Spatio-temporal gene expression analysis from 3D in situ hybridization images

Welten, M.C.M.

Spatio-temporal gene expression analysis from 3D *in situ* hybridization images

Cover design by Joep Büsdorf
Figures by Martin Brittijn
Printed by UFB Grafische producties

Spatio-temporal gene expression analysis from 3D *in situ* hybridization images

PROEFSCHRIFT

ter verkrijging van de graad van doctor aan de Universiteit Leiden,
op gezag van de Rector Magnificus prof.mr. P.F. van der Heijden,
volgens besluit van het College voor Promoties
te verdedigen op dinsdag 27 november 2007
klokke 16.15 uur

door
Monica Cornelia Maria Welten
geboren te Heemstede
in 1960

PROMOTIECOMMISSIE

Promotores
Prof. Dr. S.M. Verduyn Lunel
Prof. Dr. H.P. Spaink

Co-promotor
Dr. Ir. F.J. Verbeek

Referent
Prof. Dr. C.A. Tickle (University of Bath, UK)

Overige leden
Prof. Dr. A.J. Durston
Prof. Dr. A.P.J.M. Siebes (Universiteit Utrecht)
Prof. Dr. M.K. Richardson
Dr. H. Berkhoudt
Dr. A.H. Meijer

This study was financially supported by Netherlands Research Council through the BioMolecular Informatics programme of Chemical Sciences (grant number #050.50.213). The preparation of the thesis was supported by grants from **ZFScreens BV.**

Aan Jan en Frieda Welten - Hund

Aan Wim Welten

Spatio-temporal gene expression analyses from 3D *in situ* hybridization images

Contents

Chapter 1 **General introduction** **9**

A tool to visualize gene expression:

Chapter 2 **ZebraFISH: Fluorescent in situ hybridization protocol and 3 D imaging of gene expression patterns.** **19**

Case study – early zebrafish development

Chapter 3 **Expression analysis of genes encoding 14-3-3 gamma and tau proteins using the 3D digital atlas of zebrafish development** **33**

Chapter 4 **3D Reconstruction of gene expression patterns in the developing innate immune system of the zebrafish** **53**

Case study – late zebrafish and cross species development

Chapter 5 **Gene expression and digit homology in the chicken wing** **69**

Chapter 6 **Application of frequent episode mining in developmental pattern analysis, based on gene expression and morphological characters.** **87**

Chapter 7 **Discussion and conclusions** **105**

References **115**

Summary **133**

Samenvatting **137**

Curriculum vitae **143**

Color supplement **145**

Chapter 1

General introduction

1. Introduction

Understanding developmental processes requires a broad range of approaches and tools. These comprise biological (molecular-biological and genetic) as well as computational tools.

In this thesis, several developmental processes in both zebrafish and chicken embryos are investigated in two groups of case studies. The focus is on imaging spatial as well as temporal gene expression patterns during embryonic development, exploring *in situ* hybridization methods and computer assisted tools. Based on the use of these tools, a workflow has been developed in order to generate a large amount of biological data in a straightforward manner, thus allowing statistical analysis and pattern recognition.

Developmental biologists use a wide range of vertebrate model species such as zebrafish, clawed toad, mouse and chicken to elucidate developmental processes and as models to study human disorders. In recent years, a large amount of molecular data from these model systems has become available from developmental genetics and functional studies of genes involved in human development and disorders. This abundance of molecular data is generated with the mere goal to provide insight in developmental processes and - in some cases- evolution, and supplements to the existing knowledge. Now that all these molecular data are available, genes involved in developmental processes can be analyzed and compared across model species, to extrapolate experimental findings to other model systems and human.

2. Zebrafish as a model system

During the last decades, zebrafish has become an increasingly popular model system. In the late 1960s of the past century, George Streisinger (University of Oregon) started working with zebrafish as a model system. He had experienced its many advantages such as high fecundity, small size, short generation time, external fertilization, and numerous transparent embryos (Grunwald and Eisen, 2002). In the mid 1970s, Streisinger developed a technique to produce recessive mutations present in the maternal germ line, facilitating the analysis of mutants in zebrafish, a vertebrate model system (Streisinger et al.1981). In the mid-1980s, a research community was founded in Oregon by Streisinger's colleagues Kimmel, Westerfield and others, focusing on genetic and developmental studies in zebrafish (Grunwald and Eisen, 2002). In 1993, large screenings of embryonic zebrafish mutants were initiated in Tübingen, Germany (Haffter and Nüsslein-Volhardt, 1996) and Boston (Driever et al. 1996). These genetic screenings provided the possibility to analyze the molecular mechanisms underlying specific developmental processes. In recent years, large amounts of data from developmental marker genes have become available from functional genomics, clinical studies and molecular developmental research (Grunwald and Eisen 2002; Stern and Zon, 2003). These data are available from internet resources (e.g. www.zfin.org, http://cegs.stanford.edu/search.jsp) and include both micro array and spatial, i.e. *in situ* gene expression data.

In this thesis we will not further exploit the genetics of zebrafish, but rather analyze the spatial gene expression profiles in developmental time series of wild-type zebrafish.

3. Tools to visualize gene expression

Temporal gene expression patterns can be analyzed in several ways, such as RT-PCR, Northern blot, or immunolocalization of the proteins, i.e. the product of transcription. Recently, micro-RNAs (miRNAs) have been described as non-coding small RNAs that regulate expression of target mRNAs (reviewed by Ruvkun, 2001).

Nowadays, microarrays are a popular instrument to study gene expression (Lipshutz et al. 1995; Schena, 1996). These methods reveal gene expression profiles for a large number of genes at different time-points. In general, however, they are limited in providing spatial information of gene expression patterns during development. Tetko et al. (2006) describe spatio-temporal gene expression patterns in *Arabidopsis thaliana*. In this study, genes expressed in specific regions of the plant, e.g. root, inflorescence and leaves, are analyzed using microarrays. Though gene expression is extensively studied in a wide variety of plant organs as well as developmental stages, no true spatial – i.e. in situ - gene expression patterns are shown. Also, isolating specific organs from plant embryos is probably easier than from zebrafish embryos and early embryos of other animal models.

In order to investigate spatial patterns of gene expression*, in situ* hybridization (ISH) is the most suitable tool. This method facilitates visualization of spatial characteristics of cell and tissue specific gene expression patterns (Wilkinson, 1998; Darnell et al. 2006). Moreover, large numbers of embryos can be hybridized simultaneously (Wilkinson, 1998) – though the amount of genes that are analyzed in microarrays rises to ten thousands. In zebrafish research ISH is in most cases applied to whole mount embryos, using digoxigenin-labeled antisense RNA probes and the alkaline phosphatase (AP) detection method (Wilkinson, 1998). A high resolution ISH protocol with the AP detection method has been developed by Thisse et al. (Thisse et al, 1993, 2004), and has shown to be suitable for high throughput genomic screens. Spatial patterns of gene expression are compared by microscope images of the whole-mount ISH, providing two-dimensional information (Thisse et al.1993, 2004; www.ZFIN.org). However, ISH in itself is not the most suitable tool to provide true spatial information. Accurate visualization of the gene expression domains and their spatial relationship requires additional serial sectioning of the hybridized embryos. But even though these techniques provide complementary information, reconstruction of the gene expression patterns is still required since the information is only in 2D.

For mouse as well as for *Xenopus*, a digital 3Datlas of embryonic development and a gene expression database have been developed (mouse: http://genex.hgu.mrc.ac.uk; Davidson et al. 1997; *Xenopus*: http://www.xenbase.org3DModels, http://3dexpress.org, http://xlaevis.cpsc.ucalgary.ca; Gerth and Vize, 2004). The 3D atlas of mouse development is based on serial sections of mouse embryos. 2D gene expression patterns from ISH as well as 3D gene expression patterns obtained by optical projection tomography (Sharpe et al. 2002; http://genex.hgu.mrc.ac.uk/OPT_Microscopy) can be mapped on the anatomical structures of the 3D mouse atlas, thus providing a clue in the genetic pathways underlying developmental processes. For *Xenopus,* images obtained with FISH, ISH and immunohistochemical RNA detection can be viewed and compared with the 3D models built from whole mount confocal images (Gerth et al.2007).

3.1 3D atlas of zebrafish development

In our research group (http://bio-imaging.liacs.nl), we are developing and maintaining a 3D digital atlas of zebrafish development (Verbeek et al, 1999). The 3D atlas is intended for use as an online reference for researchers. In addition it may serve as a template to map gene expression patterns on the developing anatomical structures. Supplementary to the 3D atlas of zebrafish development, currently a zebrafish gene expression database is under construction (Belmamoune and Verbeek, 2006). During early development, changing patterns of gene activity are essential for developmental processes and the final form of anatomical structures (Wolpert et al., 2002). Therefore, the zebrafish gene expression database can be considered as the molecular counterpart of the 3D atlas. It enables mapping spatial and temporal activity of genes on developing anatomical structures, comparison of co- localization and co-expression of genes; providing insight in the genetic pathways underlying the formation of complex anatomical structures.

3.2 Zebrafish gene expression database

The zebrafish gene expression data from the experiments for research described in this thesis are stored in the Gene Expression Management System (GEMS) (Belmamoune and Verbeek 2006). Besides these gene expression data, images using GFP labeling can also be stored in GEMS. This system enables both management and retrieval of 3D spatiotemporal gene expression data. To allow interoperability of the spatiotemporal data in this database with other resources, the annotation system uses two ontologies: the zebrafish developmental anatomy ontology (DAOZ; http://bio-imaging.liacs.nl/liacsontology.html), and the gene ontology (GO; http://geneontology.org). The anatomical terms of the DAOZ are extracted from the standard vocabulary provided by the zebrafish information network (ZFIN; http://zfin.org). It uses approved nomenclature by the zebrafish community and it is intended to serve as an annotation tool for zebrafish scientific images. The GO combines biological processes and corresponding molecular and cellular functions of genes (The Gene Ontology Consortium 2000; Camon et al. 2004) and is based on a dynamic controlled vocabulary. This common, standard vocabulary is updated when information changes or accumulates; making it possible to annotate genes, proteins and biological processes in a wide variety of organisms (The Gene Ontology Consortium 2000). Integration of the zebrafish gene expression database with the GO and other Internet resources facilitates the extraction of information (Belmamoune and Verbeek, 2006).

3.3 Obtaining 3D gene expression data

In order to study developmental processes and the differentiation and patterning of specific organ systems at specific locations, both spatial and temporal information is required. Therefore, 3D data of gene expression patterns as well as anatomical structures provide most information about the state of development. To that end, we developed a straightforward technique for fluorescent *in situ* hybridization (FISH) of whole mount zebrafish embryos: the ZebraFISH protocol. This protocol is the counterpart of the high resolution whole mount ISH protocol described by Thisse et al. (2004). It is developed to enable 3D imaging with the confocal laser-scanning microscope (CLSM). A 3D image

from the CLSM, basically serial optical sections are prepared for processing with TDR-3Dbase software (Verbeek et al. 2000, Verbeek et al. 2002). This allows schematic 3D visualization of the spatial characters of gene expression patterns, as well as analytical approaches in future functional studies. For this thesis the most laborious method of TDR-3Dbase was used (Verbeek et al. 2004) in order to obtain more accurate 3D models. However, we were able to generate a large amount of 3D patterns in a straightforward and non-destructive manner**.**

In order to obtain large amounts of spatial and temporal gene expression data in a straightforward manner, we developed a workflow based on ZebraFISH, CLSM and 3D reconstruction (Fig. 1)

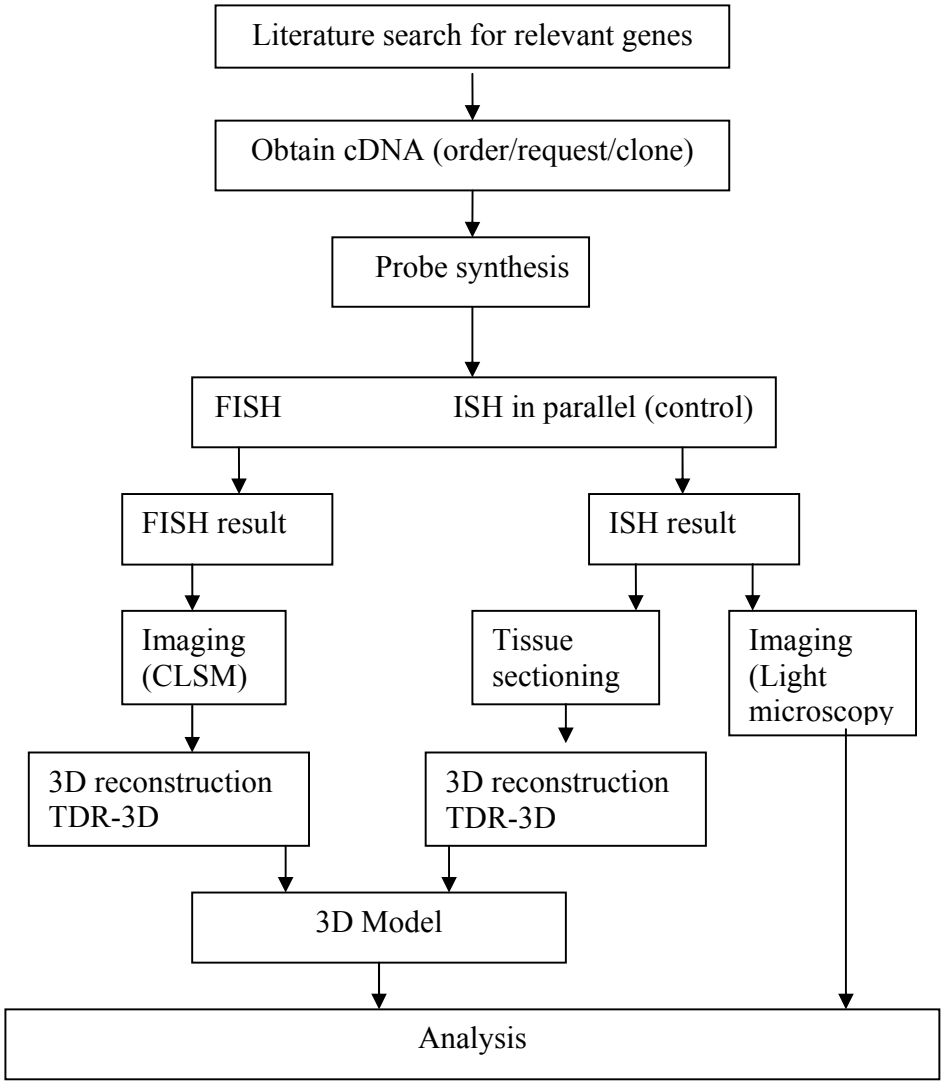

Fig.1: workflow used for obtaining *in situ* gene expression data and eventually, analysis of the data.

Spatial gene expression data are obtained

- by combining ZebraFISH (cf C**hapter 2**) and 3D reconstruction with TDR-3Dbase.

Temporal in situ gene expression data are obtained

- by application of zebraFISH to produce developmental series of zebrafish embryos,
- by analysis of spatiotemporal expression data with Frequent Episode Mining in Developmental Analysis (FEDA, cf. **Chapter 6**)
- by analysis of microarrays. Besides in situ gene expression analyses, we also generated and analyzed temporal (i.e. micro array) gene expression data (Corredor et al. 2006; Meuleman et al. 2006). The microarray data provide a quantitative analysis for a large variety and a large number of genes expressed during time series of development, but are poor in spatial information in the zebrafish embryos studied (Linney et al. 2004).

4. Case studies

In this thesis, ISH and ZebraFISH have been applied on a wide variety of genes. We analyzed gene expression patterns of more than 35 genes, in 4 different functional systems, during 4-10 developmental stages (cf. Chapter 3 – 6). In Table 1, a summary of the functional systems, developmental stages and genes is given.

Consequently, we have obtained a large amount of data from both standard marker genes and less specific genes. We were able to study relationships between genes in a spatial and temporal context. 3D spatiotemporal analysis can be used to characterize expression patterns of certain genes very precisely. We have applied ZebraFISH to two case studies to support this:

1) gene expression during early zebrafish development

2) gene expression during late zebrafish and cross species development, with a focus on limb and pectoral fin formation.

4.1 Case study early zebrafish development

In this case study, two processes in early zebrafish development were investigated:
Case study 1a) Gene expression analysis of 14-3-3 proteins in brain development.
In this study we aimed to accurately map gene expression patterns that have a diffuse appearance over a specific part of the body, to developing anatomical structures in zebrafish embryos during the early stages of development.
The 14-3-3 protein family is a highly conserved family of small dimeric proteins, found in eukaryotes. 14-3-3 proteins are involved in numerous cellular processes (cf. **Chapter 3**). Recent studies have indicated that the 14-3-3 proteins play a role in human disorders such as cancer and neurological disorders (Dougherty and Morrison, 2004), Expression of 14-3-3 during zebrafish development was previously analysed by Besser et al. (2006). In this study, the ISH results for the 14-3-3 genes exhibited diffuse expression patterns that were difficult to annotate on anatomical structures. Moreover, gene expression patterns in zebrafish were not yet localized in detail, i.e. by means of tissue sectioning, and gene expression patterns appeared difficult to characterize from 2D images. To study the zebrafish 14-3-3 family members in relation to human development, neurological disorders and cancer, it is important to accurately characterize the gene expression patterns of 14-3-3 isoforms in the zebrafish brain.

Table 1. Summary of functional systems, organ systems, genes and developmental stages used for this thesis.

Zebrafish Functional system	**Locomotion**		**Innate Immune system**	**Central nervous system**	**Develop-mental**
Organ	Fin	Skeleton & Musculature	Blood, haematopoietic tissues	Brain, spinal cord	Body axis
Process	initiation development patterning identity	development	development distribution	development	development patterning
Developmental Stages Kimmel et al. 1995	24-120 hpf	36-120 hpf	18-96 hpf	10-48 hpf	10-24 hpf
Number of stages	7	6	7	10	8
Genes	*fgf8* *tbx5* *shh* *msx-b* *hoxa9a* *hoxc4a* *hoxd9a* *hoxd11a*	*sox9a* *sox9b* *bmpr1b* *runx2a* *runx2b* *chm 1* *myoD*	*l-plastin* *mpx* *draculin* *fms* *lysC*	*hoxb1a* *hoxb3a* *krox20* *otx2* *pax2* *six3.1* *14-3-3 ε* *14-3-3ι* *14-3-3ζ* *14-3-3γ* *14-3-3τ*	*hoxb6a* *hoxb8a* *hoxb13a* *hoxc12a*
Chicken Organ		wing hindlimb			
Developmental Stages Hamburger & Hamilton, 1951		24-34			
Number of stages		10			
Process		development			
Genes		*sox9* *bmpr-1b* *wnt-14*			

Case study 1b) Gene expression analysis of markers of the innate immune system.
In this case study we annotate gene expression in single white blood cells -or precursors thereof- to larger anatomical structures. We analyze the temporal distribution of marker gene expression in these cells over the embryo during early stages of development. In this study the focus is on *l-plastin*, a general marker of leukocytes, and *mpx*, a specific marker of neutrophil granulocytes. These marker genes are expressed in single cells and show a very distinct expression pattern.

4.2 Case study late zebrafish and cross species development
In this case study, the focus is on marker genes involved in zebrafish pectoral fin as well as in chicken limb development. Marker genes involved in zebrafish fin and chicken limb development are analyzed and compared with limb development in other tetrapods. The chicken is another well-studied model system, and a large amount of gene information is available to study chicken limb development in a developmental as well as in an evolutionary context.
The teleost pectoral fin and the tetrapod limb are well studied in evolutionary - developmental biology. Data from the fossil record suggest that the transition from fin to limb occurred approximately 410 million years ago (Shubin et al, 2006). However, many similarities can be observed in both the teleost fin and the tetrapod limb. Highly conserved organizing structures are found in limbs as well as in paired fins, and the same genetic pathways involved in patterning and outgrowth are found in teleost fins and in tetrapod limbs (Hinchliffe, 2002; Tickle, 2002).
Though skeletal structures in tetrapod limbs are more complex than in teleost fish such as zebrafish (Coates and Cohn, 1998; Grandel and Schulte-Merker, 1998), the molecular marker genes present in early cartilage formation are conserved in both tetrapods and teleosts.
The timing of limb and fin development, however, displays a lot of variation (Richardson, 1995). All considered, it is interesting to compare gene expression data involved in fin and limb development in vertebrates. Such studies are an example to facilitate extrapolation between model systems as well as to human.
In this case study on limb development, we analyze

1) Gene expression patterns of three early cartilage marker genes in chicken embryo wings and hindlimbs. In this study ISH in combination with tissue sectioning was used to reveal a rudimentary structure (cf. **Chapter 5**) and to compare timing of gene expression within one species.
2) Gene expression of marker genes involved in pectoral fin development and cartilage formation in zebrafish embryos from 30-120 hpf., using ISH and zebraFISH.
3) Gene expression data from known orthologues in other tetrapod model species. Here, gene expression patterns for clawed toad, axolotl, mouse, as well as supplemental data for chicken are retrieved from literature.

Eventually, the relative timing of gene expression during fin and limb development is compared between all five model species, using the frequent episode mining algorithm (FEDA).

In this case study, we have specifically focused on difference in timing of gene expression, in one species i.e. chicken, as well as cross – species, i.e. in zebrafish and four tetrapod model species; using ISH, FISH, as well as data acquisition.

5. Outline of the thesis

In **Chapter 2** the methodology of the ZebraFISH is presented and discussed. The FISH method is based on the high resolution whole- mount ISH protocol developed by Thisse et al. (1993, 2004). This protocol is used for high throughput genomic screens; excellent results have been shown (www.ZFIN.org). To test and optimize our ZebraFISH protocol, we used a panel of five standard marker genes, with a wide range of gene expression patterns (cf. **Chapter 2**)

Following the application with standard markers in **Chapter 2**, we have worked out two case studies with more specific markers.
In **Chapter 3**, we present a spatiotemporal characterization of the 14-3-3 γ and τ isoforms with the focus on the developing zebrafish brain, using ZebraFISH, TDR-3Dbase software and the 3D atlas of zebrafish development as a reference. In addition, we demonstrate that the techniques presented facilitate a precise localization of complex gene expression patterns.

In **Chapter 4**, cell-based gene expression patterns of *mpx* and *l-plastin* are analysed in their spatial relation to anatomical structures such as developing blood vessels and heart. Distribution of these cells over the embryo is visualized in 3 dimensions and at subsequent time points during embryonic development, using TDR-3Dbase software.

In **Chapter 5**, *in situ* hybridization is applied to investigate a rudimentary structure in another model system, the chicken. Traditional histological methods might detect a rudimentary cartilage structure too late, when it already starts to disappear. Marker genes used in **Chapter 5** are expressed before condensation of mesenchyme in future skeletal elements (Akiyama et al, 2002; Chimal- Monroy et al, 2003), or in early differentiating chondrocytes (Karsenty and Wagner, 2002; Pizette and Niswander, 2002).
In **Chapter 6,** *in situ* gene expression data from marker genes involved in limb and pectoral fin development are compared between five model species. A new method to analyze limb and fin gene expression data with a focus on heterochrony in gene expression, is presented: Frequent Episode Mining in Developmental Analysis (FEDA).
A general discussion is presented in **Chapter 7**, followed by the conclusions from the work described in this thesis. Finally, in **Chapter 8** a summary and a summary in Dutch are given.

Chapter 2

ZebraFISH: Fluorescent *in situ* hybridization protocol and 3 D imaging of gene expression patterns.

M.C.M. Welten [1,2], S.B De Haan[1,2], N. Van den Boogert [1], J.N. Noordermeer [3], G.E.M. Lamers [2], H.P. Spaink [2], A.H. Meijer [2] and F.J. Verbeek.[1]

1. Imagery and Media, Leiden Institute of Advanced Computer Science, Leiden University, Niels Bohrweg 1, 2333 CA Leiden, the Netherlands
2.Institute of Biology, Leiden University, Clusius Laboratory, Wassenaarseweg 64, 2333 AL Leiden, The Netherlands
3.Leiden University Medical Center, Developmental neurobiology group, Dept. of molecular cell biology, Wassenaarseweg 72, 2300 RA Leiden, The Netherlands

Originally published in Zebrafish, 2006: Vol. 3, No. 4: 465-476
Modified and updated version

.

A Tool to visualize gene expression

ABSTRACT

We present a method and protocol for fluorescent *in situ* hybridization (FISH) in zebrafish embryos to enable three-dimensional imaging of patterns of gene expression using confocal laser scanning microscopy. We describe the development of our protocol and the processing workflow of the three-dimensional images from the confocal microscope. We refer to this protocol as zebraFISH. FISH is based on the use of tyramide signal amplification (TSA), which results in highly sensitive and very localized fluorescent staining. The zebraFISH protocol was extensively tested and here we present a panel of five probes for genes expressed in different tissues or single cells. FISH in combination with confocal laser scanning microscopy provides an excellent tool to generate three-dimensional images of patterns of gene expression. We propose that such three-dimensional images are suitable for building a repository of gene expression patterns, complementary to our previously published three-dimensional anatomical atlas of zebrafish development (bio-imaging.liacs.nl/). Our methodology for image processing of three-dimensional confocal images allows an analytical approach to the definition of gene expression domains based on the three-dimensional anatomical atlas.

INTRODUCTION

The zebrafish is an excellent model system for developmental and molecular genetics, for functional analysis of genes, as well as to gain understanding of genetic networks involved in human disease (Stern and Zon, 2003).The basis for such analysis is the *in situ* study of gene expression. The best tool for studying spatial characteristics of patterns of gene expression is *in situ* hybridization (ISH) (Wilkinson, 1998). In zebrafish research it is, in most cases, applied on whole-mount embryos, using digoxigenin-labeled antisense RNA probes and the alkaline phosphatase (AP) detection method (Wilkinson, 1998). A high resolution ISH protocol with the AP detection method for high throughput genomic screens that utilize spatial patterns of gene expression as readout has been developed by Thisse et al. (Thisse et al, 1993, 2004). Patterns of gene expression are then compared by microscope images of the whole-mount ISH, providing two-dimensional information; excellent results and observations have been shown (Thisse et al, 1993). For analytical approaches, a true three-dimensional spatial representation of the pattern of gene expression is required (Verbeek et al, 1999). Three-dimensional images can be acquired by using the confocal laser scanning microscope (CLSM). Up to a certain age, zebrafish embryos and larvae can be very well visualized with CLSM and true three-dimensional images of high resolution can be produced. With CLSM, visualizing a pattern of gene expression is based on tagging a fluorescent molecule such as Cyanine 3 or Cyanine 5 (Cy3 or Cy5, PerkinElmer) to the RNA probe.

We argue that a suitable protocol for fluorescent *in situ* hybridization (FISH) can easily be adapted from existing protocols and be used in high-throughput applications in zebrafish (zebraFISH). To adapt this protocol as much as possible to common laboratory practice of the zebrafish researcher as well as to high-throughput screening, we used the standard ISH AP detection protocol developed by Thisse et al. (Thisse et al, 1993, 2004) as a foundation. Whole-mount FISH has been successfully applied in *Drosophila* (Kearny et al, 2004; Paddock, 1999) and the protocol used in the *Drosophila* community was taken as the starting point to develop and optimize the fluorescent labelling steps for zebraFISH. The first steps of our FISH protocol are identical to the standard Thisse (Thisse et al, 1993, 2004) protocol and it diverges at the point of application of the fluorescent substrate. The protocol uses an amplification step in order to obtain sufficiently high signal-to-noise ratios for visualization and localization for three-dimensional imaging. This amplification step, achieved by the tyramid signal amplification (TSA) technique, is an essential ingredient in our zebraFISH protocol; the result is an amplification of the Cy3/Cy5 signal. Horseradish peroxidase (HRP) is used to catalyze the deposition of a fluorophore-labelled tyramide amplification reagent at the site of probe binding. This approach is, in a way, complementary to AP detection substrates (i.e., NBT/BCIP) that precipitate diffusely near the location of gene expression. In TSA, a relatively short defined staining procedure provides as strong expression signal with relatively low background staining (Zaidi et al, 2000). Even weak probes and small gene expression domains can be visualized using our approach for TSA detection. Independent of our research and testing of the zebraFISH protocol, another protocol for fluorescent *in situ* hybridization, also based on TSA, has been developed by Clay and Ramakrishnan (2005). The focus of their protocol was on multiplex detection of genes with overlapping expression patterns, with AlexaFluor conjugates used to

demonstrate colocalization expression within single cells. In the zebraFISH protocol described here, we also use multiple fluorescent labels. The purpose is however different. In order to reveal both outline and anatomical structures of the embryo, we combine TSA/Cy3 or TSA/Cy5 staining with a nuclear counter staining, using SYTOX Green or SYTOX Orange. In this way the gross texture of the embryo is visualized by clusters of nuclei. The interpretation of the three-dimensional image is greatly facilitated in this manner and we use this to colocate anatomical domains with respect to the expression patterns. Our protocol differs from that of Clay and Ramakrishnan in that we use a one-step antibody detection procedure (HRP-conjugated anti-dioxigenin antibody) instead of a two-step detection procedure that uses sheep anti-dioxigenin and HRP-conjugated anti-sheep antibodies.
Our one-step approach results in a procedure that is one day shorter; this is a major advantage for high-throughput applications. In this paper we demonstrate that our zebraFISH protocol with one-step TSA detection provides adequate sensitivity to detect expression of a variety of developmental marker genes, such as *myoD*, *krox20*, *otx2*, *pax2.1*, and *mpx.*

MATERIALS AND METHODS

Zebrafish maintenance and embryonic staging

Embryos were collected from a laboratory breeding colony of albino zebrafish kept at 28°C on a 14:10 h light/dark rhythm and raised under standard conditions (zfin.org). Embryos were staged at 28°C according to hpf and morphological criteria (Kimmel et al, 1995).

cDNA clones and RNA probe synthesis

cDNA clones of *myoD*, *krox20*, *otx2*, and *pax2.1* were provided by J. Bakkers (NIOB, Utrecht, the Netherlands). An *mpx* cDNA clone (BC056287) was obtained from RZPD (Berlin, Germany). Antisense riboprobes labeled with digoxigenin-11-UTP (Roche) were synthesized from linearized cDNA clones using T7, T3, or Sp6 RNA polymerases (Maxiscript kit, Ambion) according to the manufacturer's instructions.

Fluorescent in situ *hybridization (FISH)*

In brief, embryos were manually dechorionated, fixed overnight in 4% buffered paraformaldehyde (PFA) at 4°C, dehydrated through a graded methanol series and stored at -20°C in methanol. Endogenous peroxidase activity was inhibited by incubation in 3% H_2O_2 in methanol for 20 min at room temperature. Embryos were rehydrated through a graded methanol series to 100% PBST (phosphate buffered saline, pH 7.0, containing 0.1% Tween 20) and permeabilized with 10 ug/ml proteinase K (Promega) in PBST at 37°C from 15 min (24 hpf embryos) to 30 min (36–120 hpf embryos). To stop the reaction, the embryos were washed in PBST for 5 min. Embryos were refixed in 4% buffered PFA and washed 5 times in PBST for 5 min. Next, the embryos were prehybridized for 2–5 h at 55°C in hybridization buffer containing 50% formamide, 5xSSC(20xSSC = 3M NaCl, 300 mM trisodium citrate), 0.1% Tween 20, 500 ug/ml tRNA (Sigma), and 50 ug/ml heparin (Sigma), pH 6.0–6.5. Hybridization was carried out overnight at 55°C in 200 ul hybridization buffer containing 50–100 ng of digoxigenin-

labelled riboprobe. After hybridization, the embryos were briefly washed in hybridization buffer (without tRNA and heparin) and next washed at 55°C in 15-min steps over a gradient of hybridization buffer and 2xSSC (75%/25%, 50%/50%, 25%/75%) to a final wash in 100% 2xSSC. Subsequently, the embryos were washed 2 times in 0.2x SSC for 30 min at room temperature and washed in 10-min steps at room temperature over a gradient of 0.2xSSC and PBST (75%/25%, 50%/50%, 25%/75%) to a final wash in 100% PBST. Embryos were preabsorbed for 2 h at room temperature under slow agitation in antibody buffer consisting of PBST containing 2% sheep serum and 2 mg/ml bovine serum albumin. Meanwhile, anti-DIG-HRP antibody (anti-DIG-POD, Roche) was diluted 1:1000 in antibody buffer and preadsorbed for 2 h at room temperature under gentle agitation. After pre-incubation, the antibody buffer was replaced by the preadsorbed 1:1000 diluted anti- DIG-HRP solution and embryos were incubated overnight at 4°C under gentle agitation. After antibody incubation, embryos were washed 6 times for 15 min in PBST and stained with TSA/Cy3 reagent (PerkinElmer) diluted 1:50 in amplification buffer (provided with the TSA/Cy3 amplification kit) for 30 min at room temperature. After staining, embryos were washed 8 times for 15 min in PBST, and a nuclear counterstaining with 100 nM SYTOX Green (Molecular Probes) was performed for 30 min. Embryos were washed 6 times for 15 min in PBST. For microscopy, embryos were mounted and stored in Gelvatol containing 100 mg/ml DABCO (1,4-diazabicyclo[2.2.2]octane) in a glass-bottom dish. (See Appendix for complete protocol.) For control of the *in situ* reaction and comparison with FISH results, probe detection with alkaline-phosphatase-conjugated anti-digoxigenin (Roche) and nitroblue tetrazolium salt/5-bromo-4-chloro-3-indolyl phosphate substrate (NBT/BCIP, Roche) as described by Thisse et al.(1993, 2004) was carried out in parallel. Each control ISH was examined on a stereo microscope and photographed with a digital camera for later reference.

Microscopy and image processing

Images of NBT/BCIP-stained embryos were acquired using a Leica MZFL-III12 stereomicroscope equipped with a Leica DC 500 digital camera. Confocal imaging of embryos was performed using a Leica TCS/SP DM IRBE confocal laser scanning microscope (inverted setup) equipped with an Ar/Kr laser. Excitation and emission wavelengths of used fluorophores are summarized in Table 1.

Table 1. Overview of fluorophores, excitation, and emission spectra described in ZebraFISH.

Fluorophore	*Excitation (nm)*	*Excitation in zebraFISH protocol (nm)*	*Emission (nm)*	*Emission in zebraFISH protocol (nm)*
Cyanine 3	550	568 (Kr laser)	570	580
Cyanine 5	648	NA	667	NA
ELF	345	350 (Zeiss Axioplan)	530	NA
SYTOX Green	504	488 (Ar laser)	523	523
SYTOX Orange	547	NA	570	NA

In our setup, excitation resulted in a green and a red channel. All images shown were obtained with a 10x plan apo lens with a large working distance (NA 0.24). The images are sampled isometrically, taking the resolution in the xy plane as the guide for the z-axis sampling; each image slice is sampled to 1024 x 1024 pixels. The CLSM images are saved as two-channel multiple TIFF files and these files were processed with dedicated image processing software (Bei et al.2006).

The three-dimensional reconstructions (see Fig. 1) were produced from the CLSM images using the TDR-3Dbase annotation and reconstruction software (Verbeek et al. 2000; Verbeek, 2000). By means of the TDR- 3Dbase software, gene expression and anatomical domains in the three-dimensional images were traced, either manually or via automated procedures, to result in the three-dimensional models.

RESULTS

To test and optimize the zebraFISH protocol, we used a panel of 5 probes which we consider represent a range of patterns, from expression in single cells (*mpx*) to expression in different tissues of the brain (*krox20*, *otx2*, *pax2.1*) and in the somites (*myoD*). Figures 1 and 2 present an overview of the results with the panel of 5 genes. In Figure 1, results of both chromogene and TSA detection are shown for each of these genes. In all cases, the TSA/Cy3-based detection FISH expression patterns perfectly corresponded to those obtained through standard AP detection. In agreement with previous reports, at 24 hpf, *MyoD* expression is detected in the somites (Weinberg et al, 1996), *krox20* is expressed in rhombomeres 3 and 5 (Woo and Fraser, 1998), *otx2* is expressed in the diencephalon and mesencephalon (Mercier et al, 1995), and *pax2.1* shows expression domains in the midbrain-hindbrain boundary, the optic stalk, and the otic vesicle (Lun and Brand, 1998). In addition to the three-dimensional images, we provide three-dimensional reconstructions for these four expression patterns, using the three-dimensional image stack as input to our three-dimensional reconstruction software, TDR-3Dbase (Verbeek et al, 2000; Verbeek, 2000).

The reconstruction process results in a geometric model through which the expression patterns and some of the surrounding tissues can be visualized (Fig. 1D). These three-dimensional visualizations give further insight into spatial relationships of the pattern and the three-dimensional models underlying the visualizations can be used for quantitative analysis. TSA/Cy 3 detection reveals clear and specific expression patterns even for genes expressed in small domains, as illustrated in particular by the *mpx* expression pattern (Fig. 2). Lieschke et al (2001) reported previously that neutrophil granulocytes

expressing mpx are scattered over the yolk sac, the head region, and the ventral venous plexus of the 48 hpf embryo. TSA/Cy3 detection clearly revealed the expression pattern in single cells.
In order to obtain optimal and reproducible results from zebraFISH we examined several important parameters of the procedure. From laboratory practice we have learned that some fine tuning is required for the critical steps in every probe.

Embryo culture
The addition of methylene blue during embryo culture is often used to prevent fungal growth; however, it also induces autofluorescence. Therefore, embryos should be grown in egg medium (www.zfin.org) without methylene blue.

In situ hybridization
One of the crucial parameters of the zebraFISH protocol is to adjust the pH of the prehybridization and hybridization mix to 6–6.5. All our hybridizations were carried out at 55°C. In our experiments, hybridization at this temperature yielded the best signal and the most stable signal complex; for standard ISH, Thisse et al. (1993, 2004) suggest hybridization at 70°C.

Antibody incubation and blocking reaction
If the background is too high, lower the antibody concentration. Titration of the used antibody is recommended by the manufacturer (Roche) to obtain the optimal antibody dilution with every new batch of anti-DIG-HRP. We have learned that use of 1:1000 to 1:2000 dilution of the anti-DIG-HRP antibody yields good results to decrease background staining. Alternatively, the background can be further reduced by preadsorbing the antibody either with zebrafish acetone powder (Jowett, 2001, Zaidi et al, 2000) or with prehybridized zebrafish embryos (Thisse et al, 2004).

Fluorescent RNA and nuclear staining
For HRP-conjugated antibodies (anti-DIG POD, Roche 1 207 733), TSA can be performed with either of the fluorescent labels Cy3 or Cy5 (PerkinElmer NEL 704A and NEL 705A). For reasons of our local CLSM setup, we concentrated on the TSA/Cy3 fluorescence system; the TSA/Cy5 protocol is very similar to the method described in this paper. To visualize the outline of the embryos in relation to the gene expression location, an additional nuclear staining with SYTOX Green (Molecular Probes S-7020) is performed. To make optimal use of the nuclear staining, it should be applied just prior to the CLSM imaging session. Fading can be overcome by storing embryos in an antifading reagent (e.g., Gelvatol- DABCO) before mounting them for microscopy. In an antifading agent, the specimen and the fluorescent signals remain more stable for a longer period, allowing repeated imaging of the same specimen.

FIG. 1. A panel of marker genes expressed in 24 hpf zebrafish embryos. Row **A** depicts the results of the standard AP detection. Row **B** depicts a characteristic optical section from the 3D image obtained with zebraFISH, using TSA/Cy3-SYTOX Green. Row **C** is a projection of that same image stack into one image. Row **D** depicts 3D reconstructions of the expression pattern, the embryo outline, and some surrounding tissues as obtained from the 3D image.
Column **1** shows *myoD* expression in the somites: (**B1, C1**) *myoD* expression detected in an image stack of 64 slices; (**D1**) 3D reconstruction of *myoD* expression in white, yolk extension in green, and embryo outline in blue. Column 1 is visualized in oblique dorsal orientation. Column **2** shows *krox20* expressed in rhombomeres 3 and 5: (**B2, C2**) *krox20* gene expression in an image stack of 13 slices; (**D2**) 3D reconstruction of *krox20* expression in white, third ventricle in cyan, partial eye outline in salmon, and embryo outline in blue. Column 2 is visualized in oblique lateral orientation. Column **3** shows the *pax2.1* expression pattern at the midbrain-hindbrain boundary and the optic stalk: (**B3, C3**) show gene expression detected in an image stack of 97 slices; (**D3**) 3D reconstruction of *pax2.1* gene expression patterns in white, embryo outline in blue, optic cup in salmon. Column 3 is visualized in oblique lateral orientation. Column **4** shows *otx2* expressed in the diencephalon and mesencephalon: the image stack in (**B4, C4**) is 74 slices; (**D4**) 3D reconstruction of *otx2* gene expression in white, embryo outline in blue, optic cup in salmon. Column 4 is visualized in oblique lateral orientation. For all four genes, the pattern generated with zebraFISH corresponds to the pattern generated with AP detection. The 3D reconstructions give insight into the extension of the pattern within the embryo as well as clear spatial relations with a number of anatomical domains. These domains coincide exactly with the domains annotated in the three-dimensional digital atlas of zebrafish development (bio-imaging.liacs.nl).
FIG. 2. Gene expression patterns of *mpx* in 36 hpf and 48 hpf zebrafish embryos with TSA/Cy3 detection. (**A**) At 36 hpf, an image stack of 70 slices. For this image only TSA detection was applied. The *mpx* expressing cells are clearly visible as dispersed over the yolk and also visible in the head; *mpx* expressing cells also accumulate in the ventral venous plexus (not shown). (**B–D**) At 48 hpf, image stacks of 78 slices using TSA/Cy3-SYTOX Green detection. Expression is visible in single cells scattered over the yolk and in the head. Characteristic slices show single cell imaging (arrow pointing to *mpx* expressing cell) in the brain (**B**) and yolk sac (**C**). (**D**) A projection of the whole stack showing the pattern of the *mpx* gene at 48 hpf.

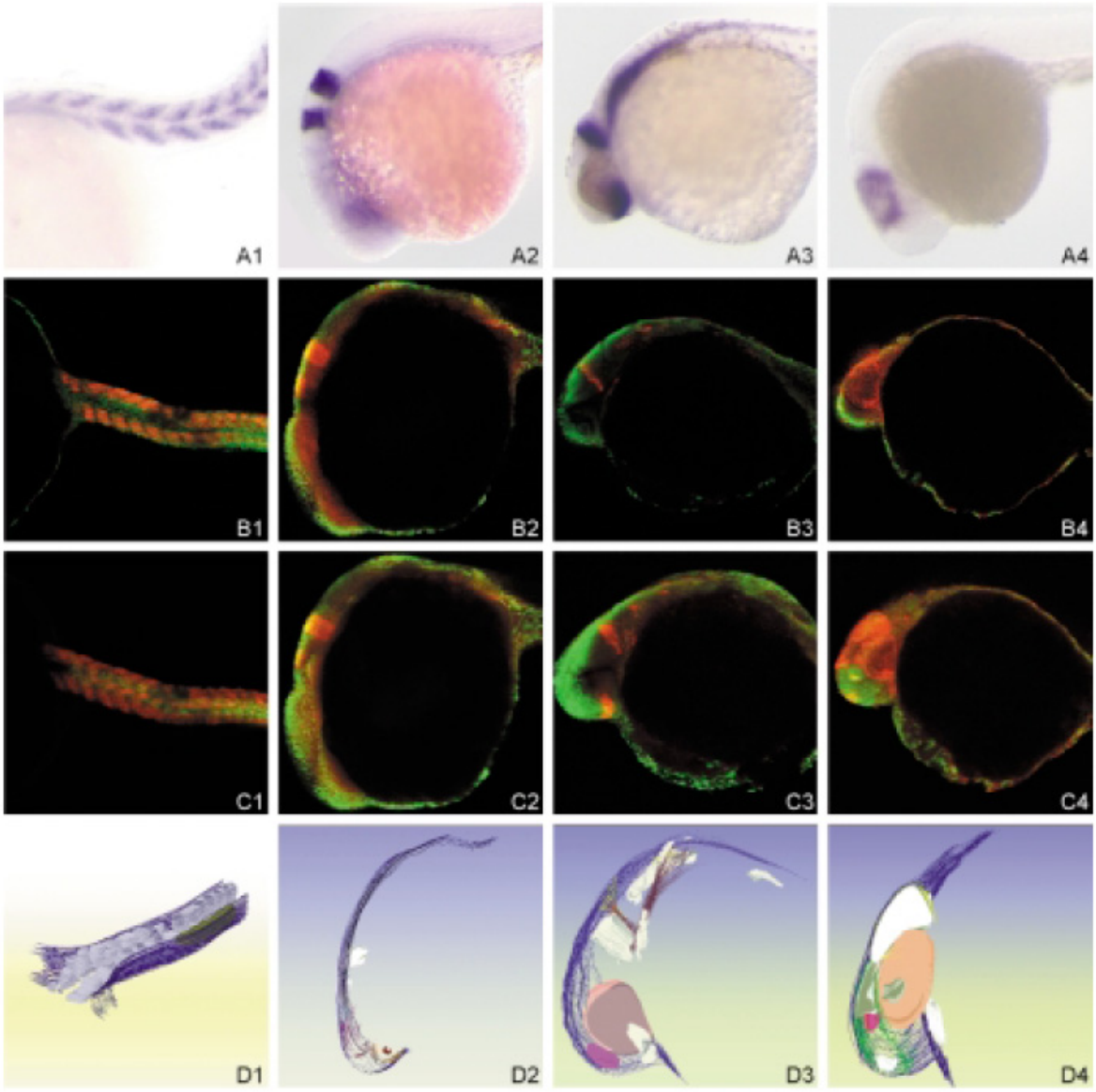

FIG. 1.

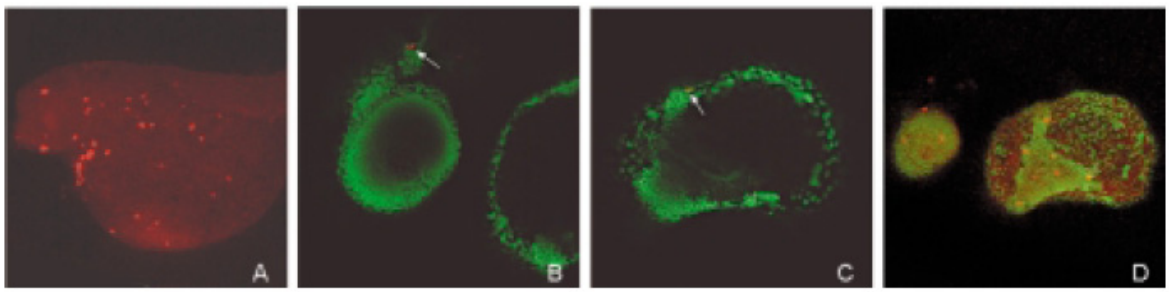

FIG. 2.

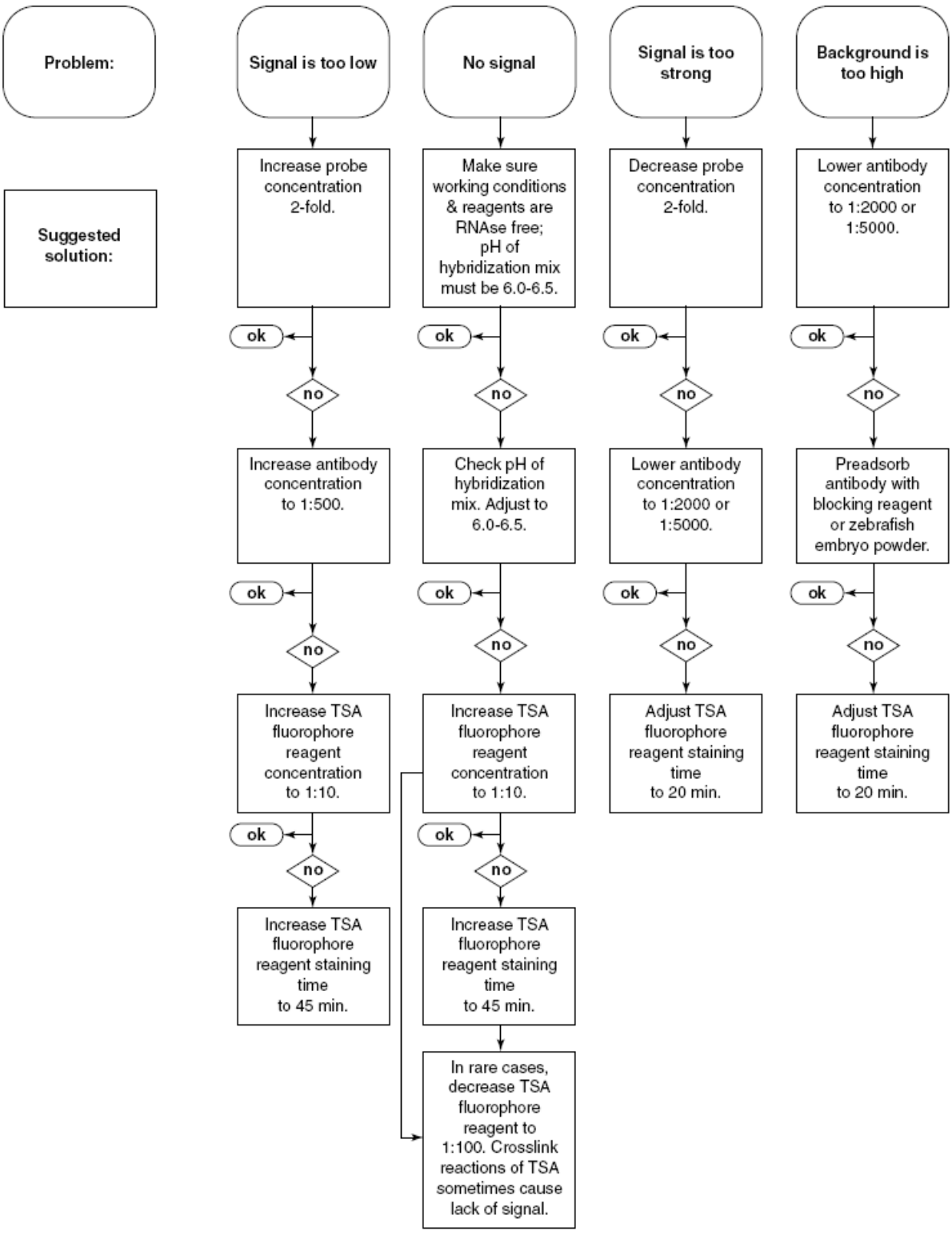

FIG. 3. Schematic summary of possible problems, with flowchart for problem-solving.

Optimization of TSA reaction
In order to obtain optimal results for the amplification reaction we found it necessary to titrate both anti-DIG-HRP antibodies and the TSA fluorophore working solution for every new batch. If adjusting the probe or antibody concentration still results in low signal, the TSA/Cy3 or Cy5 concentration needs to be adjusted; this is also recommended by the manufacturer (personal communication, Grootjans, PerkinElmer Europe). These suggestions for optimization are summarized in Figure 3.

Mounting and storage
The embryos are mounted in glycerol or Gelvatol- DABCO for CLSM on glass bottom dishes (WillCo). After imaging, embryos are stored in Gelvatol-DABCO at 4°C. It should be noted that the glass bottom dishes were selected because an inverted CSLM setup was used.

Control reaction
To check the *in situ* hybridization procedure and the used solutions and reagents, each ISH procedure is performed simultaneously with an NBT/BCIP (Roche) for anti-DIG AP and DAB or BMblue (Roche) for anti-DIG-HRP. Since every probe requires some fine tuning, AP detection gives an indication of the probe concentration to obtain sufficient signal for FISH. Eventually, antibody concentration can be adjusted.

DISCUSSION

In this paper we present a method and protocol for FISH in zebrafish embryos to visualize patterns of gene expression. This protocol is particularly suitable for three-dimensional imaging of zebrafish embryos with confocal laser scanning microscopy.
In order to make FISH applicable for a wide range of probes, signal amplification is used. In parallel with the protocol for FISH, a methodology for image processing of the CLSM images is being developed. Processing these images allows analytical approaches to patterns of gene expression which can be assisted by our three-dimensional atlas of zebrafish development.
The FISH protocol based on the TSA fluorescence system yields clear, strong, specific, and localized expression patterns with a low background. The staining procedure and time is short (30 minutes). In combination with the protocol, we have provided a range of solutions to possible problems. In addition to our findings on reducing background staining, Clay and Ramakrishnan (2005) suggest using Western blocking solution (Roche) and have shown good results with that reagent.
The FISH protocol described in this paper is adapted from the protocol described by Thisse (1993, 2004) with modifications, especially for the fluorochrome tagging and staining. The combination of the SYTOX nuclear staining with TSA/Cy3 or Cy5 detection provides an excellent pair of fluorescent markers to discern gene expression patterns, the outline of the embryo, and the outline of anatomical structures. An alternative to the TSA/Cy3 or Cy5 method based on the AP detection protocol described by Thisse et al (1993, 2004) is enzyme-linked fluorescence signal detection (ELF, Molecular Probes),which also produces a strong signal. For the ELF approach, the staining reaction needs to be monitored. Moreover, it requires a longer staining time,

which can result in higher background. ELF signal detection therefore is a possible alternative but produces less specifically localized precipitate.
Using CLSM imaging, three-dimensional images from the gene expression patterns are produced in a nondestructive manner. Application of the zebraFISH protocol for a range of zebrafish marker genes will result in collections of three-dimensional images of gene expression patterns. Our goal is to make these patterns comparable in a quantitative manner. In some cases, comparing gene expression patterns can be realized using multiple channels in the CLSM. This is restricted by the laser lines available, and thus different for each CLSM. Therefore, we argue that patterns should be compared on an individual basis as well as to a standard. For developmental genetics, a whole range of marker genes and their three-dimensional patterns should be made available in an internet repository, so that researchers can appreciate each pattern separately and combine such results with their own findings.
The results presented in this paper concern embryos that are opaque; using CLSM, a certain depth penetration can be realized, but for older embryos and larval stages, this is difficult. We therefore propose to handle these embryos and larvae with multiphoton laser microscopy, which has a considerable higher potential for depth penetration in the specimen.
In our research we are in the process of providing the necessary computerized tools to make comparisons of spatial patterns possible through digital three-dimensional images and models. We have developed a general three-dimensional reference system for the developing zebrafish embryo, the three-dimensional digital system is used to project the three-dimensional patterns of gene expression that are obtained from application of zebraFISH. A database for these images has been developed: the gene expression database (Bei et al, 2006; Verbeek et al, 2002) directly relates to the three-dimensional atlas of zebrafish development (bio-imaging.liacs.nl). Dedicated tools for the mapping of these CLSM images have also been developed (Verbeek et al, 2004). Three-dimensional visualizations of the patterns of gene expression can provide additional insight into the spatial distribution of gene expression. We have shown this with the three-dimensional reconstructions we have made from the sample FISH images. Different modes of visualization further help in the understanding of complex patterns. The three-dimensional models underlying these visualizations are stored with the three dimensional images.
In the near future, zebraFISH will also be used in combination with transgenic GFP-lines and immunostaining to analyze colocalization (Manders et al, 1993). Our prime focus remains on generating three-dimensional patterns for a gene expression database.

ACKNOWLEDGMENTS

This work is partially supported by The Netherlands Research Council through the Bio-Molecular Informatics Programme of Chemical Sciences, and the ZF-Models programme supported through the European Community Sixth Framework Programme (grant LSHGCT- 2003-503496). We would like to thank Marjo den Broeder, who worked with F.J. Verbeek on FISH while he was at the Hubrecht Laboratory; Dr. Jeroen Bakkers, who kindly provided us with probes; and Laura Bertens for her contributions on the *mpx in situ* hybridizations. We also thank Dr. J. Grootjans (PerkinElmer Europe, Brussels) for his valuable advice, and Peter Hock for his assistance with the preparation of the figures.

APPENDIX

Fluorescent *in situ* hybridization (zebraFISH) protocol

Note: Up to the first post-hybridization wash step, all work should be carried out under RNAse free conditions. Use gloves, sterile disposable tubes, pipette tips and transfer pipettes, and sterilized glassware. Autoclave buffers for 20 min at 120°C. Nuclease-free Tween 20, proteinase K, tRNA, and heparin are added after autoclaving.

1. Embryo fixation

Dechorionate embryos and fix overnight in 4% paraformaldehyde in PBS at 4°C.
Wash 3 times for 5 min in PBST at room temperature.
Dehydrate through methanol series: 5 min 25%, 10 min 50%, 5 min 75% methanol in PBST, wash twice in 100% methanol.
Place embryos in 100% methanol for at least 24 h at -20°C or store at -20°C up to several months.

2. Pretreatment and prehybridization

Inhibit endogenous peroxidase activity in 3% H_2O_2 in methanol for 20 min at room temperature.
Rehydrate embryos through methanol series: 5 min 75%, 10 min 50%, 5 min 25% methanol in PBST.
Wash 4 times for 5 min in PBST at room temperature.
Permeabilize the embryos by digestion with 10 ug/mL proteinase K (Promega V3021) at 37°C.
Duration depends on developmental stage:
Blastula, gastrula, and somitogenesis (<18 somites) stages 30 sec to 1 min
24 hpf stage up to 10 min
Embryos older than 24 hpf 20–30 min
Wash in PBST for 5 min.
Refix embryos in 4% paraformaldehyde in PBST for 20 min at room temperature.
Wash 5 times for 5 min in PBST at room temperature.
Prehybridize in hybridization buffer pH 6.0–6.5 for 2–5 h at 55°C.
Continue directly with hybridization, or store embryos in hybridization buffer at -20°C up to several weeks.

3. Hybridization

Remove the hybridization buffer and discard.
Replace with fresh hybridization buffer containing 100 ng of digoxigenin-labeled antisense riboprobe.
Hybridize overnight at 55°C.

4. Post-hybridization washes

Remove probe mix from embryos and store at -20°C. Probes can be reused up to 3 times.
Wash briefly in hybridization buffer without tRNA and heparin.
In the following wash steps, tRNA and heparin are also omitted from the buffer.
Bring embryos to 2x SSC environment by successive 15 min wash steps at 55°C over the following
gradient:
75% hybridization buffer/25% 2x SSC
50% hybridization buffer/50% 2x SSC
25% hybridization buffer/75% 2x SSC
100% 2x SSC.
Wash 2 times for 30 min in 0.2x SSC at room temperature.
Bring embryos to PBST environment by successive 10 min wash steps at room temperature over

the following gradient:
75% 0.2x SSC/25% PBST
50% 0.2x SSC/50% PBST
25% 0.2x SSC/75% PBST
100% PBST.

5. Antibody incubation and blocking reaction
Incubate embryos for 2–5 h at room temperature in antibody buffer with slow agitation.
Meanwhile, dilute DIG POD (Roche 1207733) for anti-DIG-HRP detection 1:1000 in antibody buffer and preadsorb for 2 h at room temperature with slow agitation.
Optional: Preadsorb anti-DIG-POD in zebrafish acetone powder as described by Jowett (2001), or with a batch of prehybridized embryos as described by Thisse (2004) with Western blocking reagent (Roche 11921673001).(Clay and Ramakrishnan, 2005)
Remove antibody buffer with the preadsorbed anti-DIG-POD antibody solution and incubate overnight with slow agitation at 4°C.

6. Post-antibody washes and detection with fluorescent dyes
Remove POD-conjugated antibody solution from embryos.
Wash 6 times for 15 minutes in PBST at room temperature.
Prepare TSA/Cy3 or TSA/Cy5 substrate according to instructions of the manufacturer (PerkinElmer): dilute Cy3/Cy5 reagent 1:50 in the amplification buffer supplied by manufacturer.
Incubate at room temperature in the dark for 30 minutes.
Wash 8 times for 15 minutes in PBST.

7. Nuclear staining with SYTOX Green
Preferably perform just prior to microscopy, as the staining will diminish over time. Stain with 100 nM SYTOX Green (Invitrogen-Molecular Probes, S-7020) for 1 h at room temperature.
Wash 6 times for 15 min in PBST.

8. Mounting for microscopy
Mount embryos in Gelvatol containing 100mg/ml DABCO (1,4-diazabicyclo[2.2.2]octane) in a glass-bottom dish (Willco Wells).
Preserve embryos in Gelvatol DABCO at 4°C in the dark. Storing in Gelvatol DABCO preserves nuclear staining up to 3 weeks.

Solutions
PBS 10x stock solution: 75.97g NaCl, 12.46g $NaH_2PO_4 \cdot 2H_2O$, 4.80g $Na_2HPO_4 \cdot H_2O$ in 1 L of milliQ water. Adjust pH to 7.0.
PBST: PBS + 0.1% Tween 20
SSC (20x stock solution: 3M NaCl, 300 mM trisodium citrate)
1 M citric acid
Hybridization buffer: 50% deinonized formamide (Sigma F9037), 5x SSC, 0.1% Tween 20, pH adjusted to 6–6.5 with 1M citric acid, 50 ug/ml heparin (Sigma H3393), 500 ug/ml tRNA (Sigma R7876) (Thisse et al. 2004)
Antibody buffer: PBST containing 2% sheep serum (Sigma S-2263) and 2 mg/ml BSA
Gelvatol containing 100mg/ml DABCO (1,4-diazabicyclo[2.2.2]octane)

Additional remarks to the ZebraFISH protocol

4:**To improve background reduction: replace PBST by TBST for the following gradient**:

Bring embryos to **TBST** environment by successive 10 min wash steps at room temperature over the following gradient:

75% 0.2x SSC/ 25% **TBST**
50% 0.2x SSC/ 50% **TBST**
25% 0.2x SSC/ 75% **TBST**
100% **TBST**

And 5: **Replace PBST by TBST for the Antibody buffer:**
- Dilute DIG POD, Roche 1207733 for anti DIG- Horse Radish Peroxidase detection 1: 1000 in antibody buffer Antibody buffer : **TBST** containing 2% sheep serum (Sigma., cat. nr. S-2263), and 2 mg/ ml BSA.

6: To improve background reduction during post-antibody washes and detection with fluorescent dyes:
- Replace PBST by TBST at room temperature.
- Optional: wash 6 x 1 hr at room temperature,
- Optional: wash overnight at +4° to obtain higher background reduction.

To improve signal of weak or short probes (< 450 bp): use TSA™ Plus Cyanine 3 System
(NEL744, Perkin Elmer).
Dissolve TSA Plus - Cy3 / Cy5 reagent in 150 ul DMSO (molecular grade).
Dilute Cy3 / Cy5 reagent 1: 50 in the amplification buffer supplied by manufacturer.

7. Nuclear staining with SYTOX Green:
Stain with 100 nM SYTOX Green (Invitrogen-Molecular Probes, S-7020) in **TBST**. Add 0.01 % Triton X.
- Stain for at least 1 h at room temperature
- Wash 6 x 15 min in **TBST**.
- Optional: stain overnight at +4°.

Solutions:

1xTBS:
6.05 g Tris (50mM)
8.76 g NaCl (150 mM) in 1 liter of milliQ water. Adjust pH to 7.5.
TBST: TBS + 0.1 % Tween 20

SYTOX Green (Invitrogen-Molecular Probes, S-7020): 100 nm in **TBST;** add 0.01% Triton X-100 (Sigma-Aldrich 234729

Chapter 3

Expression analysis of the genes encoding 14-3-3 gamma and tau proteins using the 3D digital atlas of zebrafish development

M.C.M. Welten[1, 2], A. Sels [1,2], M.I. Van den Berg – Braak[1], G.E.M. Lamers[2], H.P. Spaink[2] and F.J. Verbeek [1]

1. Imagery and Media, Leiden Institute of
Advanced Computer Science,Leiden University, Niels Bohrweg 1, 2333 CA Leiden, The Netherlands.
2. Section Molecular Cell Biology, Institute of Biology, Leiden University, Clusius Laboratory, Wassenaarseweg 64,
2333 AL Leiden, The Netherlands

Paper in preparation

Case study Early zebrafish development

ABSTRACT

The 14-3-3-protein family is a highly conserved family of small dimeric proteins, found in all eukaryotes. Extensive studies in yeast, plants, insects and vertebrates have shown that the 14-3-3 protein family members play a role in numerous cellular signaling processes, e.g. cell division, metabolism, apoptosis, and differentiation. Studies by Muslin et al. (1996) and Morrison et al. (1993) reveal functions for 14-3-3 in Raf phosphorylation and phosphoserine binding. Although the 14-3-3 proteins are ubiquitously expressed in all tissues, they are abundantly expressed in the vertebrate brain. Extensive studies of 14-3-3 expression patterns in mouse and rat brain show altered 14-3-3 protein levels in neurodegenerative diseases like Alzheimer's disease, Creutzfeld-Jakob disease and scrapie. Furthermore, the 14-3-3 proteins have been indicated to play an important role in several other neurological disorders such as epilepsy; and epithelial cancers such as breast and gastric cancer (reviewed by Dougherty and Morison, 2004).
Recently, gene expression patterns of the genes encoding 14-3-3 isoforms in zebrafish were described by Besser et al. (2006). This research paved the way for a more complete, exact localization of zebrafish 14-3-3 gene expression patterns.
In this paper, we present an analysis of zebrafish 14-3-3 γ and τ isoforms, using whole mount fluorescent *in situ* hybridisation (FISH), *in situ* hybridisation (ISH) and TDR-3Dbase reconstruction software. From confocal laser scanning microscopy (CLSM) images as well as from serial sections, 3D reconstructions are obtained to analyze expression patterns of genes encoding 14-3-3, thereby using the 3D atlas of zebrafish development as a reference. The methods presented facilitate a more sensitive and precise spatiotemporal analysis of genes encoding 14-3-3 γ and τ isoforms during zebrafish embryonic development, and yield more gene expression domains at earlier stages than previously observed. Moreover, the methods are less time-consuming than those previously used. In future functional studies, the 3D reconstructions made with TDR-3Dbase reconstruction software allow an analytical approach to the gene expression domains.

Keywords: 14-3-3 proteins, fluorescent *in situ* hybridisation, 3D reconstruction, zebrafish brain development

INTRODUCTION

The 14-3-3 protein family members are a highly conserved family of proteins, present in yeast, plants (Lu et al, 1994), insects (Swanson and Ganguly, 1992) and vertebrates (Koskinen et al. 2004 Watanabe et al. 1993; Wu et al. 2002). The name of the 14-3-3 proteins is derived from their migration position on DEAE cellulose chromatography and starch gel electroporesis (Aitken et al. 1995). In *Xenopus*, 6 isoforms (Lau et al. 2006), in mammals 7 isoforms (Rosner and Hengstschlaeger, 2006) and in zebrafish, 11 isoforms are found. During vertebrate development, 14-3-3 proteins are mainly expressed in neural tissue and brain structures (Koskinen et al. 2004; Wu et al. 2002). Recent studies show that 14-3-3 proteins are involved in cancer and neurological disorders (reviewed by Dougherty and Morrison, 2004).

Both sequence and structure of the 14-3-3 proteins are remarkably conserved in all eukaryotes. Human 14-3-3 γ protein shows 95%, similarity with zebrafish 14-3-3 γ protein; the sequence of the human 14-3-3 τ gene shows 76 % similarity with zebrafish 14-3-3 τ gene). The crystal structure of the 14-3-3 proteins shows that they are dimeric proteins. They are predominantly helical and form a negatively charged groove. The interior of this groove consists of almost invariant amino acids in all 14-3-3 family members (Aitken, 1996) and forms a phosphoprotein-binding surface that interacts with a large amount of cellular proteins (Dougherty and Morrison, 2004). 14-3-3 binding of a target protein may (i) protect it from dephosphorylation or proteolysis, (ii) modulate its activity, (iii) alter its ability to interact with other partners, (iv) modify its cytoplasmic/nuclear partition, or (v) serve as an adapter or scaffold to bridge proteins (Rosner and Hengstschlaeger, 2006). The 14-3-3 protein family is involved in numerous cellular pathways, such as metabolism, cell cycle, differentiation, signalling and apoptosis (Dougherty and Morrison, 2004). Therefore, it is not surprising that 14-3-3 proteins are involved in pathogenesis and progression of neurological disorders and cancer, where altered regulation of 14-3-3 proteins may influence the activity of binding partners. Also, loss of anti-apoptotic functions and tumor suppressor functions of 14-3-3 may lead to progression of certain cancers (reviewed by Dougherty and Morrison, 2004).

14-3-3 γ isoform

In vertebrates, 14-3-3 γ isoforms are expressed in the developing and adult brain. During *Xenopus* embryonic development, the 14-3-3 γ isoform shows variable levels of expression in cranium and central nervous system. Extensive studies with 14-3-3 γ specific morpholino injections in 2-cell stage *Xenopus* embryos result in reduction and even inhibition of eye development (Lau et al. 2006). The mechanism of this inhibition of eye development is still unknown. In rat embryos, expression of the gamma isoform is found throughout the brain and spinal cord (Watanabe et al, 1994). In zebrafish two highly similar isoforms of the 14-3-3 γ isoform are found (called γ1 and γ2). During embryonic development of zebrafish, expression of the gene encoding the 14-3-3 γ1 isoform was found in telencephalon, diencephalon, the tegmentum of the mesencephalon and the cranial ganglia (Besser et al. 2006). However, it is likely that the probes used in the previous study are not able distinguish between the two representatives of the 14-3-3 γ gene.

14-3-3 τ isoform

Recent studies show that 14-3-3 τ isoform is involved in vertebrate brain development, and that it remains expressed during adulthood. In *Xenopus* embryos, 14-3-3 τ isoforms were abundantly expressed in trunk, skeletal myotomes, and tail fin regions. Injections with antisense τ specific morpholinos in 2 cell stage embryos, led to severe gastrulation defects (Lau et al. 2006).

In mouse and rat embryos, 14-3-3 τ protein expression is found throughout the brain. At postnatal stages however, it is mostly found in the white matter and in the hippocampus (Baxter et al. 2002, Watanabe et al. 1994). In zebrafish embryos, two highly similar τ isforms (called τ1 and τ2) are found. The 14-3-3 τ1 isoform shows diffuse expression in substructures of the eye and several brain structures (Besser et al. 2006). However, for both the zebrafish τ1 and τ2 isoforms it is likely that the probes used in previous experiments could not distinguish between the two representatives of these genes.

14-3-3 and neurological disorders

Analysis of 14-3-3 isoforms in the brain of rat embryos showed that the isoforms are involved in neuronal proliferation, migration and differentiation (Watanabe et al.1993, 1994). Experiments in mouse and rat reveal altered 14-3-3 protein levels in the brain, in epilepsy (Schindler et al. 2006) and scrapie (Baxter et al. 2002). In humans suffering from Creutzfeld –Jakob disease, Alzheimer's disease and multiple sclerosis, 14-3-3 proteins are released into the cerebrospinal fluid as a consequence of extensive destruction of the brain, e.g. destruction of neurons. The presence of 14-3-3 γ proteins in cerebrospinal fluid is used as a diagnostic marker for neurodegenerative disorders like Alzheimer's disease (Fountoulakis et al. 1999; Van Everbroek et al. 2005), Creutzfeld Jakob disease (Shiga et al. 2006) and multiple sclerosis (Bartosik and Archelos 2004).

The aim of our study is to accurately localize gene expression of 14-3-3 isoforms in the developing zebrafish brain as well as in other structures.

Neurogenesis

In adult mammals, production of new neurons – i.e. adult neurogenesis – is found in two restricted areas in the central nervous system: in a particular region of the hippocampus and in the lateral ventricular zones, from which newly formed neurons migrate towards the olfactory bulb (Fig.1). In teleost fish however, numerous brain regions are able to form new neurons, also during adulthood (Zupanc et al, 2005). In zebrafish, neuronal proliferation zones are found in almost all brain divisions (Fig.1), including the olfactory bulb and the dorsal telencephalon - where a region was found, presumably homologous to the hippocampus in mammals (Zupanc et al. 2005). This might implicate a different role for 14-3-3 proteins during embryonic and adult neurogenesis. In addition, identification of cellular mechanisms that enable formation of new neurons in almost all regions of the adult fish brain might provide a clue for therapeutic approaches for the treatment of neurodegenerative diseases in the future.

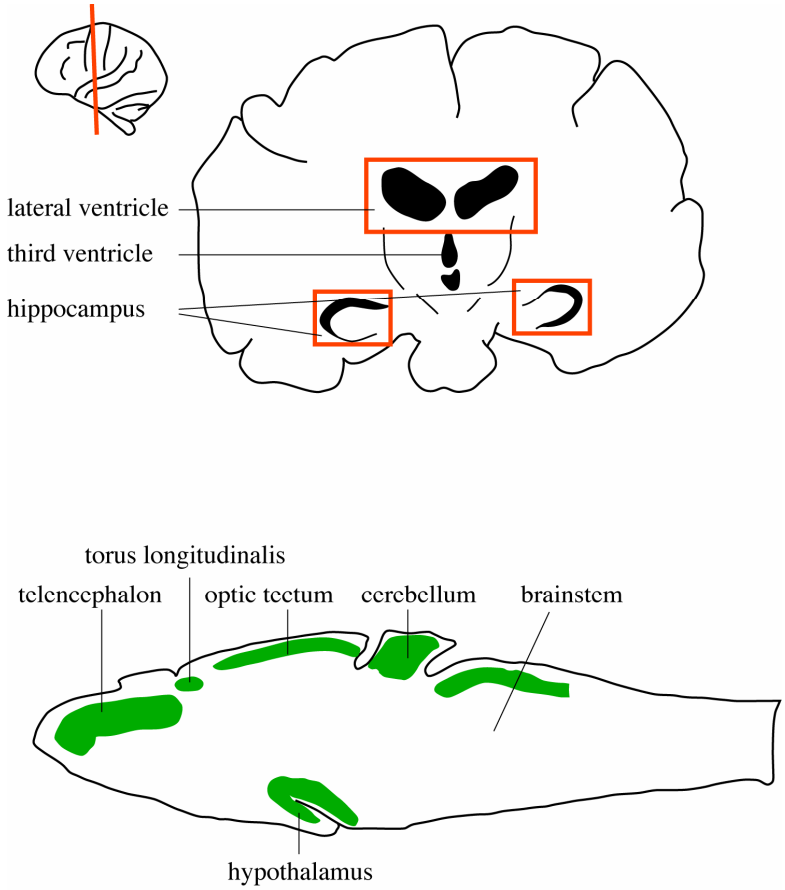

Fig.1, upper panel: author's impression of zones of adult neurogenesis in the human brain, boxed areas.
Lower panel: author's impression of the zebrafish brain. Zones of adult neurogenesis are marked in green (after Zupanc et al. 2005; Mueller and Wulliman, 2005)

3D atlas of zebrafish development
In our research group, we have developed a 3D atlas of zebrafish development. In addition, a zebrafish gene expression database is under construction (Verbeek et al. 2000; http://bio-imaging.liacs.nl). Results of experiments can be stored in this database**.**
Gene expression data are produced using the ZebraFISH protocol (Welten et al. 2006) to facilitate 3D imaging with confocal laser scanning microscopy (CLSM). These 3D images can be processed with TDR-3D software to make 3D reconstructions, thus providing a schematic modelling of the structures and patterns observed in the CLSM images. The gene expression patterns can be mapped on anatomical structures, using the 3D atlas of zebrafish development as a reference. In this way, more insight in the spatial relationships of gene expression domains is obtained (Verbeek et al. 2002, Verbeek et al. 2004).
In recent years, the zebrafish has proven to be an excellent model system to study human disorders, amongst these, cancer and neurological diseases (Stern and Zon, 2003). Gene expression patterns for the zebrafish 14-3-3 isoforms were described in generic context. (Besser et al.2006). However, gene expression patterns in zebrafish were not yet exactly localized. Given the involvement of 14-3-3 proteins in development and human

disorders, it is important to accurately map the gene expression patterns of 14-3-3 isoforms in zebrafish brain development. So as to pave the way for further functional analyses of the 14-3-3 isoforms and their involvement in diseases.
In this study, we present a three-dimensional analysis of gene expression for genes encoding the 14-3-3γ and τ isoforms in the zebrafish embryo using fluorescent *in situ* hybridisation (zebraFISH) (Welten et al. 2006) during subsequent stages of development. *In situ* hybridisation (ISH) (Thisse et al.2004) is used in parallel as a control for the procedure. In addition, ISH stained embryos are processed for serial sectioning. 3D images from FISH stained embryos are obtained by CLSM and these images are used to produce 3D reconstructions with TDR-3Dbase software (Verbeek et al. 1995). Moreover, 3D models are obtained in the same manner from serial sections. The techniques presented in this study provide an accurate spatiotemporal characterization of gene expression patterns encoding the 14-3-3 proteins in the developing zebrafish. Furthermore, the 3D techniques allow more analytical approach in future functional studies.

MATERIALS AND METHODS

Obtaining gene expression data
Zebrafish were maintained under standard conditions (http://zfin.org) in our facilities.
Zebrafish embryos were harvested and staged to 18, 24, 36 and 48 hours post fertilization (hpf) as described by Kimmel et al. (1995) and processed for *in situ* hybridization (zebraFISH; Welten et al, 2006) and *in situ* hybridization (ISH; Thisse et al. 2004).
Cloning and antisense RNA probe synthesis of the genes encoding 14-3-3 γ1 and τ1 used in this study have been described by Besser et al (2006). Our results are based on these γ1 and τ1 probes. From now on, we will refer to these probes as 14-3-3 γ and τ. Supplementary information concerning genes encoding zebrafish 14-3-3 γ1 and τ1 proteins, ZFIN gene name and genomic location are described by Besser et al (2006).

Microscopy and imaging
Confocal images were acquired according to a standard protocol (Welten et al., 2006) using a Leica TCS/SP DM IRBE confocal laser-scanning microscope equipped with an Ar/Kr laser. Excitation of the used fluorophores (Cy3 and SYTOXGreen) resulted in emission in a red and green spectrum; detected with separate laser channels (Kr and Ar, respectively). All images were obtained with a 10x plan apo lens (NA 0.24). For every image, photo multiplying tube (PMT) gain and offset were optimised to reduce the signal to noise ratio. Images were saved as two-channel multiple TIFF files.
Images of ISH-stained embryos were acquired using a Leica MZFL-III12 stereomicroscope equipped with a Leica DC 500 digital camera.

Tissue sectioning
After ISH, whole mount embryos were overstained for 3 days in NBT/BCIP staining solution (Roche). Overstained embryos were embedded in Technovit 7100 (Heraeus Kulzer Gmbh, Wehrheim, Germany). Sagittal sections of 4 μm were cut on a Leica Ultracut E 388542 microtome. From the serial sections, 3D reconstructions were made as previously described (Verbeek, 2000).

3D reconstructions

From the 3D images produced with CLSM, 3D reconstructions were made using TDR-3Dbase with a Wacom LCD graphical tablet. To annotate gene expression patterns in relation to the anatomical structures, the 3D reconstructions were compared with corresponding 3D embryos from the 3D atlas of zebrafish development (http://bio-imaging.liacs.nl.html).

As a reference for the annotation of brain structures, otx2 and pax2.1 and neurogenin-1 were used as molecular markers for diencephalon, mesencephalon, optic stalk and cranial ganglia in zebrafish (Welten et al. 2006). Additional anatomical and molecular data for were extracted from literature (cranial ganglia: Holzschuh et al. 2005, Wilson et al. 2007; anatomy: Mueller and Wulliman, 2005) and www.zfin.org.

RESULTS

14-3-3 γ and τ expression patterns

In table 1 and 2, a summary of expression patterns for genes encoding 14-3-3 γ and τ proteins is given. Gene expression domains are compared to those described by Besser et al (2006).

However, the application of ZebraFISH yielded more gene expression patterns, and at earlier stages than those found in previous studies. These results were consistent after repeating the experiments, and for almost all hybridized embryos.

Likewise in the study of Besser et al., it is expected that the used probes are not able to distinguish the difference between the two different representatives of the isoforms. From the 3D reconstructions no conclusive evidence could be produced.

14-3-3γ

Our FISH detection method yielded more expression pattern domains for genes encoding 14-3-3 γ than described in previous experiments. Supplementary to the patterns described by Besser et al (2006), application of the zebraFISH protocol detected more gene expression domains and at earlier stages. These gene expression domains were consistent with those found in literature for other model systems (*Xenopus:* Lau et al., 2006; rat: Watanabe et al. 1993 and 1994). Our FISH experiments yielded clear expression signals for the γ isoform in the diencephalon, the optic stalk, the optic cup, the lens and the future heart region in 18 hpf (n=17, 88%) and 24 hpf embryos (n=12, 100%), as visible from Fig. 2A-D.

Moreover, the FISH detection revealed weak expression for 14-3-3 γ in the optic tectum of the mesencephalon at 24 hpf (12/12, 100%) (Fig.2A, B, G and H).

At 48 hpf, a strong gene expression signal was localized in the heart region (n=5, 80%) (Fig.2C and D). These findings were constant over multiple FISH experiments. ISH experiments were carried out in parallel. Our FISH results were confirmed through serial sectioning of embryos after overstaining the ISH samples for 3-4 days (Fig.2 G and H). In previous studies, ISH detection yielded only weak expression signal in these structures at 24 hpf (Besser et al, 2006), and there was no conclusive evidence if this was background or weak signal. In table 1, gene expression patterns for 14-3-3 γ are

summarized and compared with those found by Besser et al. Samples for imaging were taken at random from a staged batch.
3D modelling with TDR-3Dbase further established expression for 14-3-3 γ in or adjacent to the otic vesicle, most likely in the future cranial ganlion VIII (Holzschuh et al. 2005, Wilson et al. 2007); cranial ganglion V (trigeminal ganglion), and the spinal cord neurons at 20 hpf (data not shown) and 24 hpf (Fig.2 B and D). 3D reconstruction also confirmed 14-3-3 γ expression in the presumptive heart, the diencephalon and the optic stalk (Fig.2B). From 36 to 48 hpf, the total number of brain structures showing 14-3-3 γ expression decreased. At 48 hpf, distinct expression patterns were only found in the cranial ganglia and the heart (Fig.2C and D).

Fig.2 A: FISH result for the gene encoding 14-3-3γ in a 24 hpf embryo. The picture is a confocal slice.

C: 14-3-3 **γ** FISH result in a 48 hpf embryo; a so-called z-projection of the confocal image.
A and C: Gene expression is in red, i.e. the red channel of the CLSM image. The green depicts a background staining of the cell nuclei with SYTOX Green.
2 B,D: 3D reconstruction of the embryos shown in 2A and 2B respectively. Gene expression for 14-3-3 **γ** is depicted in white. Both FISH images and 3D reconstruction clearly reveal gene expression patterns in otic vesicle (salmon), optic stalk (orange), cranial ganglia (light yellow), ganglion V (light orange), spinal cord neurons and heart primordium (red) at 24 and 48 hpf.
2 E, F: ISH results for 14-3-3 **γ** at 24 and 48 hpf. Dorsal view; anterior is to the left.
G: 14-3-3 γ ISH result at 24 hpf. Tissue section after overstaining, revealing gene expression in eye, tectum of the mesencephalon, cranial ganglia and around the otic vesicle.
H: 3D reconstruction of the embryo shown in 5A. In 5B, gene expression is displayed in relation to anatomical structures. 14-3-3 γ gene expression domains are depicted in white.
In all images, anterior is to the left, dorsal is to the top.
The findings after overstaining, tissue sectioning and 3D reconstruction of ISH results confirm our findings with FISH.
Abbreviations: ccv, common cardinal vein; cer, cerebellum; c g, cranial ganglia; c g V, fifth cranial ganglion; di, diencephalon; h: heart primordium; o v, otic vesicle; sp n, spinal cord neurons; tec, tectum of the mesencephalon; rh: rhombencephalon.
Color legend: gene expression: white; gill primordia: light green; cerebellum: blue; common cardinal vein: clear blue; diencephalon: orange; eye: salmon; lens: brown; heart primordium: red; otic vesicle: dark green; rhombencephalon: lilac; tectum (mesencephalon): purple; telencehpalon: dark blue; 4^{th} ventricle: clear blue.

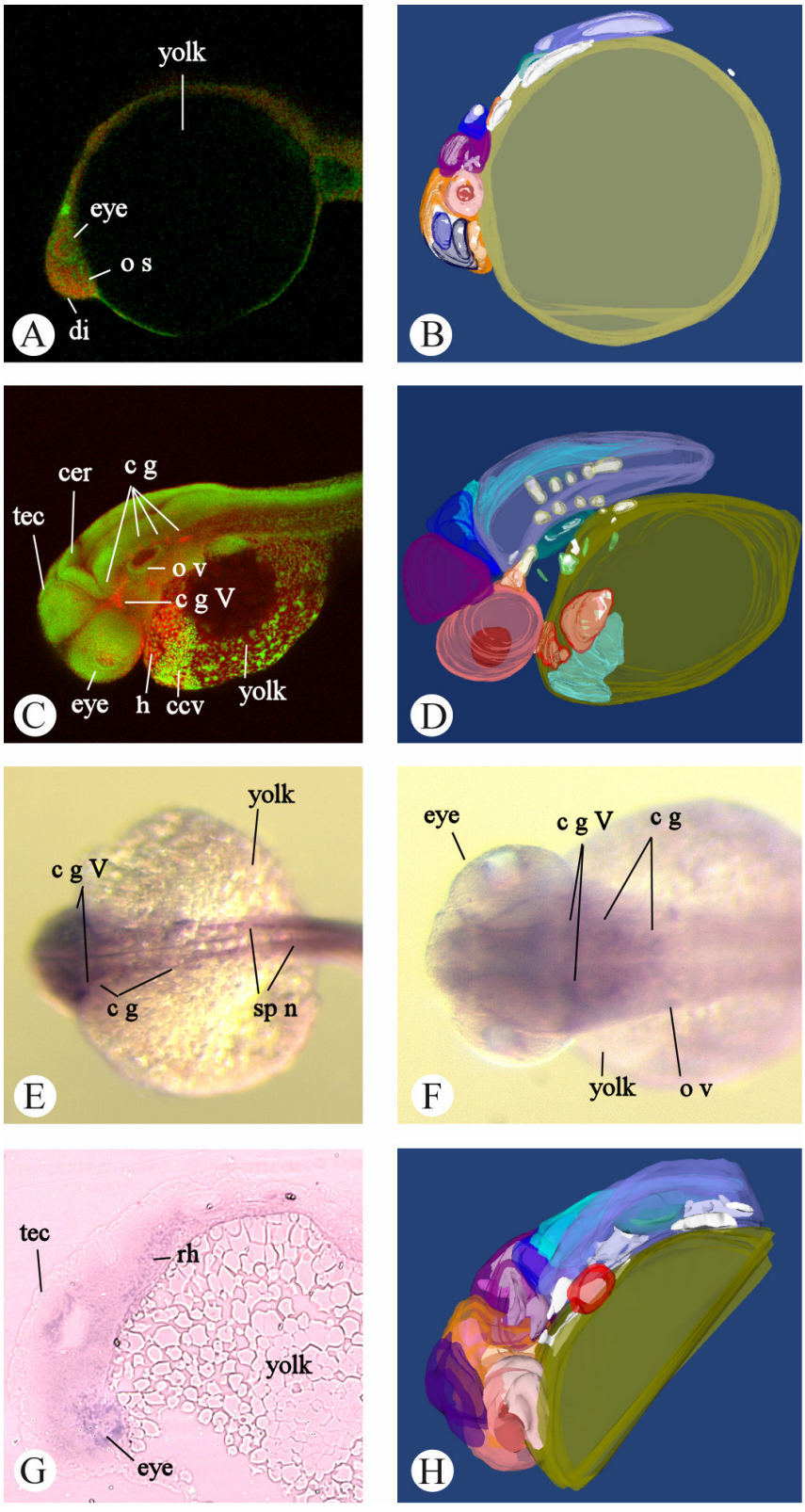
yolk
eye
o s
di
A
B
cer
c g
tec
o v
c g V
eye
h
ccv
yolk
C
D
yolk
c g V
c g
sp n
E
eye
c g V
c g
yolk
o v
F
tec
rh
yolk
eye
G
H

Fig. 2

14-3-3 τ

Our results show diffuse expression all over the brain structures and a prominent expression pattern in the in the optic cup and substructures of the eye; see Table 2 and Figure 3 A and B.

3D modelling for the τ isoform reveals a distinct expression pattern in cranial ganglion V at 24 hpf (Fig. 5E, F). Furthermore, the τ isoform displayed a more diffuse expression pattern throughout the brain structures from 20 hpf up to 48 hpf.
Two marker genes of brain development were used to verify and map our results: the *otx2* gene showed expression in diencephalon and mesencephalon (Mercier et al.1995), and *pax2.1* showed expression domains in the midbrain-hindbrain boundary, the optic stalk and the otic vesicle (Lun and Brand, 1998) (Fig. 4 A and B).
In figure 6, gene expression for 14-3-3 *3 γ* and *τ* in brain structures is compared over time.

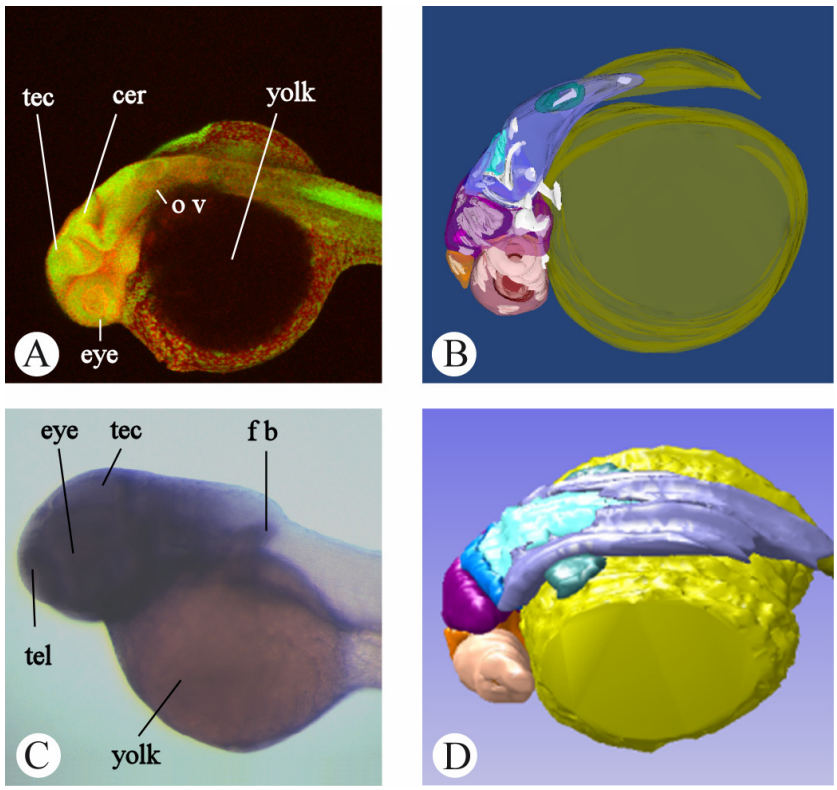

Fig. 3 A: 14-3-3 τ FISH result in a 24 hpf embryo; z-projection of a confocal image.
B: 3D reconstruction of the embryo shown in 3A. 14-3-3 τ gene expression (white) is visible in most brain structures.
C: Gene expression for 14-3-3 τ at 36 hpf, ISH detection.
D: Reference image from the 3D atlas, in the same orientation as the embryo in 3A and B.
Abbreviations: cer, cerebellum; f b: fin bud; o v, otic vesicle; tec, tectum of the mesencephalon; tel: telencephalon. In all images, anterior is to the left, dorsal is to the top.

Color legend: gene expression: white; cerebellum: blue; diencephalon: orange; eye: salmon; lens: brown; otic vesicle: dark green; rhombencephalon: lilac; tectum (mesencephalon): purple; 4th ventricle: clear blue.

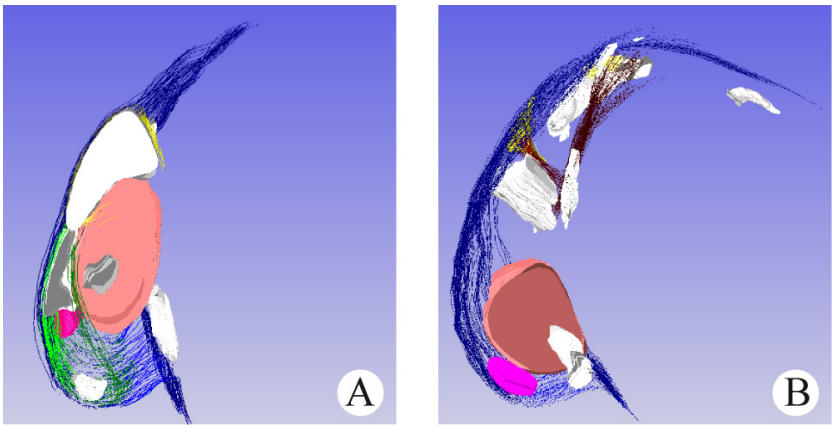

Fig.4 A, B: 3D reconstructions of *pax2* (4A) and *otx2* (4B) expression domains at 24 hpf, used as a reference for the brain structures.
In all images, anterior is to the left, dorsal is to the top. Color legend: gene expression: white; optic cup: salmon; embryo outline: dark blue.

Table 1. Summary of gene expression patterns found with ISH (Besser et al, 2006) and FISH (this study) for the 14-3-3 γ1 isoform

Probe	ISH 18 hpf (Besser et al, 2006)	FISH 20 hpf n=17
γ	diencephalon spinal cord neurons	diencephalon optic stalk mesencephalon tectum tegmentum cranial ganglia cranial ganglion V spinal cord neurons otic vesicle/ cranial ganglion VIII? eye retina and lens heart primordium
	ISH 24 hpf (Besser et al, 2006)	**FISH 24 hpf n=12**
	telencephalon diencephalon mesencephalon tegmentum rhombencephalon cranial ganglia spinal cord neurons otic vesicle	telencephalon diencephalon optic stalk mesencephalon tectum tegmentum rhombencephalon cranial ganglia cranial ganglion V spinal cord neurons otic vesicle/cranial ganglion VIII? eye retina and lens heart primordium
	ISH 36 hpf	**FISH 36 hpf n=2**
	no data available	diencephalon rhombencephalon cranial ganglia cranial ganglion V otic vesicle/cranial ganglion VIII? eye retina heart primordium
	ISH 48 hpf (Besser et al, 2006)	**FISH 48 hpf n=11**
	diencephalon hypothalamus mesencenphalon tegmentum rhombencephalon cranial ganglionV otic vesicle	diencephalon rhombencephalon cranial ganglia cranial ganglion V otic vesicle/cranial ganglion VIII? heart

Table 2. Summary of gene expression patterns revealed by ISH (Besser et al. 2006) and FISH (this study).

τ1	ISH 18 hpf (Besser et al, 2006)	FISH 20 hpf n=11
	optic cup	telencephalon diencephalon mesencephalon tectum rhombencephalon cranial ganglion V spinal cord neurons eye lens retina boundary
	ISH 24 hpf (Besser et al, 2006)	FISH 24 hpf n=42
	telencephalon mesencephalon tectum rhombencephalon ventricular zone spinal cord neurons eye lens retina boundary	telencephalon diencephalon mesencephalon tectum rhombencephalon fourth ventricle zone cranial ganglion V spinal cord neurons eye lens retina boundary
	ISH 36 hpf (Besser et al, 2006)	FISH 36 hpf n=12
	no data available	telencephalon diencephalon mesencephalon tectum rhombencephalon cranial ganglion V spinal cord neurons eye retina boundary
	ISH 48 hpf (Besser et al, 2006)	FISH 48 hpf n=53
	diencephalon rhombencephalon cranial ganglion V otic vesicle eye retina fin buds /liver	telencephalon diencephalon mesencephalon tectum rhombencenphalon cranial ganglion V eye retina boundary

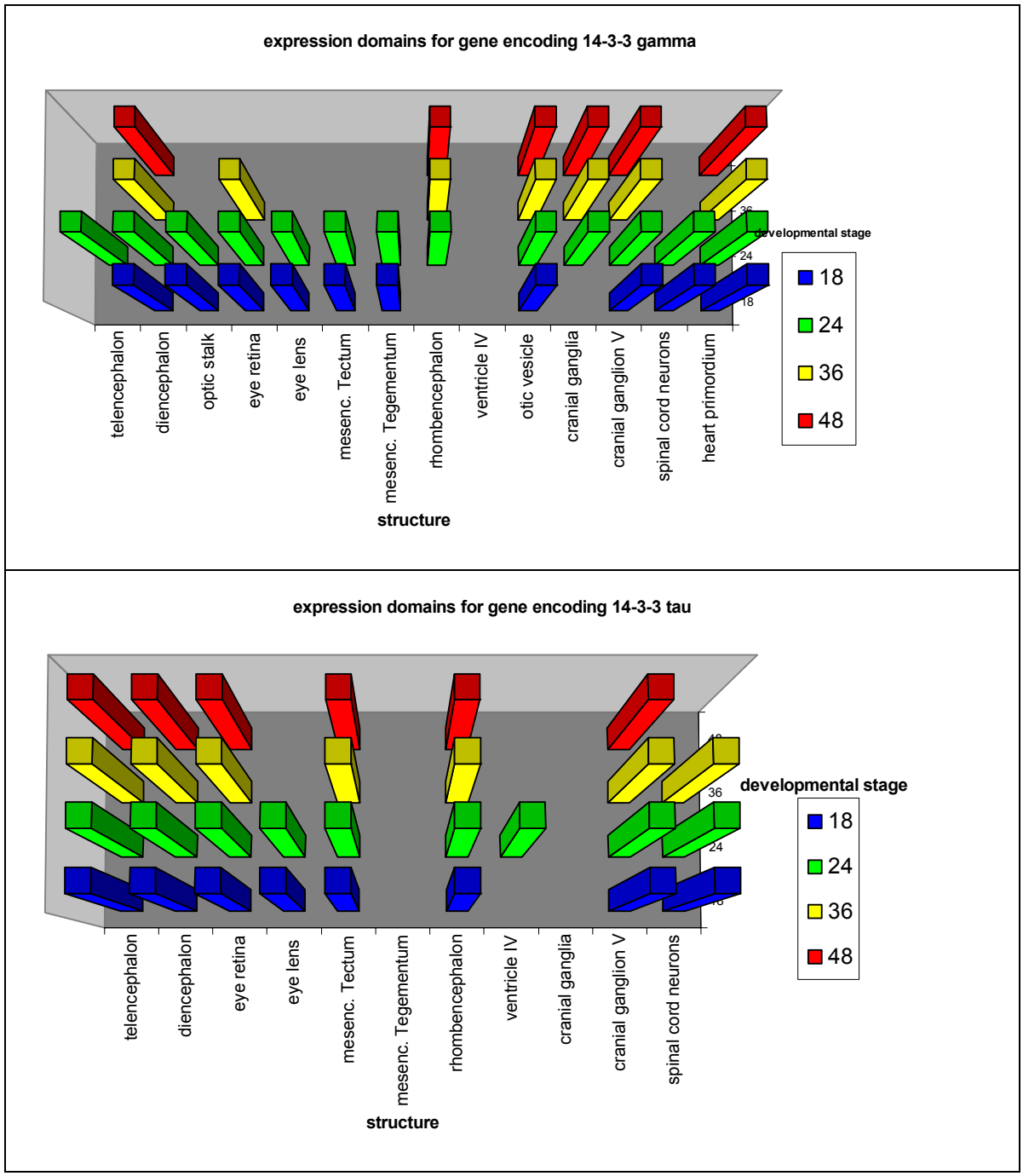

Fig. 6. Diagrams showing the total number of gene expression domains for 14-3-3 γ (upper panel) and τ (lower panel) in developmental time series from 18 up to 48 hpf. For the γ isoform, the number of expression domains decreases over time, where 14-3-3 τ remains more evenly expressed over brain structures at the same stages.

DISCUSSION

The gene expression patterns revealed by zebraFISH confirm findings from a previous study (Besser et al. 2006) but in addition, due to higher sensitivity of the method, much more gene expression domains were found; especially at earlier stages of development. At 24 and 48 hpf, a strong signal for the gene encoding 14-3-3 γ was observed in the dorsal region of the diencephalon and in the retina and lens. The Tyramide Signal Amplification (TSA) method used in our study is an amplification method, based upon the patented catalyzed reporter deposition (CARD) technology using derivatized tyramide. In the presence of hydrogen peroxide, immobilized Horse Radish Peroxidase converts the labeled tyramide substrate into a short-lived, extremely reactive intermediate that rapidly reacts with and covalently binds to electron rich regions of adjacent proteins (Jowett, 2001; Zaidi et al. 2000). Therefore, it is more sensitive than the Alkaline Phosphatase (AP) detection used in the in situ hybridisation. So, regions that show only a weak gene expression for 14-3-3 γ in the AP detection might yield a stronger signal with TSA detection.

In our study, gene expression patterns for 14-3-3 γ were found in substructures of the eye at 24 hpf. Expression patterns for the γ isoform in the eye are described for lower vertebrates such as the rainbow trout (Koskinen et al. 2004) and *Xenopus* (Lau et al. 2006). *Xenopus* embryos injected with 14-3-3 γ specific morpholino show inhibition of eye development (Lau et al. 2006). Though little is known about the role of 14-3-3 isoforms in eye development, recent studies show that 14-3-3 γ and τ are expressed in the adult chick retina (Pozdeyev et al.2006) and rat retinal ganglion cells, and play a role in maintaining these cells (Ivanov et al. 2006).

In mouse and rat embryos (embryonic day 7.5 and 13 respectively), expression of the 14-3-3 γ protein is found in the ventral horn of the spinal cord, in the dorsal root ganglia and in the 5th ganglion (Baxter et al.2002, Watanabe et al.1993, 1994); our data for the gene encoding 14-3-3 γ in zebrafish show expression in by and large the same structures. 14-3-3 expression was described in the neural crest of the rainbow trout (Koskinen et al. 2004). This also corresponds with our findings, since the neural crest has a broad developmental potential and gives rise to many cell types such as glial neurons (Wolpert, 2002).

Our FISH results show hybridization in the future heart region at 20-24 hpf embryos, and in the heart at 48 hpf. After overstaining with the AP detection method, serial sections from ISH stained embryos displayed weak but distinct gene expression patterns in the same region, confirming our FISH results. Interestingly, for rat and humans, 14-3-3 γ has been indicated to play a role in heart disorders (He et al. 2006; Horie et al. 1999).

In our experiments, the gene encoding 14-3-3 τ shows diffuse expression throughout the brain from 20 up to 48 hpf. Prominent expression is found in the lens, the outer boundary of the retina and the spinal cord neurons from 20 somites up to 36 hpf in 92 % of the hybridized embryos at these stages (60/65, n = 65). Expression patterns were also found in telencephalon, diencephalon and mesencephalon (in the optic tectum) from 20 somites up to 48 hpf, in 95% of all hybridized embryos (106/111, n= 111). Besser et al. (2006) also describe gene expression for 14-3-3 τ expression in the pectoral fins the liver at 48 hpf, though this expression is very weak and might be an artifact. We found no FISH and ISH signal for this structure. No distinct FISH and ISH signal could be found in the liver.

In *Xenopus* embryos, the τ isoform was expressed over the body surface, and later on in

the posterior trunk, tail fin region and in the skeletal myotomes (Lau et al. 2006). The latter might be a result of a difference in projection of the results. The pattern shown in Fig. 3 (Lau et al. 2006) is a 2D image. 3D reconstruction might reveal that the gene expression pattern found in the skeletal myotomes, is also located in the spinal cord neurons, as found in other vertebrates (Baxter et al.2002; Besser et al. 2006). The expression pattern of genes encoding 14-3-3 τ in zebrafish is consistent with gene and protein expression patterns found in mouse and rat embryos.

In the different model species, gene and protein expression patterns for 14-3-3 γ and τ are described either from the onset of neurulation up to subdivision of the prosencephalon into telencephalon and diencephalon (Baxter et al.2002, Watanabe et al. 1993 and 1994), or at later developmental stages (Besser et al.2006, Lau et al.2006), after completion of the five brain subdivisions.

Though our analysis portrays that the expression patterns for genes encoding zebrafish 14-3-3 γ and τ are found in the same structures as their orthologues described in the higher vertebrates, it might be interesting to compare gene expression at even earlier stages of zebrafish brain development. From extensive studies it is also evident that the 14-3-3 isoforms remain expressed in a wide variety of tissues and organs during adulthood (Bartosik and Archelos 2004, He et al. 2006, Horie et al. 1999, Kawamoto et al. 2006, Shiga et al. 2006).

In summary, the ZebraFISH and 3D reconstruction methods used in our study enabled a fast and precise localization of expression patterns of genes encoding 14-3-3 γ and τ in the zebrafish. Overstaining and tissue sectioning of ISH samples confirmed our FISH results. The gene expression patterns found in our study were consistent with those described for other model species (Koskinen et al. 2004; Lau et al. 2006; Watanabe et al. 1993 and 1994) and those described by Besser et al (2006). Our study also demonstrates that 3D analysis based on the 3D atlas of zebrafish development as a reference, provides an accurate localization of the genes encoding 14-3-3 γ and τ isoforms.

Conclusions and future work

In this study, we present a 3D analysis of the genes incoding 14-3-3 γ and τ in several structures of the zebrafish brain and the developing central nervous system, in time series of early embryonic development. The 3D reconstructions, composed from CLSM images as well as from serial sections, provide detailed information on the spatial relations of the gene expression patterns during zebrafish brain development. Moreover, 3D reconstruction of 14-3-3 isoforms allows an analytical approach for functional analysis in the future. The spatial and temporal (i.e., during subsequent stages of embryonic development) analysis of 14-3-3 gene expression data and the techniques presented in this study, further facilitate studies of 14-3-3 family members in zebrafish development and in relation to in human disorders. For a more accurate localization of the genes encoding 14-3-3 γ and τ, colocalization experiments can be carried out with markers for cranial and lateral line ganglia. Also, timing of zebrafish 14-3-3 gene expression can be compared with other model species, using data acquisition methods.

ACKNOWLEDGEMENTS

This project is partially supported by the Netherlands Research Council through the BioMolecular Informatics programme of Chemical Sciences (grant number #050.50.213) and by a BSIK project (Cyttron) from the Dutch Ministry of Economic Affairs (H.P.S). The authors would like to thank Dr. Jeroen Bakkers, who kindly donated *otx2* and *pax2* probes and Jeroen Korving and Merijn de Bakker for their helpful advice. The authors also would like to thank M. Brittijn for his help with the figures.

Chapter 4

3D Reconstruction of gene expression patterns in the developing innate immune system of the zebrafish

M.C.M. Welten [1,2], L.F.M. Bertens[1,2(a)], W.M.E.M. Spoor[1,2(b)], A.H.Meijer[2] and F.J. Verbeek[1]

1 Imagery and Media, Leiden Institute of Advanced Computer Science, Leiden University, Niels Bohrweg 1, 2333 CA Leiden, the Netherlands
2 Institute of Biology, Leiden University, Clusius Laboratory, Wassenaarseweg 64, 2333 AL Leiden, The Netherlands

(a and b equally contributed)

Paper in preparation

Case study Early zebrafish development

ABSTRACT

The zebrafish develops both an innate and an adaptive immune system, closely resembling the innate and adaptive immune system of higher vertebrates (mammals and birds). The innate immune system of zebrafish develops already during de first day of embryogenesis. The zebrafish macrophages and granulocytes are essential cell types involved in the innate immune system and show striking similarities with their counterparts in mammals. On the molecular level, marker genes expressed by zebrafish macrophages and granulocytes are found to be homologous to those in mammals. In this study we make a contribution to the existing knowledge by presenting a three dimensional characterization of marker genes of the zebrafish macrophage and granulocyte lineage. In our study we focus on two maker genes, i.e. *l-plastin*, a general marker of leukocytes; and *mpx*, a specific marker of neutrophil granulocytes. The aim of this study was to analyze complete time series. Analysis was accomplished by investigating the number of cells during normal development. We report data from a pilot study that provides a good basis for further experiments. Gene expression patterns were studied in time series of zebrafish embryos, using fluorescent *in situ* hybridisation (FISH), *in situ* hybridization (ISH) and confocal laser scanning microscopy (CLSM). 3D reconstructions of the gene expression patterns were made using 3D reconstruction software. In this manner, distribution of *l-plastin* and *mpx* expressing cells could be presented in a three dimensional matrix. Furthermore, the techniques presented allow an analytical approach to distribution and migratory behavior of single cells.

Keywords: macrophages, neutrophil granulocytes, zebrafish development, fluorescent *in situ* hybridization, time series, 3D reconstruction.

INTRODUCTION

In recent years the zebrafish, *Danio rerio,* has become an increasingly important model system for several reasons: small size, high fecundity and short generation time (Stern and Zon, 2003). The embryos are completely transparent which makes it possible to study developmental processes in vivo, most of which are completed within a few days. Invertebrates like *Drosophila* and *C. elegans* are thoroughly studied in relation to the immune system. These species however, restrict to development of an innate immune system. The zebrafish develops both an innate and an adaptive immune system (Phelps and Neely, 2005), which closely resemble that of mammals. In the phylogenetic sense, the innate immune system is older than the adaptive immune system. The latter evolved after the divergence of invertebrates and vertebrates. The innate immune system provides a broad protection, without previous exposure to pathogens. The innate immune system responds instantaneously to a pathogen whereas the adaptive immune response needs days or weeks to further develop (Kimbrell and Beutler, 2001). Vertebrates exhibit two distinct cell lineages that are involved in the immune system: the myeloid and the lymphoid lineage. Cells from the myeloid cell line, i.e. granulocytes and macrophages, are very important in the innate immune system (Kimbrell and Beutler, 2001). Different types of granulocytes are able to phagocytose foreign material and destruct parasites. Macrophages are able to engulf invading micro-organisms and cellular debris, and also play a role in adaptive immunity (Kimbrell and Beutler, 2001).
Homologues of white blood cell types and marker genes involved in the haematopoiesis and the immune system in higher vertebrates have also been identified in zebrafish (Crowhurst et al. 2002, De Jong and Zon 2005, Herbomel et al.1999, Lieschke et al. 2001). This is one of the reasons that the zebrafish can be employed as a model to study the interaction of the innate as well as the adaptive immnune system with pathogens; and experimental findings can be extrapolated to human.

Hematopoiesis and white blood cells

Haematopoiesis is the process of formation of all blood cell types. In amniotes (birds and mammals), early haematopoiesis starts in an extra-embryonic region: the yolk sac **(**Bennett et al. 2001; Godin and Cumano, 2005)**.** In later embryonic development, haematopoiesis occurs in the aorta-gonad-mesonephros (AGM) region and the fetal liver. An exception can be found in marsupials and monotremes where embryonic haematopoiesis occurs in an intraembryonic region, in the liver (Old and Deane, 2003). In both birds and mammals, adult haematopoiesis takes place in the bone marrow and the thymus (Bennett et al. 2001; Godin and Cumano, 2005). In the amphibian *Xenopus*, early haematopoiesis starts in the intraembryonic antero–ventral region of the embryo. At larval stages, intraembryonic heamatopoiesis occurs in the dorsolateral plate and the liver; extaembryonic haematopoiesis takes place in the ventral blood island (Chen and Turpen 1995; Robb, 1997; Smith et al 2002). In teleosts such as zebrafish, haematopoiesis starts initially in two distant anatomical areas, both being intraembryonic (Herbomel et al. 1999; Rombout et al. 2005). The embryonic zebrafish erythrocytes arise from posterior lateral plate mesoderm forming the intermediate cell mass (ICM) of the trunk, whereas the myeloid cells form in the anterior lateral plate mesoderm beneath the embryonic heart (Herbomel et al. 1999, Willett et al. 1999). Subsequently, like in

mammals, a wave of haematopoiesis starts in the AGM (Murayama et al. 2006, Willett et al. 1999). Recently, a new, transitional haematopoietic location was revealed during larval stages: the caudal haematopoietic tissue (CHT) (Murayama et al.2006). Around 3-4 days of development, cells from the CHT start seeding the kidney and thymus, which remain haematopoietic locations in the adult zebrafish (Murayama et al. 2006, Willett et al. 1999).
In mammals, a common pluripotent haematopoietic stem cell (HSC) gives rise to three progenitors: a lymphoid, a myeloid and an erythroid progenitor. The myeloid progenitor gives rise to four myeloid cell lineages: 1) macrophages and three types of granulocytes i.e. 2) neutrophils, 3) eosinophils and 4) basophils.
In zebrafish, the myeloid progenitor develops into macrophages and two types of granulocytes: the neutrophils (or heterophils) - closely resembling the mammalian neutrophils - and the eosinophils (Bennett et al. 2001, Crowhurst et al. 2002, Lieschke et al. 2001). A summary of zebrafish blood cells is given in Table 1.

Table 1. Overview of blood cell lineages in zebrafish

Haematopoietic stem cell			
Myeloid lineage			Erythroid lineage
Macrophages	Granulocytes		Erythrocytes
	Neutrophils	Eosinophils	

Macrophages and granulocytes in zebrafish
In zebrafish, a macrophage lineage has been identified which is morphologically and functionally similar to its mammalian counterpart (Crowhurst, 2002; Bennett, 2001; Lieschke, 2001). Macrophages are characterized by an agranular cytoplasm which is large compared to the nucleus. The cytoplasm contains cytoplasmic phagosomes, and vacuoles in which phagocytic materials can be found (Crowhurst et al. 2002; Lieschke et al. 2001).
The neutrophil is the most abundant granulocyte cell type in zebrafish, comprising more than 95% of all observed granulocytes (Lieschke et al. 2001). This cell type closely resembles the mammalian neutrophil, though the segmented nuclei of the zebrafish heterophils are divided into 2 or 3 lobes instead of into 5 lobes like the human neutrophils. Another granulocyte cell type is in the literature often referred to as eosinophil (Lieschke et al. 2001; Crowhurst et al. 2002). The morphological appearance of the zebrafish eosinophil differs considerably from the mammalian eosinophil: the zebrafish eosinophil exhibits characteristics of both mammalian eosinophils and basophils (Bennett et al. 2001; Crowhurst et al. 2002). Both cell types contain granules that are filled with enzymes.
In this study we will especially focus on specific marker genes expressed by macrophages and neutrophil granulocytes, since these cell types play a crucial role in the response to inflammation in both zebrafish and mammals.

Macrophage- and granulocyte - specific gene expression

The first marker investigated in this study is *l-plastin* (leucocytosolic plastin). *L-plastin* was shown to be expressed in macrophages (Herbomel et al. 1999) and this gene has subsequently been used as macrophage-specific marker (Liu and Wen 2002, Renshaw et al. 2006). However, partial overlap with *mpx*-expressing cells has also been reported (Bennett et al. 2001) and recent multicolor FISH studies indicated that *l-plastin* is expressed in all leukocytes (Meijer et al., in press). Therefore, *l-plastin* appears to be a general leukocyte marker, although it is possible that expression in macrophages is stronger than in neutrophils at certain developmental stages.

l-plastin is an actin bundling protein. It is a homologue of the leukocyte-specific plastin found in mammals; it is involved in adhesion and activation of macrophages (Herbomel et al.1999, Jones et al. 1998). It is expressed in an early macrophage population when it spreads over the yolk sac as well as in a dispersed axial population of cells in the anterior yolk, in the region of the hatching gland and the pericardium (Crowhurst et al., 2002). At 24 hpf, *l-plastin* expression is found in cells dispersed over the cranial mesenchyme, the body and in the posterior intermediate cell mass (ICM). From 24 up to 60 hpf, *l-plastin* expressing cells start to colonize the cephalic mesenchyme and eventually, brain compartments and retinas. At around 60 hpf the macrophages in the brain compartments undergo a phenotypical transition into early microglia (Herbomel et al.2001) and the expression of *l-plastin* in this cell type decreases. From 60 hpf onwards, the number of *l-plastin* expressing cells in the head diminishes (Herbomel et al.2001).

The second marker we will study is myeloid-specific peroxidase *(mpx)*, expressed by the neutrophil lineage of zebrafish (Clay and Ramakrishnan 2005, Crowhurst et al. 2001, Lieschke et al. 2001, Meijer et al, in press). It is a peroxidase ezyme, stored in the azurophilic granules of the neutrophils and is involved in the primary defense of the cell. It is the zebrafish homologue for mammalian myeloid- specific peroxidase known as *mpo* (Lieschke et al. 2001). Phylogenetic analyses suggest that it may represent an ancestral peroxidase gene (Crowhurst et al, 2002).

3D atlas of zebrafish development

In our research group, a 3D digital atlas of zebrafish development has been developed (Verbeek et al. 2002). Complementary, a zebrafish gene expression database is under construction in which 3D zebrafish gene expression data can be stored and retrieved (Belmamoune and Verbeek, 2006). 3D gene expression patterns are produced using fluorescent *in situ* hybridization (ZebraFISH) (Welten et al.2006); 3D images are obtained by confocal laser scanning microscopy (CLSM). Currently, the dominant group of images in the zebrafish gene expression database is generated using ZebraFISH, but images using GFP can also be stored in the database. The 3D multichannel images are preprocessed for 3D modeling using TDR-3Dbase software (Verbeek et al. 2000). 3D reconstructions of the gene expression patterns are made and mapped on anatomical structures, using the 3D digital atlas of zebrafish development as a reference. To annotate gene expression patterns in relation to the anatomical structures, the 3D reconstructions are compared with corresponding 3D embryos from the 3D atlas of zebrafish development (http://bio-imaging.liacs.nl/atlasbrowserstart.html).

In this study we present an analysis of two marker genes expressed in macrophages and neutrophil granulocytes during zebrafish development: *l-plastin* and *mpx*, respectively. Three dimensional gene expression patterns in developmental time series of whole mount zebrafish embryos were generated by fluorescent *in situ* hybridization (Welten et al.2006). As an initial study for future research, the spatiotemporal distribution of *mpx* and *l-plastin* expressing cells was characterized during normal development. The visualization of gene expression in 3D, the analysis of cell numbers during normal development, and the gene expression analysis from developmental time series will contribute to a better understanding of the innate immune system in zebrafish and facilitate further analytical studies in the future.

MATERIALS AND METHODS

Embryo collection and in situ hybridization

Zebrafish were kept under standard conditions (www.zfin.org) in our facility. Embryos were staged according to Kimmel et al. (1995), fixed in 4% paraformaldehyde and processed for fluorescent *in situ* hybridization (FISH) (Welten et al. 2006).

In situ hybridization (ISH, Thisse et al. 1993 and 2004) was performed in parallel, as a control for the FISH procedure.

Probe synthesis

cDNA clones for *l-plastin* (BC 062381) and *mpx* (BC056287) were obtained from RZPD (Berlin, Germany) and linearized with EcoRI and BamHI respectively. Digoxigenin-labeled antisense RNA probes were synthesized from linearized cDNA clones, using T7 RNA polymerase (Maxiscript kit, Ambion) following the manufacturer's instructions.

Microscopy and imaging

For embryos stained using our ZebraFISH protocol, microscopy and imaging were carried out as previously described. Confocal images were acquired according to a standard protocol (Welten et al., 2006), using a Leica TCS/SP DM IRBE confocal laser scanning microscope (inverted setup) equipped with an Ar/Kr laser. Excitation of the used fluorophores (Cy3 and SYTOXGreen) resulted in a red and a green channel. All images were obtained with a 5x and a 10 x plan apo lens with a large working distance (NA 0.24). For every image, photo multiplying tube (PMT) gain and offset were averaged to optimise the signal to noise ratio. Images were saved as multi-channel TIFF files. Z-projections of the TIFF images were made using SCIL Image.

Images of NBT/BCIP-stained embryos were acquired using a Leica MZFL-III12 stereomicroscope equipped with a Leica DC 500 digital camera. From a single embryo images were made in different focal planes using Adobe Photoshop image processing software; composite images were made from these images.

Analysis of gene expression patterns

In order to observe the distribution of *mpx* and *l-plastin* expressing cells in relation to heart development, vascularization and haematopoietic events over total embryos, *mpx* and *l-plastin* expressing cells, the body of the embryo was subdived into 1) yolk, 2) tail

(caudal from the yolk extension) and 3) head and trunk. These subdivisions are depicted in Fig.1.

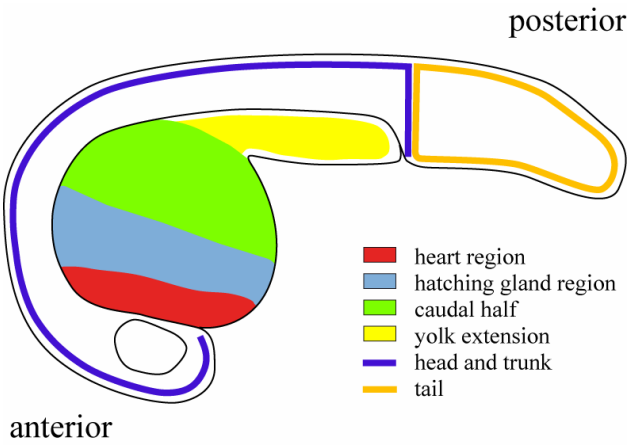

Fig.1 Author's impression of a 24 hpf zebrafish embryo. Overview of regions in the zebrafish embryo, as used for the analysis of cell numbers. In every region, cells were counted in subsequent stages of development.

On the yolk itself, several important vascularization events occur. To investigate the distribution of *mpx* and *l-plastin* expressing cells in relation to haematopoietic events and development of vessels in the yolk region, the yolk was also subdivided. The cells were also counted over four subdivisions of the yolk: 1) heart region, 2) hatching gland region, 3) caudal region of yolk sac, and 4) yolk extension (Fig.1).
From the projections of CLSM images (cf *microscopy and imaging*) as well as from composite light microscopy images from 24 hpf up to 72 hpf embryos, *mpx* and *l-plastin* expressing cells were counted in the subdivisions of 1) the total embryo and 2) the yolk and processed with Excel software. For *mpx*, n = 3-6 embryos and for *l-plastin* n= 3-4 embryos were analyzed. In the analysis, percentages of expressing cells over the above mentioned regions of the total embryos were calculated for all stages. Trendlines were added to demonstrate shifts in cell numbers in certain subdivisions.

3D reconstructions
The multichannel 3D images generated with confocal laser scanning microscopy, were prepared with Scil Image and imported into TDR-3Dbase. 3D reconstructions were made using TDR-3Dbase (http://bio-imaging.liacs.nl/tdr3dbase.html#). Anatomical structures and gene expression patterns were delineated, using TDR-3Dbase and a Wacom LCD graphical tablet.

RESULTS

l-plastin gene expression patterns
In zebrafish, the blood circulation starts at approximately 28 hpf. At this stage, the blood stream flows freely over the yolk sac in the duct of Cuvier, i.e. the future common cardinal vein (Herbomel et al. 1999; Isogai et al. 2001). In our study, the majority of *l-*

plastin expressing cells were indeed found on the yolk at 24 hpf; confirming this important event in blood formation and circulation. From 36 hpf onwards, an increasing number of *l-plastin* expressing cells was found in the head, as visible from the trendline in Fig. 2A. Herbomel et al.(2001) describe migration of macrophages into head mesenchyme and brain structures, and a phenotypical transformation of these macrophages into early microglia at around 60 hpf**.** Indeed, our analysis shows that from 60 hpf onwards, the number of *l-plastin* expressing cells in the head starts to decrease. In 72 hpf embryos, *l-plastin* expression is found in the head, ventrally from the optic cup, and in the anterior part of the trunk. The amount of cells expressing *l-plastin* in the tail increased, as visible from the trend lines in Fig. 2A. On the yolk, the trend lines portray a shift in distribution from the hatching gland region towards the heart region from 36 hpf up to 72 hpf (Fig.2B). This can be explained by the development of the common cardinal veins, which also develop into a more cranial position during these stages (Isogai et al. 2001) and to the regression of the yolk sac from 72 hpf onwards (Herbomel et al.2001).
In Fig. 3 A-E, *l-plastin* expression is shown in a developmental time series of zebrafish embryos at 24, 36, 48 and 60 hpf. At 96 hpf, only few *l-plastin* expressing cells were found in the head. In the tail, though expression was weak in all observed embryos, a string-like pattern of *l-plastin* expressing cells was seen in the ventral part. This is in agreement with the caudal haematopoietic tissue (CHT) described by Murayama et al. (2006). Expression was also found in the dorsal longitudinal anastomotic vessels, as shown in Fig.5A. No expression was seen in the intersegmental vessels.
3D reconstruction for *l-plastin* gene expression at 36 hpf confirms *l-plastin* expressing cells in the head and in the region of the presumptive heart (Fig. 6A and B). 3D reconstruction of a 60 hpf embryo confirms *l-plastin* gene expression inside brain divisions, mainly in the optic tectum and on the roof of the 4th ventricle (Fig. 6 C and D).

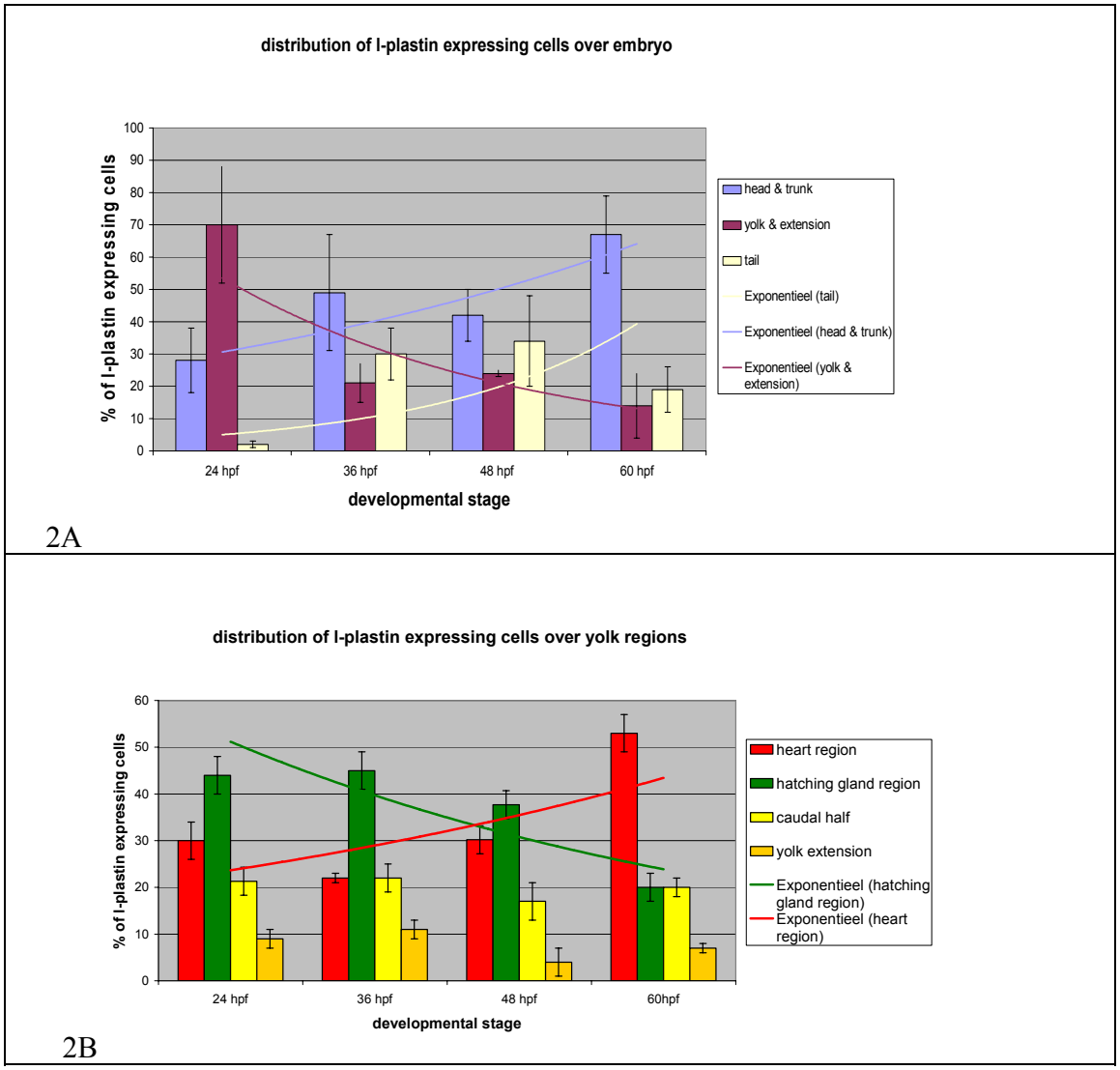

Fig.2. A: Distribution of *l-plastin* expressing cells over the whole embryo (upper panel). The trendlines show an increasing number of *l-plastin* expressing cells in the head up to 60 hpf and in the tail, and decreasing number on the yolk. Lower panel: distribution of *l-plastin* expressing cells over different yolk regions. The trendlines are added to support the idea that an increasing number of *l-plastin* expressing cells can be found in the heart region over time.

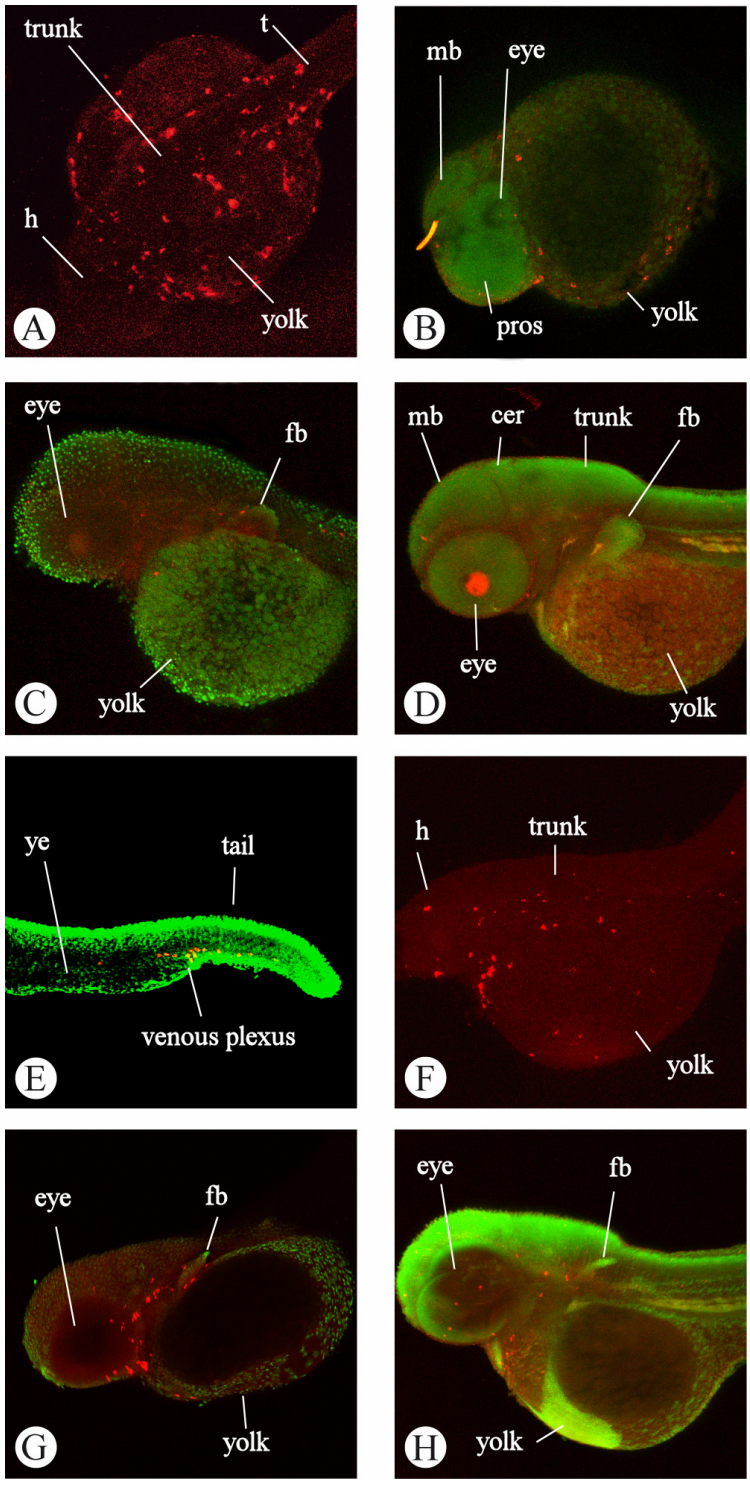
trunk
t
h
yolk
A
mb
eye
pros
yolk
B
eye
fb
yolk
C
mb
cer
trunk
fb
eye
yolk
D
ye
tail
venous plexus
E
h
trunk
yolk
F
eye
fb
yolk
G
eye
fb
yolk
H

Fig. 3

Fig. 3. Panels A-D: developmental series of *l-plastin* expression in zebrafish embryos at 24, 36, 48 and 60 hpf.
Panels E-H: developmental series of *mpx* expression at 24, 36, 48 and 72 hpf. TSA detection.
A is a dorsal view, anterior is to the left; B-H: Anterior is to the left, dorsal to the top. Images are so-called z-projections of confocal images. Gene expression is in red (TSA signal), counterstaining is in green (SYTOX Green).
Abbreviations: cer: cerebellum; fb: fin bud; h: head; mb: midbrain; pros: prosencephalon; t: tail; ye: yolk extension.

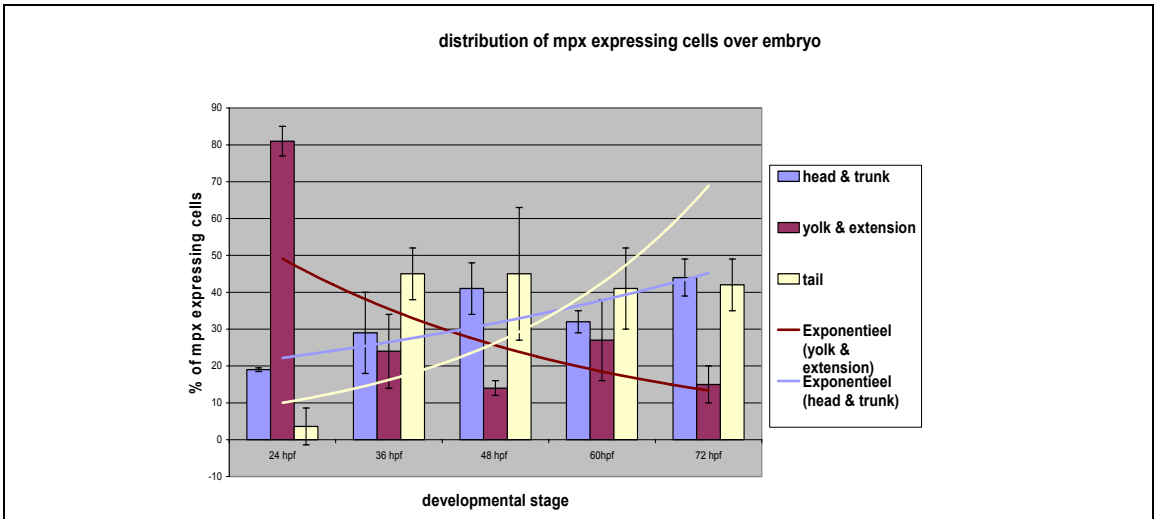

4A

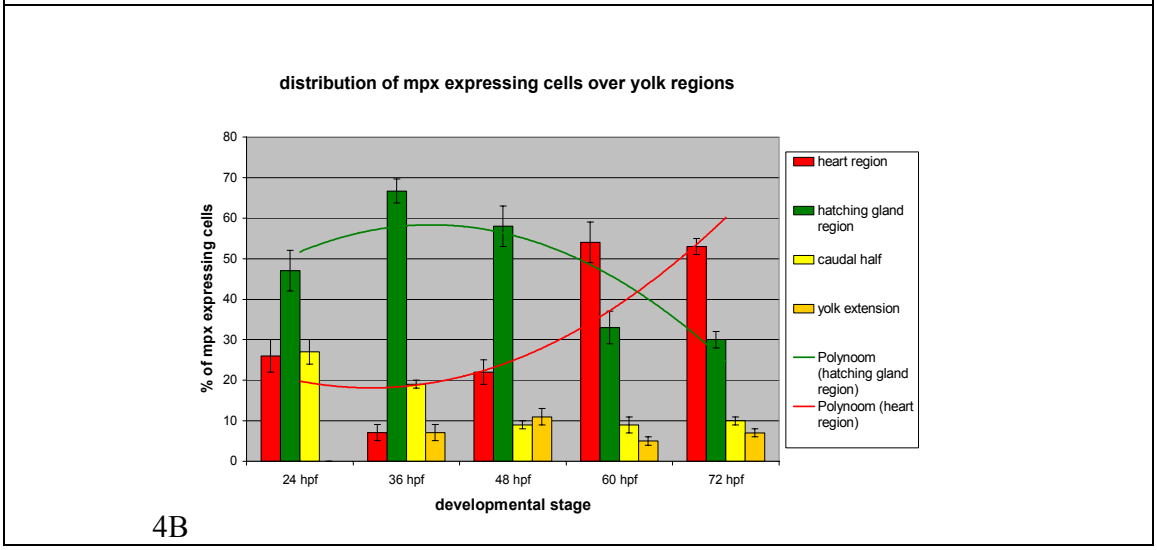

4B

Fig. 4 A: Distribution of *mpx* expressing cells over total embryo; the trendlines show increasing numbers of *mpx* expressing cells in head and trunk, and decreasing numbers on the yolk. B: the distribution of *mpx* expressing cells over different yolk regions. The trendlines are added to support the idea that a shift *in mpx* expression can be observed towards the yolk region adjacent to the heart.

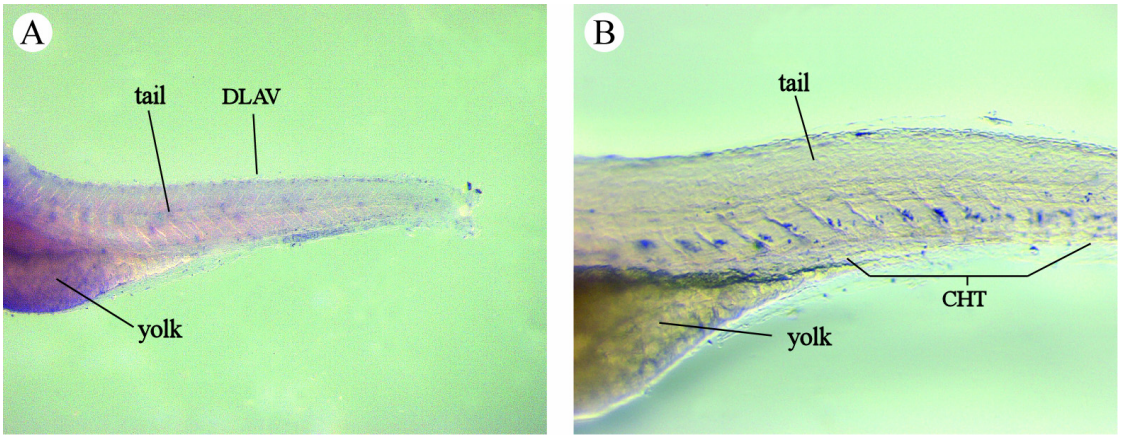

Fig. 5. A: *l-plastin* expression in the tail of a 96 hpf embryo in the dorsal longitudinal anastomotic vessels. B: *mpx* expression in the tail of a 96 hpf embryo. Notice the clusters of cells in the spaces between the somites, as a part of the CHT (Murayama et al. 2006). ISH detection with AP staining. Anterior is to the left, dorsal to the top.
DLAV: dorsal longitudinal anastomotic vessels; CHT: caudal haematopoietic tissue.

Mpx gene expression patterns

A large number of *mpx* expressing cells is found on the yolk at 24 and 36 hpf, in the same pattern as described for the *l-plastin* expression pattern. This is consistent with the onset of circulation at 24 hpf and the pattern of the duct of Cuvier at these stages (Isogai et al.2001). In Fig3 E-H, *mpx* expression is shown in developmental time series at 24, 36, 48 and 72 hpf. From 36 hpf onwards, the number of *mpx* expressing cells on the yolk decreases.

The trend lines suggest a migratory pattern towards the head and trunk (Fig. 4A and 4B), closely following the pattern of vascularization (Isogai et al. 2001) and the development of the heart. At 48 hpf the majority of *mpx* expressing cells is found in the head region and in the tail. At 60 and 72 hpf, expression is found in the head, the tail, the caudal veins and also in the region described as the caudal haematopoietic tissue (Murayama et al. 2006).

At 96 hpf, throughout almost all of the trunk and tail small clusters of *mpx* expressing cells were found in the spaces between the somites on the ventral side of the notochord, forming a part of the CHT (Murayama et al. 2006) (Fig.5B).

Some *mpx* expressing cells were also seen in the caudal vein and dorsal to the spinal cord, in the dorsal longitudinal anastomotic vessels, connected to the intersegmental vessels (Isogai et al. 2001). Scattered *mpx* expressing cells were found in the posterior part of the head and in the heart cavity, as well as in the trunk.

3D reconstruction for *mpx* gene expression patterns portrays *mpx* expressing cells in the common cardinal vein at 48 hpf (Fig. 6 E and F). 3D reconstruction of a 72 hpf embryo depicts *mpx* gene expression in the tail (Fig. 6 G). In the tail, *mpx* expressing cells are visible in the CHT (Fig. 6H).

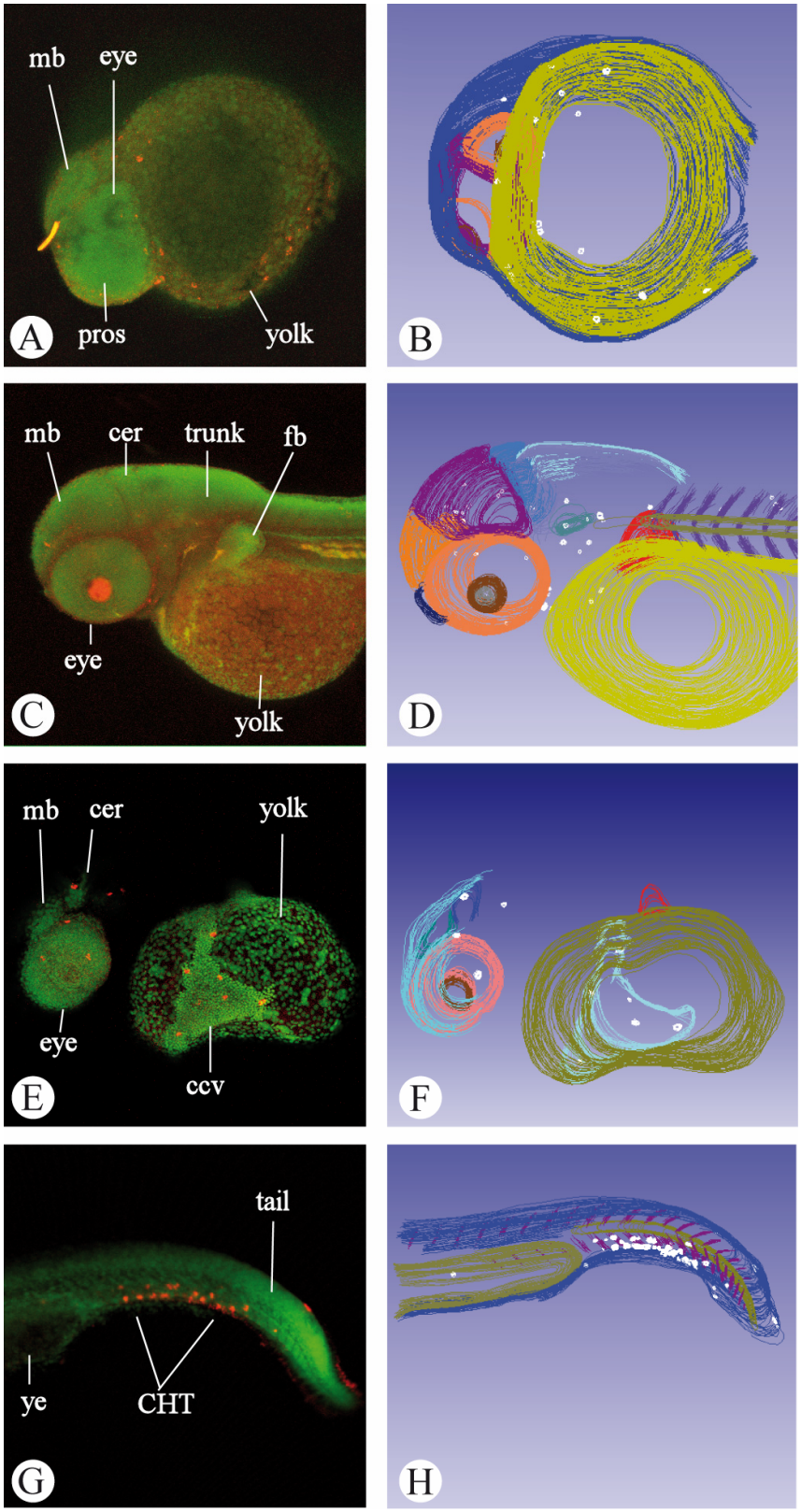
mb
eye
pros
yolk
A
B
mb
cer
trunk
fb
eye
yolk
C
D
mb
cer
yolk
eye
ccv
E
F
tail
ye
CHT
G
H

Fig. 6

Fig.6. A-D: *l-plastin* gene expression at 36 hpf (panel A and B) and at 60 hpf (panel C and D), In panel B and D, the 3D reconstructions of the embryos in panel A and C are depicted. The 3D reconstruction in panel B is magnified and slightly rotated.

E: *mpx* expression in a 48 hpf embryo. F: 3D reconstruction of the same embryo, depicting *mpx* expressing cells in the common cardinal vein i.e. the light blue structure on the yolk (ochre), visible from the confocal image as well as in the 3D reconstruction.
G: *mpx* expression in the tail of a 72 hpf embryo. H: 3D reconstruction of the same embryo, portraying *mpx* expressing cells in the CHT.
The images of the embryos in panel A, C, E and G are the result of TSA detection; The images are so-called z-projections of a confocal image stack. Gene expression is in red (TSA signal), counter staining is in green (SYTOX Green signal). Anterior is to the left, dorsal to the top.

Color legend for the 3D reconstructions in panel B, D, F and H:

l-plastin or *mpx* positive cells (white). embryo outline (dark blue), diencephalon (orange), yolk and yolk extension (ochre), mesencephalon (purple) optic cup (salmon), pectoral fin (red).

Abbreviations: ccv: common cardinal vein; cer: cerebellum; CHT: caudal haematopoietic tissue; fb: fin bud; h: head; mb: midbrain; pros: prosencephalon; t: tail; ye: yolk extension.

DISCUSSION

Gene expression patterns

In our study, the developmental series, cell number analysis and 3D reconstructions portray an increase of *l-plastin* expressing cells in the head up to 60 hpf (Fig.2). From that stage onwards, the number of *l-plastin* expressing cells decreased and at 96 hpf, only a few *l-plastin* expressing cells were found in the head. Herbomel et al. (2001) describe a migration pattern of macrophages from 22 hpf onwards, towards the head mesenchyme. The macrophages then start to colonize brain compartments and the retina. By 60 hpf, the number of *l-plastin* expressing cells in the head signal starts to diminish. The macrophages present in brain and retina undergo a phenotypical transformation into microglia; this is also demonstrated by expression of a marker for the neurotrophic factor *apolipoprotein E* in these cells at 72 hpf (Herbomel et al. 2001).
Between 24 and 60 hpf, by ISH and FISH experiments 20 - 160 *l-plastin* and *mpx* positive cells were detectable on the yolk; 20 - 180 were detectable in the head and 5 - 40 in the tail (Herbomel et al. 1999, Herbomel et al. 2001, this study). However, the total amount detected per embryo showed large variation in our study, probably due to differences in detection sensitivity between experiments. For comparative analysis, we therefore decided to express data as percentages of total cell numbers in different areas. For some developmental stages, only a few datasets were available for analysis. Therefore, the spatio-temporal analysis of distribution of *mpx* and *l-plastin* expression should be considered as a pilot study for future analysis.
Since our study focuses on whole mount FISH and ISH, it has not been not possible to investigate migration of cells over time. However, studies by Herbomel et al. (1999,

2001) and Murayama et al. (2006) demonstrate that both macrophages and granulocytes exhibit migratory behavior as well as cell proliferation.

3D reconstructions
With the confocal microscope settings used in this study, only a limited number of optical sections can be made. Therefore, 3D reconstruction is based on only a part of the embryo. Observations from the 3D models of both *l-plastin* and *mpx* gene expression from 24 hpf up to 72 hpf, are consistent with the gene expression patterns described in literature. In addition, the schematic 3D modeling also allows better inspection of the distribution of the single *l-plastin* and *mpx* expressing cells, and their relation to anatomical structures.

Conclusions and future work
In this study we present 3D gene expression patterns for *mpx* and *l-plastin*. Spatiotemporal gene expression patterns are depicted in developmental time series of zebrafish embryos, and further characterized in 3D models. Exploratory experiments were performed to demonstrate the spatial and temporal distribution of neutrophils and macrophages during development. Both the semi-quantitative data and the 3D reconstructions provide a contribution to the existing knowledge.
In future research, the use of multi-photon microscopy can provide a better depth penetration of the total embryo. Different fluorescent tags will provide the possibility study co-localization of marker genes of leukocytes and other cell types. Eventually, 3D reconstruction of total embryos allows an accurate analysis of cell numbers and distribution in timing series of whole mount embryos, in future functional studies such as inflammation and wounding experiments. The techniques demonstrated in this study, will further facilitate the application of zebrafish as a model to investigate the human immune system.

ACKNOWLEDGEMENTS

This project is supported by The Netherlands Research Council through the BioMolecular Informatics programme of Chemical Sciences (grant number # 050.50.213). We thank G.E.M. Lamers for her valuable advice on confocal microscopy and M. Brittijn for his help with the preparation of the graphical layout of the figures.

Chapter 5

Gene expression and digit homology in the chicken wing.

M.C.M. Welten[1], F.J. Verbeek[2], A.H. Meijer[1] and M.K. Richardson[1].

1. Institute for Biology, Leiden University, Kaiserstraat 63, 2311 GP Leiden, The Netherlands
2. Imagery and Media, Leiden Institute of Advanced Computer Science, Leiden University, Niels Bohrweg 1, 2333 CA Leiden, The Netherlands

Originally published in Evolution & Development 7:1, 18-28 (2005)
Modified and updated version

Case study: late zebrafish and cross species development

ABSTRACT

The bird wing is of special interest to students of homology and avian evolution. Fossil and developmental data give conflicting indications of digit homology if a pentadactyl ‘‘archetype’’ is assumed. Morphological signs of a vestigial digit I are seen in bird embryos, but no digit-like structure develops in wild-type embryos. To examine the developmental mechanisms of digit loss, we studied the expression of the high-mobility group box containing *Sox9* gene, and bone morphogenetic protein receptor 1b (*Bmpr-1b*), markers for precondensation and prechondrogenic cells, respectively. We find an elongated domain of *Sox9* expression, but no *Bmpr-1B* expression, anterior to digit II. We interpret this as a digit I domain that reaches precondensation, but not condensation or precartilage stages. It develops late, when the tissue in which it is lodged is being remodelled. We consider these findings in the light of previous Hoxd-11 misexpression studies. Together, they suggest that there is a digit I vestige in the wing that can be rescued and undergo development if posterior patterning cues are enhanced. We observed *Sox9* expression in the elusive ‘‘element X’’ that is sometimes stated to represent a sixth digit. Indeed, incongruity between digit domains and identities in theropods disappears if birds and other archosaurs are considered primitively polydactyl. Our study provides the first gene expression evidence for at least five digital domains in the chick wing. The failure of the first to develop may be plausibly linked to attenuation of posterior signals.

INTRODUCTION

The homology of avian wing digits is of interest to palaeontologists and evolutionary biologists because it bears on the important question of the evolution of birds. Digit homology is also important for experimental developmental biologists who use the phenotypes (‘‘identities’’) of digits as markers of position along the anteroposterior axis of the limb. Furthermore, because the wing is a well-studied experimental model, it provides opportunities to explore the mechanistic basis of developmental homology. Finally, the history of ideas about the avian wing presents us with an unrivaled catalog of archetypes and recapitulation. Our aim in this article is not to overturn current hypotheses of avian phylogeny, but to ask how developmental mechanisms were modified in the transition from the presumed ancestral state. We also wish to ask whether alternative hypotheses of avian digit homology have been overlooked. We begin by reviewing some of the relevant evolutionary and developmental issues. (Note: all references to ‘‘digits’’ in this article are to those of the forelimb, unless otherwise stated.)

Avian phylogeny

Archaeopteryx lithographica (Fig. 1) has always been central to the debate about avian origins because of its historical fame as a ‘‘missing link,’’ and its possession of a mosaic of avian and more inclusive theropod characters (Ostrom 1976; Christiansen and Bonde 2004). Cladistic analyses support the hypothesis that birds belong to the ‘‘Coelurosauria,’’ a clade of theropod dinosaurs (Gauthier 1986; Sereno 1999). Recent discoveries of nonavian maniraptorans with feathers or feather-like coverings (e.g., *Protarchaeopteryx robusta* and *Caudipteryx zoui*; Ji et al. 1998, 2001; Zhou et al. 2003) support the inclusion of birds in Theropoda. The fossil *Rahona ostromi* also shows a mosaic of avian and theropod features, and phylogenetic analysis places it as a sister species to *Archaeopteryx* (Forster et al. 1998). Although other ancestries for birds have been proposed (notably the thecodont and crocodilian hypotheses; Tarsitano and Hecht 1980; Hecht and Tarsitano 1982; Thulborn and Hamley 1982; Hecht 1985; Moinar 1985; Walker 1985), we will adopt here the consensus view that birds are theropods (Fig. 1).

Digit position and digit phenotype

Digits are traditionally assigned Roman numerals I–V, with reference to a pentadactyl archetype (Fig. 2). These designations have two different meanings: as positional references, the terms I–V describe the spatial relations of digits along the anteroposterior axis of the limb. By contrast, the phenotypes or identities I–V apply to different complexes of morphological characters that relate to the skeleton of a digit. The danger of having one numbering system with two meanings is that circular arguments may be developed about digit homologies that are not independent. Furthermore, it has been questioned whether characters such as digit shape and phalangeal formula can in fact be used to ‘‘identify’’ homologous digits in different species (Goodwin and Trainor 1983). In birds, we are faced with uncertainty both about the positional homologies of the wing digits (because only four distinct digits are seen in the wing), and also their phenotypes (because phalanges and other structures may have been lost or remodeled during evolution).

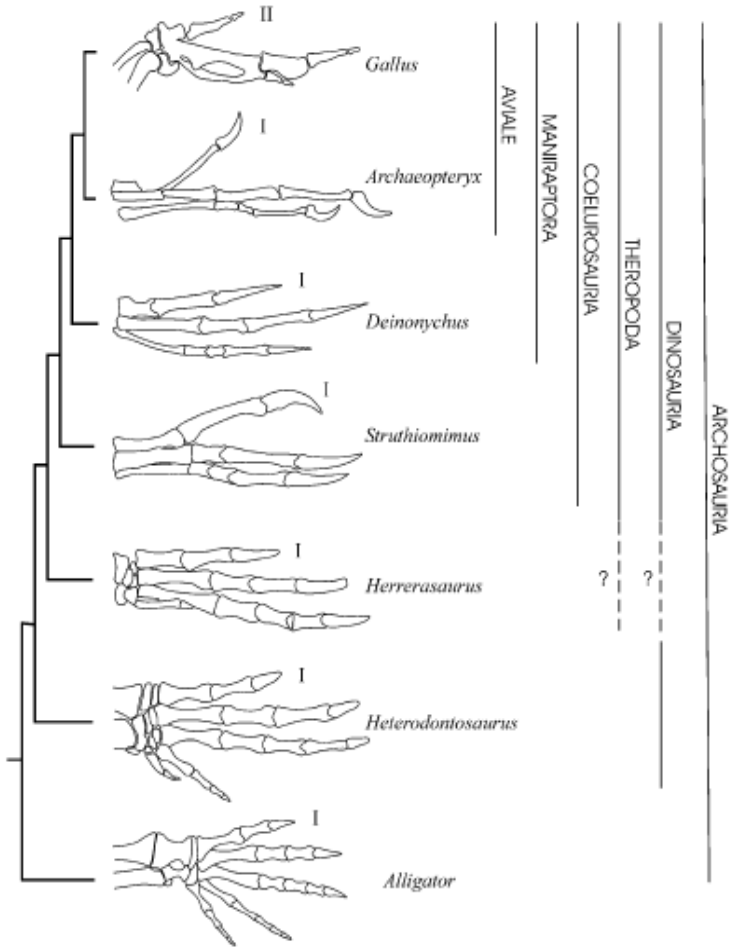

Fig. 1. Schematic illustration of some hand elements in archosaurs (anterior is to the top; some images were inverted to make comparison easier). The phylogeny is modified from Gauthier (1986) and Sereno (1999). The anterior digit is labeled with I or II according to current consensus on digit homologies. Schematic illustrations of the manus are shown and the sources for the drawings are: *Gallus gallus* (Yasuda 2002); *Archaeopteryx lithographica*, ''Maxberg'' specimen (Wellnhofer 1985); *Deinonychus antirrhopus* (Ostrom 1969); *Struthiomimus altus* (Osborn 1916); *Herrerasaurus ischigualastensis* (Sereno 1993); *Heterodontosaurus tucki* (Santa Luca 1980); *Alligator mississippiensis* (Gegenbaur 1864). Names of clades are indicated on the right. The value of the infra-order ''Coelurosauria'' is questioned by Carroll (1987). There is uncertainty, indicated in this figure by the question mark (?), about the taxonomic position of *Herrerasaurus* (Padian et al. 1999; Sereno 1999).

Positional homologies and the problem of vestigial digits

The homologies of cartilaginous and precartilaginous elements at the postaxial margin of the chicken embryo wing are a puzzle, but a plausible vestige of metacarpal V can be identified in alcian blue whole mounts (Montagna 1945; Burke and Feduccia 1997). Hinchliffe and Hecht (1984) identified an intriguing triad of postaxial elements: (a) the vestigial metacarpal V, lying laterally along the proximal part of metacarpal IV, and becoming reduced or disappearing completely; (b) the elongated pisiform, lying at the

lateral border of the wing, near the palmar aspect of the carpus; and (c) an element ‘‘X,’’ possibly an avian apomorphy, that lies near the proximal end of metacarpal IV and near the palmar aspect of the carpus, and that may persist to adulthood (see also Montagna 1945). Element X was formerly identified as an extension or process of the pisiform (Montagna 1945; Hinchliffe 1977). Part of element X was described by Montagna (1945) as fusing with his ‘‘centrale IV,’’ whereas another part was said to persist in the adult wing as a tuberosity on metacarpal III. Histogenesis at the pre-axial margin is less clear, despite numerous studies (the classical literature is reviewed by Holmgren 1933; Montagna 1945). Labelling for early cartilage matrix with $35SO_4$ (Hinchliffe 1977) fails to find a vestigial digit I. However, a condensation for distal carpal I was claimed by Montagna (1945). Recently, a small avascular zone (Kundrát et al. 2002), cell condensation (Kundrát et al. 2002; Larsson and Wagner 2002), or small cartilage nodule (Feduccia and Nowicki 2002), next to digit II, has been cited as evidence of a digit I vestige in *Gallus gallus* and *Struthio camelus* (the ostrich). There is a tuberosity for attachment of *extensor carpi alualae radialis longus* and *ligamentum elasticum prepatag*iale at the base of metacarpal II (Yasuda 2002). This tuberosity has been interpreted as evidence of a vestigial digit I, although this interpretation has been contested (Montagna 1945). A finding of great significance comes from studies of chicken wings experimentally infected with *Hoxd-11*-encoding retroviral constructs. A supernumerary digit, resembling wildtype digit II, develops in the vestigial digit I position in some cases (Fig. 4F in Morgan et al. 1992). This suggests that a digit I domain exists in that position, and can be rescued if the tissue is experimentally posteriorized. Naming a vestigial anterior digit in the chick as ‘‘digit I’’ assumes that ancestral digits have been correctly identified. Basal archosaurs are thought to show a trend toward reduction of digits IV and V (Romer 1956; Wagner and Gauthier1999). Thus the manus of the dinosaur *Herrerasaurus ischigualastensis*, possibly a basal theropod, shows reduced digits IV and V (Sereno 1993). The vestigial digits are positioned toward the palmar surface of the manus (Fig. 1). This and other evidence can be used to reconstruct a scenario in which the reduction of digits IV and V in basal archosaurs is continued in the lineage leading to birds (Fig. 1; see also Gauthier 1986; Wagner and Gauthier 1999). Debates about the taxonomic position of *Herrerasaurus ischigualastensis* (Sereno 1993; Padian et al. 1999; Sereno 1999; Galis et al. 2003; Larsson and Wagner 2003) do not completely overturn these arguments because crocodilians also show reduction of digits IV and V. For example, in the extant *Crocodylus porosus* (estuarine crocodile), digits I–III are prominently clawed, whereas IV and V are much smaller (Kükenthal 1893).

Phenotype homologies (identity) of avian digits

What are the phenotypic homologies of the three avian wing digits? Considerations of phalangeal formula, and the presence of a semilunate carpal (assumed to represent fused distal carpals I and II) have been used among other characters to assign the phenotypes I–II–III to avian digits (Wagner and Gauthier 1999; Chatterjee 2004). Adult birds commonly have an ossified phalangeal formula of 1–2–1 (our unpublished observation on specimens in the National Museum of Natural History/Naturalis, Leiden, The Netherlands), although it is always possible that tiny distal phalanges have been lost in preparation. A phalangeal formula of 2–3–3 is reported for goose embryos (*Anser sp*.; Schestakowa 1927) and 2–3–1 for adult ostriches (*S. camelus*; Kundrát et al. 2002). A

formula of 2–3–2 is reported for *G. gallus* by some authors (Chamberlain 1943; Yasuda 2002). In summary, modern birds have a lower phalangeal count for at least the third digit than nonavian theropods, where the formula is typically 2–3–4 (Wagner and Gauthier 1999). Two models have recently been proposed to account for these data. Both models assume that birds retain digit positions II–IV of nonavian theropods, and both acknowledge the incongruity that the phenotypes correspond to those of digits I–III (Fig. 2). The Frame Shift model solves the problem by proposing that embryonic digit domains II–IV have undergone a homeotic transformation so as to adopt the more anterior phenotypes of I–III (Wagner and Gauthier 1999). The solution presented by the Pyramid Reduction hypothesis (Kundrát et al. 2002) is that avian wing evolution involved bilateral loss of digits, and that the remaining central digits (II–IV) have simply been remodelled during evolution, with attendant loss of phalanges. They have thereby converged on the I–II–III phenotype (Fig. 2).

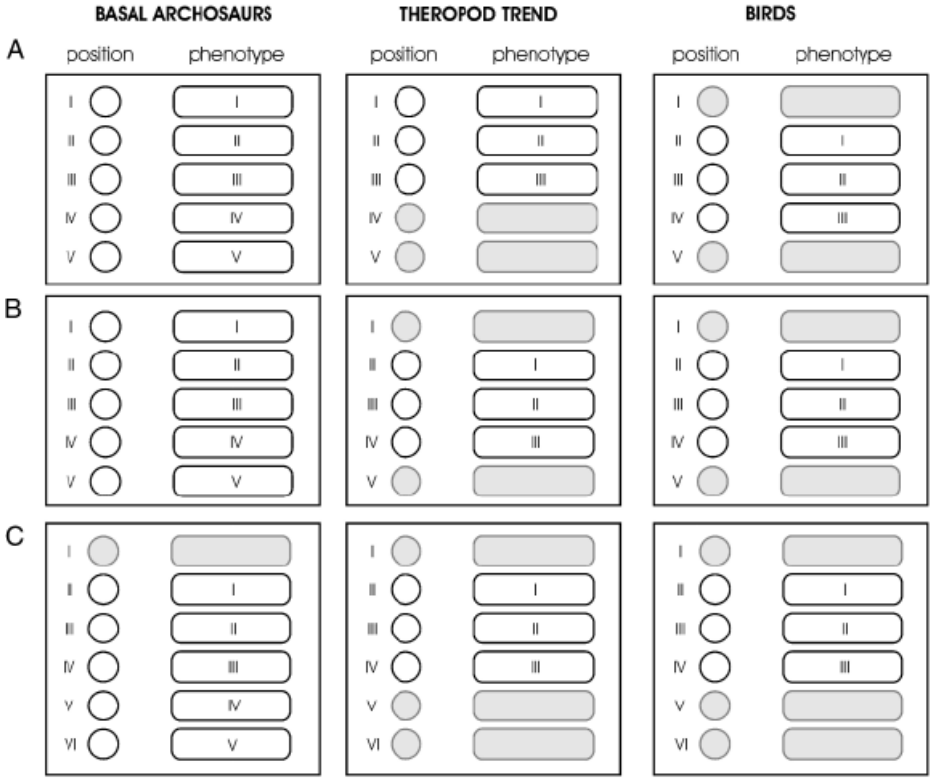

Fig. 2. Schematic representation of some models that attempt to correlate digit position with digit identity in birds. The adult situation is shown, and grey shading indicates that a particular digit is not visible in the adult (but may be present as a vestigial embryonic domain, as is likely the case for positions I and V for birds). (A) Frame Shift model, in which the digital domains take on new phenotypes (Wagner and Gauthier 1999). (B) Bilateral reduction of digits I and V, and convergence of the remaining central digits on a I– III phenotype (Kundrá t et al. 2002). (C) A model that rejects the pentadactyl archetype in favour of hexadactyly. The attraction of this model is that there is continuity of digit position and phenotype across the phylogeny. The disadvantage is that there is no direct evidence in its support.

The primary axis

One further line of evidence for the homology of chicken embryo wing digits comes from the time-sequence in which cartilage elements differentiate in the embryo, and their spatial relations with each other as they develop (Holmgren 1933; Shubin and Alberch 1986). In tetrapod embryos, alcian blue preparations show characteristic arrangements and staining intensities of limb cartilage elements. At certain stages, a chain of precociously differentiated elements may be seen running proximodistally along the limb-the primary axis of Burke and Alberch (1985).

The primary axis is presumably an expression of heterochronies in the underlying patterning mechanisms active at earlier stages. It is unlikely that the axis itself dictates the course of digit development because it only becomes visible after positional values have been encoded in a particular mesenchymal cell population (Wolpert and Hornbruch 1990; Cohn et al. 2002). Extensive surveys (Holmgren 1933; Shubin and Alberch 1986) show that the primary axis in the forelimb passes through the humerus, ulna, ulnare, distal carpal IV (if present), and digit IV. This pattern is seen in all five-fingered tetrapods except urodeles, where the axis passes through digit II. Birds show a primary axis passing through digit IV, so as to make the three bird digits II–III–IV (Burke and Feduccia 1997).

Developmental mechanisms and digit homology.

Many recent studies have expanded our knowledge of the molecular mechanisms of limb patterning (reviewed by Sanz- Ezquerro and Tickle 2003). Studies on *sonic hedgehog* (*Shh*) cast doubt on previous ideas about digit identity being a simple readout of a morphogen gradient (Yang et al. 1997; Ahn and Joyner 2004). In fact, patterning appears to be much more complex, with distinct phases. The same genes may have different roles at early stages, when broad domains are established in the limb (Dudley et al. 2002; Richardson et al. 2004) and later stages, when digits differentiate according to particular identities. Members of the bone morphogenetic protein (BMP) family of growth factors are involved both in the formation of prechondrogenic condensations and their later differentiation (Pizette and Niswander 2000). The later actions of *Bmp2* could include the specification of digit identity itself (Yang et al. 1997). The complexity of interactions, and lack of true independence between patterning mechanisms, are among possible objections (Feduccia 1999; Kundrát et al. 2002) to the Frame Shift hypothesis (Wagner and Gauthier 1999); thus, the Frame Shift might require a whole suite of mechanisms to be modified in concert to yield a phenocopy of the nonavian theropod digits. Lack of independence between mechanisms has been shown using loss-of-function studies in mice (Zákány et al. 1997). These suggest that posterior *Hox* genes regulate both the number of initial primordia formed, and the subsequent shapes of the digits. Further studies suggest that there are two critical phases of posterior *Hox* gene expression in the mouse, the first establishing anteroposterior polarity and the second involved in the readout of digit identities; in this model, posteriorly expressed *Shh* acts as a relay between the two phases (Zákány et al. 2004). The time of action of *Shh* has been analyzed in *Shh* homozygous mutant mice, leading to the suggestion that the proximal limb elements are already specified at early stages, and have normal polarity; but successively more distal elements require *Shh* both for their initial specification, and for the establishment of normal phenotype (Chiang et al. 2001). In support of the Frame Shift

hypothesis, digit primordia can undergo anterior transformation when BMP signaling is attenuated by local implantation of Noggin (Dahn and Fallon 2000). These studies also support the idea that digit phenotype is not irreversibly fixed at the early condensation stage. Time of exposure to *Shh* may also be important (Harfe et al. 2004), raising the possibility that a Frame Shift could be based on heterochrony (for more on heterochrony in limb diversification, see Blanco et al. 1998; Blanco and Alberch 1992).
Digit II specification in particular is thought to be dependent on a low threshold of *Shh* exposure (Harfe et al. 2004), and digits can undergo transformations of identity when *Hox* genes are misexpressed (e.g., the posterior transformation seen in birds injected with the RCAS-Hoxd-11 retroviral construct; Morgan et al. 1992). The Pyramid Reduction model (Kundrát et al. 2002), and its attendant loss of phalanges, can be considered in the light of studies on phalanx development. The number of phalanges on each digit may be controlled in part by the duration of limb outgrowth. In the dolphin flipper, there is evidence that prolonged outgrowth on digits II and III selectively leads to hyperphalangy (Richardson and Oelschlaeger 2002). Termination of outgrowth, and therefore formation of the distal phalanx, may be signaled by disappearance of *Fgf8* expression in the apical ectodermal ridge (Merino et al. 1998).

Aims and objectives
We have investigated these issues using whole-mount *in situ* hybridization, and alcian blue staining for hyaline cartilage matrix. Markers of early digit formation included *Sox 9*, and *BMP receptor 1B* (Merino et al. 1998; Pizette and Niswander 2000; Karsenty and Wagner 2002; Chimal-Monroy et al. 2003). The *Sox9* gene belongs to the high-mobility group (HMG) box superfamily of DNA-binding proteins, and is one of the earliest markers of limb mesoderm destined to form cartilage (Chimal-Monroy et al. 2003). It is probably a differentiation factor, and not a patterning molecule, being expressed in cells that have already been patterned with respect to the limb axes, but have not yet started to condense and differentiate (Akiyama et al. 2002). Expression has been shown to be detectable in the stage 22 chick limb (Healy et al. 1999). *Bmpr-1B*, a secreted protein receptor, follows the expression of *Sox9* closely (Healy et al. 1999; Chimal-Monroy et al. 2003). It is expressed in prechondrogenic aggregates, immature chondrocytes, and perichondrium (Pizette and Niswander 2000). *Bmpr-1B* expression has been reported in the chick limb at stage 24 (Merino et al. 1998; Healy et al. 1999). We also examined the expression of *Wnt-14*, a relatively late marker that shows hybridization to interdigital mesenchyme and future joints (Hartmann and Tabin 2001).

MATERIALS AND METHODS

Chicken embryos (*G. gallus*) of stages 26–33 (Hamburger and Hamilton 1951) were used. These stages cover the principal phases of digit formation (Sanz-Ezquerro and Tickle 2003). Limbs were dissected from embryos ranging from 4.5 to 8 days and processed for mRNA *in situ* hybridization. cDNA clones for *Wnt14, Bmpr- 1B*, and *Sox9* were kindly provided, respectively, by C. Tabin, L. Niswander, and J. M. Hurle. Anti-sense and sense RNA probes were synthesized and labeled with digoxigenin (Roche Diagnostics GmbH, Penzberg, Germany). Sense RNA probes were used as negative controls. *In situ* hybridization was performed on the dissected chick limbs according to

standard protocols (Wilkinson 1998). Samples were treated with concentrations of proteinase K ranging from 10 mg/ml for stages 25–26 to 50 mg/ml for stages 31–34 for 10–15min at room temperature. Hybridization was performed at 65–68*1*C in 50% formamide. Color reactions were developed with NBT/BCIP substrate (Roche).
To further characterize patterns of *Sox9* and *Bmpr-1B* expression, stage 30 and 31 wings from the embryos hybridized as above were embedded in Technovit 7100 (Heraeus Kulzer Gmbh, Wehrheim, Germany). Transverse sections of 10 mm were cut on tungsten knives, and counterstained with Neutral Red. Three-dimensional computer reconstructions were made as previously described (Verbeek 2000). The onset of alcian blue staining (whole limbs were stained with 0.3% in acid alcohol), and of gene expression, were recorded for each skeletal element in the chick fore- and hindlimbs. The sequences were then compared.

Homology of gene expression domains
A major problem in comparing patterns of developmental gene expression is that early expression domains may initially represent primordia of several adult bones, and then segregate into individual bone primordia. Thus there is no direct mapping of domains onto single named organs. We therefore have had to designate each domain in terms of its daughters. To make this designation, we mapped the expression domains in processed whole mounts that were then stained with alcian blue, dehydrated in ethanol, and cleared in methyl salicylate.

RESULTS

Spatial patterns of gene expression
General points
Sox9 and *Bmpr-1B* were only expressed transiently in the developing cartilage elements, and so they were not enduring markers (as alcian blue is). Thus, we only saw a primary axis in certain early stages (Fig. 3A). Later, however, the proximal elements no longer expressed the molecular markers we used, and so no continuous primary axis was seen along the full proximodistal extent of the limb. No evidence was seen of budding or branching of elements, only the segregation of discrete subdomains from within a common domain (Note: square brackets indicate a common domain for the elements enclosed).

Sox9 expression in the wing
Sox9 was expressed in the elements of the stylopodium, zeugopodium, and digital arch at stages 25 and 26. The digital arch appeared to consist of two separate domains: one for [digit V1IV], and one for the anterior digits (Fig. 3A; although we use the term “digit”, we cannot say without cell marking experiments whether the domain encompasses the entire presumptive digit, or only its metacarpal). At stages 27 and 28, strong expression patterns of *Sox9* could be observed in the three separate digit III, IV, and V domains. Anterior to digit III, another expression pattern was visible, which might be interpreted as a common domain for digit I and II anlagen (Fig. 3B). This domain appeared to divide into two at stage 29 (Fig. 3D). One daughter, which showed strong expression, was for the digit II metacarpal. The other was weaker, and we identify it as a presumptive digit I

metacarpal domain; at no stage was it resolvable into separate bones. It was lodged in the flange of tissue along the anterior margin of the wing that becomes thinned during formation of the prepatagium (Murray and Wilson 1994). A putative pisiform showed hybridization at stage 29 (Fig. 3D). Wings from stage 30 onward showed strong *Sox9* expression patterns for the posterior four digits. The weak *Sox9* domain for digit I was now very distinct, and quite elongated, and lay anterior to digit II, separated from it by a clear interdigital space (Fig. 3E). It bore a striking resemblance to the vestigial digit V domain of *Sox9* expression in the chicken foot (Fig. 3G, see below). Transverse sections through the wing (Fig. 4, B and C) showed that the *Sox9* domain for digit I was close to the ectoderm, on the palmar side of the autopodium, and in alignment with the other four digits, like the avascular zone described previously (Kundrát et al. 2002). This expression pattern was consistent in the eight embryos studied at this stage. At stage 31, hybridization became weaker and at stage 32 was no longer visible. From stage 29, *Sox9* was expressed strongly in the interzones of future joints as previously reported (Hartmann and Tabin 2001; Karsenty and Wagner 2002). At stage 30, the putative pisiform was seen to lie lateral to the ulnare; element ‘‘X’’ was visible between metacarpal V distally, and the pisiform proximally, but lying in a more ventral plane (Fig. 4, E and G).

Fig. 3. (A–E) Left chicken wings stage 26–30, after *in situ* hybridization with *Sox9* probe (anterior is to the top, ventral aspect). (F–H) Left chicken hindlimbs stage 26, 27, and 30, respectively, *Sox9* probe. Anterior is to the top, ventral aspect. Roman numerals, digit or metacarpal number; mc, metacarpal; R, radius; U, ulna; Ue, ulnare; ph, phalanx; p?, pisiform?; [mc IV1V], common expression domain for metacarpals IV and V. Some images were inverted to make the orientation consistent.

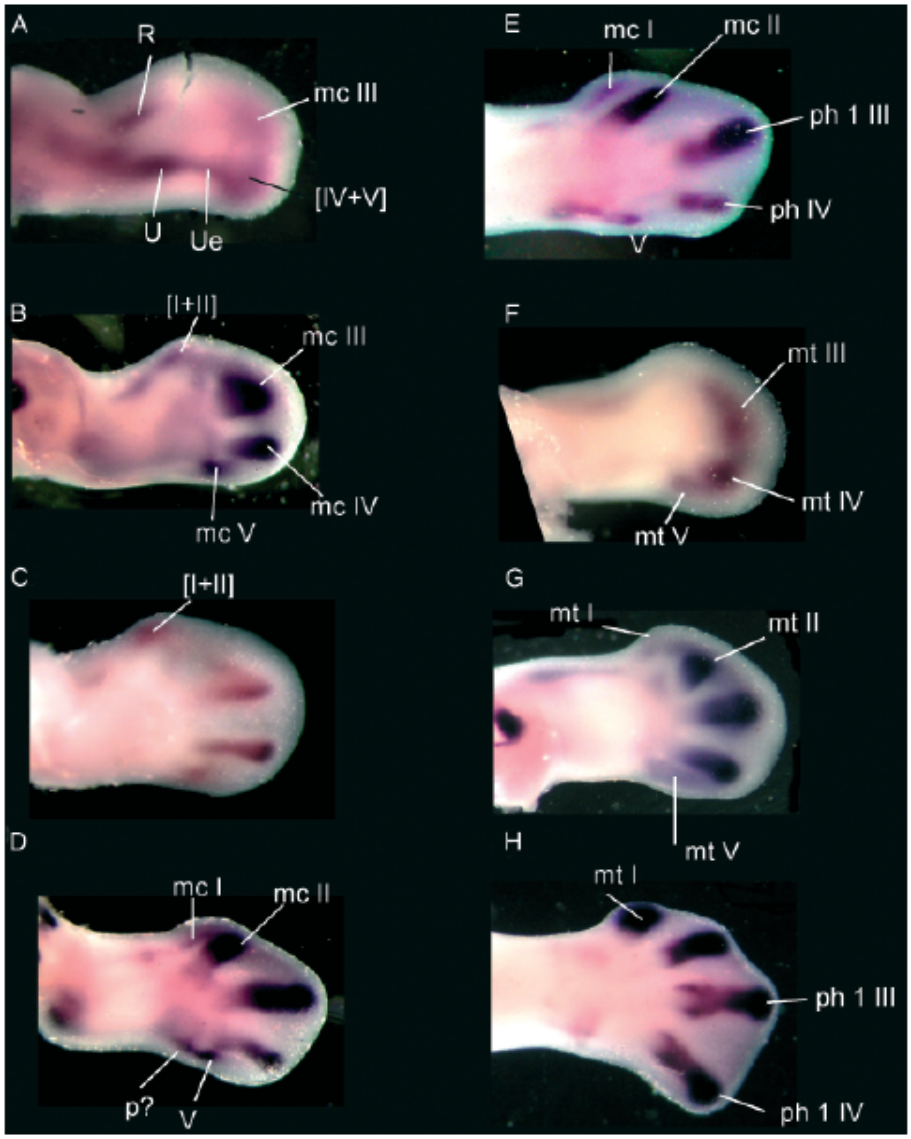

Sox9 expression in the foot

In the foot (Fig. 3, F–H), expression of *Sox9* showed a pattern similar to that in the wing. A significant difference was that we saw no common domain for digits I and II, as we had seen in the wing. Instead, the foot digit I and II domains appeared to develop as separate domains from the outset. Interestingly, the vestigial foot digit (V) showed a weak, elongated domain of expression of *Sox9* at stage 27 (Fig. 3G). This domain therefore bore a close resemblance to that of the vestigial wing digit I (Fig. 3E). We saw no evidence for more than five digit primordia in the chick foot.

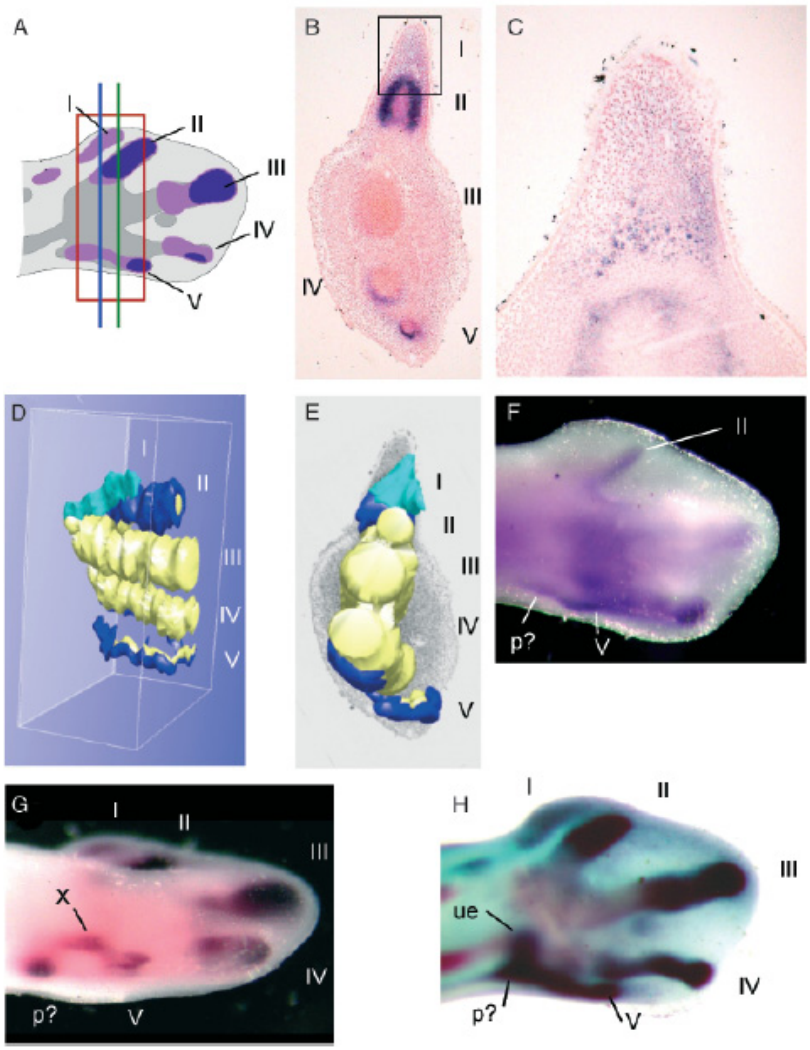

Fig. 4. (A) Schematic interpretation of the *Sox9* gene expression patterns superimposed on cartilage pattern (alcian blue/ in situ double stains).
Roman numerals, digits; vertical green line, plane of section in B; vertical blue line, plane of section in C; dark red box, area reconstructed in D, E.
(B and C) Transverse sections of wings (stage 30, hybridized with *Sox9* probe), neutral red counterstain. Sections from the same specimen, C more proximal than B. (C) Detail from boxed area in B, showing expression of *Sox9* in the noncondensed mesenchyme anterior to digit II. (D) Three-dimensional (3D) reconstruction of the same specimen. Yellow, cartilage; dark blue, gene expression digits II–V; light blue, *Sox9* expression, presumptive digit I. Anterior is to the top. Ventral view. (E) Proximal view of the 3D reconstruction. Anterior to the top. The element at the level ‘‘V’’ may consist of mc V1element X. (F) Left chicken wing, stage 30, *Bmpr-1B* probe. Anterior to the top, ventral view. Distinct prechondrogenic domains are seen in digits II–IV, but not anterior to digit II (labeled II). p?, pisiform. (G) Wing, stage 30, oblique posterior–ventral view, *Sox9* probe. X, element ‘‘X’’; p?, pisiform. (H) Wing, stage 30, overstained in NBT/BCIsubstrate after *Sox9* hybridization, then counterstained with alcian blue and cleared in methyl salicylate. p?, pisiform; ue, ulnare.

Bmpr-1B expression in the wing
The hybridization patterns followed the patterns of *Sox9* expression quite closely and appeared slightly later. At stage 30, no significant expression could be observed in the putative digit I region (Fig. 4F). *Bmpr-1B* expression showed a clear primary axis at stage 26, consisting of hybridization extending from the humerus, and through the ulna to a single common domain for digits IV and V (data not shown).

Bmpr-1B expression in the foot
The notable feature of *Bmpr-1B* expression was strong expression in the vestigial digit V, in contrast to the weak *Sox9* expression in this same digit. *Wnt14* (data not shown) expression was visible initially in the interdigital mesenchyme and along the distal margin of the digital plate. From stage 29 on, *Wnt14* was expressed in the interzones of future joints (Hartmann and Tabin 2001). *Wnt14* expression confirmed that no late digital structures, such as joints, were formed in the digit I Anlage.

Temporal analysis of gene expression during skeletal patterning and development
We made landscape maps showing the relative sequence in which the different cartilage elements were first distinct according to various markers (Fig. 5). As can be seen, there was the expected proximodistal gradient in the appearance of elements, and also some evidence of earlier differentiation along the primary axis. The most notable feature of these maps is that the presumptive *Sox9* digit I domain in the wing (Fig. 5, *Sox9*, wing, arrow) appeared relatively late in the developmental sequence. Thus the temporal homology of the anterior *Sox9* domain was consistent with predictions from the primary axis model, namely that digit I should develop late in the sequence.

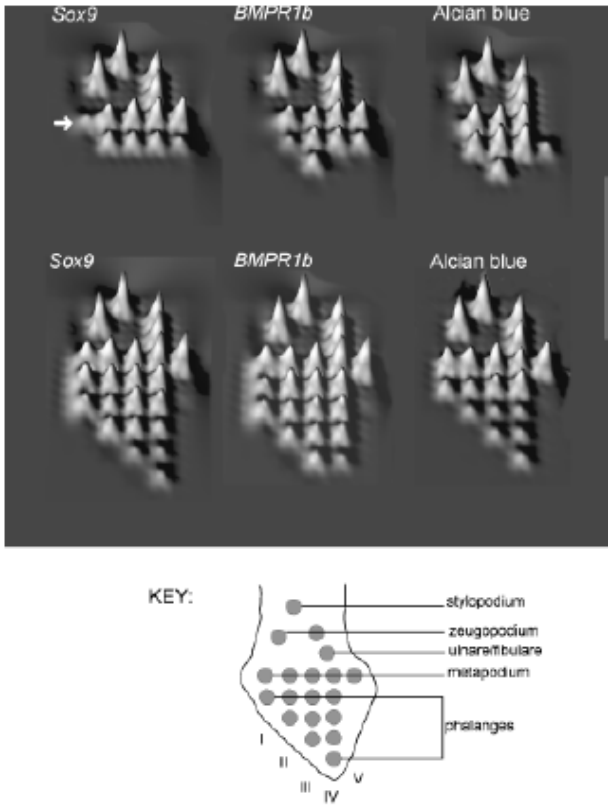

Fig. 5. Developmental timing landscapes showing the relative sequence in which various markers of skeletal formation appear. Schematic palmar views of right limb; proximal is to top, anterior to left (see key for orientation and position of elements). Each element was assigned a rank according to its place in the developmental sequence. The ranks were then inverted so that the earliest elements have a tall peak, and the latest elements have a low peak. Arrow, presumptive wing *Sox9* digit I domain.

DISCUSSION

We have shown evidence of a *Sox9*-expressing domain in the mesenchyme anterior to digit II, and separated from it by a nonexpressing zone. This *Sox9* expression domain was located at the palmar side of the hand, close to the ectoderm of the anterior margin. We suggest that it is reasonable to interpret this domain as being a vestige of digit I, and further argue, on the basis of serial expression patterns, that it splits away from a common digit I–II Anlage around stage 29. This pattern broadly conforms to the ‘‘digit I’’ condensation observed in tissue sections at this stage (Larsson and Wagner 2002). Furthermore, the avascular digit I zone (AZ-1 of Kundrát et al. 2002) resembles in location the digit I *Sox9* domain (compare their Fig. 1C with our Fig. 4B). Finally, the putative *Sox9* digit I domain develops last in the digit sequence, in agreement with the late development of digit I in pentadactyl amniotes (Shubin and Alberch 1986).

Mechanisms of digit reduction and vestige formation

Our study provides evidence that an extensive digit I domain exists in the precondensation limb mesenchyme, but fails to reach condensation and precartilage stages, as shown by lack of *Bmpr-1B* and *Wnt14* expression. This lack of differentiation could explain why no precartilage matrix was found in the putative digit I position by $35SO_4$ labeling (Hinchliffe 1985 book), and supports the idea that the digit I domain shows developmental arrest (Galis et al. 2003).The expression of *Sox9* in this domain is significant, because the gene is thought to be expressed after the initial patterning events have taken place (Akiyama et al. 2002). This supports the idea that in developmental terms, the wing is initially pentadactyl (Kundrát et al. 2002; Larsson and Wagner 2002; Galis et al. 2003). Some block must exist at later stages when digit morphogenesis normally takes place. It is significant that misexpression of *Hoxd-11* leads to formation of a supernumerary digit I in the chick wing digit I (Morgan et al. 1992). Our interpretation of these findings is that the digit I domain fails to develop because it does not receive adequate posterior signals during development; misexpression of *Hoxd-11*, a posterior *Hox* gene, provides those signals and rescues the vestigial digit. We find that other vestigial digits in the chicken show arrest at different points in the sequence of cartilage formation and differentiation (Table 1). Thus wing digit I arrests at the *Sox9*-expressing stage. Foot digit V develops further, expressing *Sox9* weakly, but then showing moderate *Bmpr-1B* expression and some cartilage differentiation. Wing digit V shows strong *Sox9* and *Bmpr-1B* expression, and some cartilage differentiation (summarized in Table 1). We saw no evidence in gene expression patterns for what other workers have described as budding or branching (Shubin and Alberch 1986; Garner and Thomas 2004).What we did observe was the establishment of discrete domains from within a common domain. We do acknowledge, though, that domains remain connected by bridges of less differentiated tissue, and this may create the impression of a branch.

Table 1. Summary of gene expression and development in normal and vestigial chicken digits

	Sox9	*bmpR-1b*	Alcian blue	Final form
Formed digits	+++	+++	+++	Fully developed
Vestigial digits				
Wing digit I	+	+/–	–	Absent
Wing digit V	+++	++	++ (small)	Greatly reduced metacarpal
Foot digit V	++	+++	++ (small)	Greatly reduced metatarsal

Note that the three vestigial digits in the chicken limbs are arrested at different points in their development and differentiation.

From approximately stage 28 onward, the interdigital region in the wing becomes greatly thinned, as does a flange of tissue along its anterior border, which becomes the prepatagium (see Figs. 3 and 4 in Murray and Wilson 1994). The *Sox9* domain for digit I is embedded in the flange, where it lies in close proximity to the ventral ectoderm (Fig. 4).

Frame shift and bilateral (‘‘pyramid’’) reduction hypotheses
Our findings cannot distinguish between the Frame Shift and Pyramid Reduction hypotheses because both of those models accept a vestigial anterior digit in the chick. We are impressed, however, by the rescue of the digit I domain in the chick by *Hoxd-11* misexpression (Morgan et al. 1992). This is consistent with the idea that a shift in anteroposterior positional signalling has occurred in the evolution of birds, such that digit I no longer receives an adequate threshold of posteriorizing signals. One could of course argue that the ‘‘rescued’’ digit I in those experiments was in fact a reduplicated digit II produced by localized mimicking of polarizing activity. However, because expression of the *Hoxd-11*-RCAS construct was ubiquitous in the limb bud, and not localized to the anterior border, we think this objection is unlikely. More recent studies reveal that *Hoxd-11* is expressed from the posterior margin of the autopodium to the cartilage condensation of digit II; it is not expressed in the anterior region of the autopodium (Nelson et al. 1996; Goff and Tabin, 1997). It has been shown that *Hoxd-11* ectopically affects condensation and segmentation of digit I (Goff and Tabin, 1997).

Alternative models
Alternatives to the Frame Shift and bilateral reduction models can be considered:
-The anterior vestige in the chicken embryo wing is not a digit but some other structure or primordium;
-Birds are not a clade within the theropods;
-Digit identities are not meaningful units of homology; rather, they are emergent patterns generated non-specifically by interactions between developmental mechanisms (Goodwin and Trainor 1983); and
-The pentadactyl ‘‘archetype’’ is false and the archosaur limb may in fact be primitively polydactylous.

We will discuss the polydactyly model in some detail, not because we consider it the most parsimonious explanation, but because it has scarcely been discussed in the context of avian evolution for many decades. It also has the unique virtue of providing continuity between digit position and digit identity across archosaur phylogeny. If the vestigial digit I domain of chicks is primitive for archosaurs, then the ‘‘vestigial digits IV and V’’ of *Herrerasaurus* and other archosaurs are in fact digits V and VI (Fig. 2). This would mean that birds could also have a vestigial digit VI as Schestakowa (1927) suggested. Element X or the pisiform are potential candidates for such a vestige. Bardeleben (1889) considered the pisiform of mammals to be a vestige of a sixth digit. This opinion was also held by Holmgren (1952), who viewed the tetrapod limb as primitively seven fingered, on the basis of his extensive developmental studies. Studies in other taxa predict that digital loss should be bilateral, affecting digit I as well as posterior digits (Alberch and Gale 1983). This has always made the asymmetric reduction in archosaurs (affecting digits IV and V) seem anomalous. However, if archosaurs are polydactyl, and have a vestigial digit I domain in their embryos, then there is no anomaly (Fig. 2). Polydactyly is not robustly supported at this time. Most evidence for digit I in birds, and for extra digits generally, is of the ‘‘nodules and shadows’’ type, where morphological vestiges in adults, or histological traces in embryos, are interpreted as recapitulated digits. Other difficulties with a polydactyly theory are: embryos from non-avian theropods are not available for

study; no adult archosaur has six distinct digits; there is no evidence for a vestigial digit I in archosaurs outside birds; and we saw no evidence of more than five digital domains of *Sox9* expression in the chick foot in this study.

Examples of supposed extra digital elements are seen in Batrachomorpha, and include the claimed ‘‘postminimus’’ in the pes of some salamanders (e.g., *Hynobius lichenatus*; Hasumi and Iwsawa 2004), and polydactyly in humans (Biesecker 2002). Late Devonian tetrapods were certainly polydactylous (Coates and Clack 1990) and the Early Carboniferous tetrapod *Pederpes finneyae* is speculated to have had a hexadactylous manus (Clack 2002). However, *Casineria kiddi*, possibly an early amniote, has a pentadactyl manus (Paton et al. 1999).

In summary, we have found molecular evidence of a digit I domain in the chicken wing that is specified by early patterning mechanisms, but fails to undergo terminal differentiation. In the light of previous studies where *Hoxd-11* was misexpressed, we suggest that the digit I domain can be rescued by increasing the strength of posterior patterning signals. Conflicts between fossil and developmental data can be eliminated by a Frame Shift, by bilateral reduction, or by assuming that archosaurs are primitively polydactyl. On the basis of current data, no one model of digit homology is more parsimonious than others.

ACKNOWLEDGEMENTS

We thank M. A. G. De Bakker for helpful advice, and C. J. Tabin, J. M. Hurle and L. Niswander for kindly providing us with the *Wnt14, Sox9*, and *Bmpr-1B* cDNA clones, respectively. R. Tibbits and M. Brittijn helped with the figures. We are especially grateful to F. Zitman for her valuable help with this project. We have had valuable discussions with M. Coates, A. Feduccia, R. Hinchliffe, M. Kundrát, C. Tickle, and G. Wagner, among many others; but this article does not necessarily reflect their views.

Chapter 6

Limb - fin heterochrony: a case study analysis of molecular and morphological characters using frequent episode mining.

R.Bathoorn [3 (a)], M.C.M.Welten [1,2 (b)], A.P.J.M Siebes [3], M.K. Richardson [2] and F.J. Verbeek [1]

1 Imagery and Media, Leiden Institute of Advanced Computer Science,
Leiden University, Niels Bohrweg 1, 2333 CA Leiden, the Netherlands
2 Institute of Biology Leiden, Leiden University, Wassenaarseweg 64, 2311 GP Leiden, the Netherlands
3 Department of Information and Computing Sciences, Utrecht University, Padualaan 14, 3584CH Utrecht, the Netherlands

(a and b equally contributed)

Submitted.

Case study Late zebrafish and cross-species development

ABSTRACT

Developmental biologists use a wide range of vertebrate model species including chicken, mouse, axolotl, clawed toad and zebrafish. In this framework, zebrafish can be considered as the “fruitfly” of the vertebrates as experimental findings are often to be extrapolated to higher vertebrates. To that end, it is important to consider phylogenetic relationships between zebrafish and other model species in order to determine whether gene networks observed in one species are indeed representative for the other. Reconstruction of phylogenetic relationships can also reveal insights into the evolution of developmental mechanisms. One approach is to look at differences in the timing of developmental events, i.e. heterochrony. Analysis of heterochrony can render important information about both development and evolution.

In this paper we address the problem of limb-fin heterochrony by analysing both molecular and morphological characters at the same time and cross species. To that end we focus on a new method for computational analysis, i.e. frequent episode mining in development analysis (FEDA), for reconstruction of phylogenetic trees based on heterochrony in gene expression; through existing methods this could not be solved. We illustrate our approach using spatio-temporal gene expression timing data from limb and fin development. Therefore we have made extensive series of *in situ* hybridizations of a panel of developmental genes in the zebrafish pectoral fin, and compared these with our data from the chick limb as well as with (gene expression) data from other species from the literature. In support of our analysis, a relative time scale of embryonic development is introduced and made part of our computational framework.

This paper explores the application of FEDA based on gene expression patterns and the results provide evidence for the limb-fin heterochrony as well as a much wider scope of application. From our case studies we demonstrate that the method provides an extensive application to complex datasets of increasing complexity. Moreover, for the case studies presented we obtained new results and insights. It can be expected that further application of FEDA will support knowledge discovery in developmental and evolutionary biology.

Keywords: *in situ* hybridization, frequent episode mining, heterochrony, gene expression.

INTRODUCTION

To analyze development, molecular genetics, and genetic networks in zebrafish and other model species, it is important to (a) study evolutionary relationships and consider the model species in the right phylogenetic context, and (b) study to what extent they are representative for each other and for human (Hanken, 1993; Metscher and Ahlberg, 1999). Zebrafish is increasingly popular as a vertebrate model species. It is a lower vertebrate model and thus interesting as a key species. A workflow in developmental biology inspired research could be that initial experiments are carried out in zebrafish, and henceforth extrapolated to other model species. We have taken this route in one of our case studies.

One way to analyze evolutionary relationships between species is based on differences in developmental timing, i.e. heterochrony. In itself, heterochrony is considered as one of the mechanisms producing evolutionary changes. Heterochrony manifests as species difference in growth patterns, in changes of developmental sequences, and changes in temporal patterns of gene expression (Jeffery et al, 2002; Richardson, 2002; Smith, 2002). Several methods have been developed to analyze heterochrony in a phylogenetic framework. These methods are based on heterochrony in sequences of morphological and developmental events (Bininda-Emonds et al, 2003; Jeffery et al, 2005; Schlosser, 2001; Schulmeister and Wheeler, 2002). In this paper we explore Frequent Episode mining in Developmental Analysis (FEDA). The theory of FEDA as a new method to analyze data with a focus on heterochrony in gene expression in an evolutionary and developmental context and with computational numerical evidence is discussed in Bathoorn et al (in preparation). The principle of the FEDA is to analyze sequences of developmental characters to find episodes; these are small ordered sets that are frequent over all developmental sequences considered. These episodes are used to determine differences between developmental sequences (Bathoorn et al., 2007).Two distinct case studies of frequent episode mining are described. These case studies focus on limb and fin development in vertebrates, but differ in the organization and focus of the data as well as model species:

1) A comparative study of gene expression in Zebrafish (*Danio rerio*) fin development and known orthologues in four other model species: African clawed toad (*Xenopus laevis* and *tropicalis*), Mexican axolotl (*Ambystoma mexicanum*), mouse (*Mus musculus*) and chicken (*Gallus gallus*). This employs our own new gene expression data and data from the literature.

2) An analysis of gene expression timing in morphological structures, carried out on data on digit formation in chicken fore and hindlimb (Welten et al, 2005). Here, we show that a heterochronic difference in gene expression can lead to developmental arrest and finally, evolutionary loss of a structure. Forelimb (derived structure) and hindlimb (ancestral condition) are analyzed in the same individual (n = 3-8; c.f. Materials and Methods). Using FEDA we do a reanalysis and evaluation of expression data from our previous study on chicken wing digit homology (Welten et al, 2005).

These studies will provide relevant biological results and at the same time they display possibilities for the applications of frequent episode mining (using FEDA) in specific areas.

The vertebrate limb and fin are well-studied structures in developmental biology and recent studies reveal that a seemingly subtle event like change in gene expression timing can produce gross macro-evolutionary changes (Smith, 2003). In several studies, examples of evolutionary changes through heterochrony in gene expression are given. One example of change in duration of gene expression and effect on outgrowth, and therefore a final structure, is the dolphin flipper (Richardson and Oelschlaeger, 2004). Other examples of heterochrony in gene expression can be found in Blanco et al. (1998); where difference in duration of *hoxa11* expression in *Xenopus* limbs affects the identity of a limb region; in Shapiro et al (2003), describing digit number affected by *sonic hedgehog (shh)* expression (Smith, 2003), and in Zakany et al (1997), showing that a slight time delay in *hox* gene expression (transcriptional heterochrony) in mutant mice leads to caudal transposition of the sacrum. Another example is loss of pelvic spines in freshwater populations of three-spine stickleback. Marine three-spine sticklebacks possess a pelvic skeleton comprising bilateral pelvic spines that articulate with the pelvic girdle (Cole et al. 2004, Shapiro et al. 2004). Several freshwater stickleback populations however, show partial or complete loss of the pelvic skeleton. The marine populations show expression of *pitx1* in the future pelvic region, while *pitx1* expression was absent in freshwater populations of three-spine stickleback (Cole et al.2004; Forster and Baker 2004; Shapiro et al. 2004). Here, the loss of *pitx1* expression leads to reduction of pelvic structures in two different populations of three-spine stickleback.

During embryonic development many genes are expressed and therefore, analysis of heterochrony in gene expression in embryos can provide useful information concerning evolutionary changes and phylogenetic relationship of vertebrate model organisms (Richardson 1995, Jeffery et al, 2002, Smith 2003). Recently, large amounts of gene expression data from different model species became available from functional genomics, clinical research and molecular developmental research (e.g. zebrafish: http://zfin.org, (http://bio-imaging.liacs.nl/), http://cegs.stanford.edu.search.isp; *Xenopus* : http://www.xenbase.org/; for mouse http://genex.hgu.mrc.ac.uk/), for chicken: http://geisha.biosci.arizona.edu/data/, and KEGG www.kegg.org). These online sources can be used to compare gene expression data and gene networks in the different model species.

Case study 1: Comparative study of heterochrony in gene expression

In this case study we want to illustrate the evolutionary relationships among different vertebrates, with a focus on differences in timing of gene expression during limb and fin development. Development of limb and fin is particularly interesting as a case study since paired appendages are unique to jawed vertebrates. Data from the fossil record suggest that the fin-limb transition occurred approximately 410 million years ago (Shubin et al, 2006). Though teleost fins and tetrapod limbs show important differences, the same, highly conserved patterns and genetic pathways are found both in teleost (main subgroup of ray-finned fish) fin and in tetrapod limb development (Coates and Cohn, 1998). For a comparative study of these highly conserved genetic pathways a selection of genes involved in zebrafish paired fin development, of which known orthologues exist in

tetrapod model species, is extracted from literature (Coates and Cohn, 1998, Hinchliffe, 2002; Tickle, 2002). For these genes, probes for Fluorescent *in situ* hybridization (FISH; Welten et al, 2006) and *in situ* hybridization (ISH; Thisse et al, 1993) are synthesized from clones or from cDNA. To obtain additional data, FISH and ISH are applied to developmental series of zebrafish embryos.
For chicken, gene expression data from a previous study were used (Welten et al, 2005). Supplemental data from chicken as well as data for mouse, *Xenopus* and axolotl are extracted from literature.
For *case study 1*, we address and assemble data from five species to apply FEDA, in order to analyse heterochrony in gene expression in five species, in a numeric and evo – devo (evolutionary-developmental) context. Though the evolutionary relationships of the model systems are evident from literature, we use this evidence to validate our algorithm. We expect that FEDA will be able to reconstruct phylogeny based on gene expression data.

Case study 2: Heterochrony within one species
Heterochrony can occur in one single species. To analyze heterochrony in gene expression in one single species, we used data from a study of early molecular markers of chondrogenesis in relation to a rudimentary digit I in the bird wing embryo (Welten et al, 2005; cf. **Chapter 5**). Other examples of heterochrony in gene expression within one species can be found in Blanco et al (1998), describing heterochronic differences in *hoxa-11* expression in *Xenopus* fore and hindlimb that affects the regional identity of tarsal bones within one individual.
In a previous study, chicken was used as a model to study digit loss (Welten et al., 2005; cf. **Chapter 5**) since chicken limb is a well-studied structure and many probes are available for developmental analysis. A *sox9* expression domain was found for a vestigial digit I (Welten et al., 2005). In the presumptive digit I domain no expression is found for subsequent markers from the molecular cascade of chondrogenesis. The onset of *sox9* in the presumptive digit I domain is relatively late compared to the other digits (Welten et al, 2005).
In *case study 2*, gene expression data of markers from the molecular cascade of chondrogenesis in chicken in hind limb and wing (Welten et al, 2005) are processed with frequent episode mining algorithm. In the chicken embryo, five digit primordia are found in the foot; in the wing 3 digit primordia are found. In the adult however, the chicken foot is four-toed while the wing is only three-fingered. In this analysis the five-toed foot of the chicken embryo is used as a reference for digit formation timing; timing data of the wing - which has three digits in the adult - are thus compared to timing data of the foot. In this particular application, FEDA is used to analyze heterochrony in gene expression in fore and hindlimb within one species.

Relative time scale of development
The onset of limb formation is variable among the different model species (Richardson, 1995). In chicken and mouse, limbs are formed during somitogenesis. In Axolotl and zebrafish, the formation of the forelimbs and pectoral fins respectively, occurs long after the end of somitogenesis (Bordzilowskaya, 1989; Kimmel et al, 1995). In *Xenopus*,

hindlimbs develop before forelimbs, relatively late, after completion of somitogenesis (Richardson 1995).
Taking these differences into consideration as well as to enable comparison, a relative time scale of development during which limb and fin development occur is computed for every single model species (cf. Materials and Methods). For the application of FEDA to gene expression data in the chicken wing and hindlimb, a different relative time scale is specified for limb development (cf. Materials and Methods).

The remaining part of this paper is structured as follows: in the Materials and Methods section we describe the pre-processing, aggregation and analysis of data, and the calculation of the relative time scale of development. In the Results section, we describe the outcome of the analysis. In the Discussion and Conclusion sections, we address the results of our experiments and we present conclusions as well as directions for future research.

MATERIALS AND METHODS

For both applications, the preprocessing of gene expression data to make them suitable for FEDA, as well as the different relative time scales are described in the next ten subsections.

Case study 1: Comparative study of heterochrony in gene expression
Selection of genes
Data regarding genes, indicated in the literature as markers genes in limb and fin development, myogenesis, cartilage and joint formation, as well as *Hox* genes involved in limb and fin development, are extracted from literature (Coates and Cohn, 1998; Duprez, 2002; Hinchliffe, 2002; Karsenty and Wagner, 2002; Tickle, 2002). In Table 1, the selected genes, a description of the expression site in limb or fin, and corresponding Gene Ontology term (http://www.geneontology.org/) are summarized. Gene Ontology terms are included as these are based on a controlled vocabulary, such providing unique identifiers for further research and interoperable search in databases. GO is applicable to a range of species, combining biological processes and corresponding molecular and cellular functions of genes (The Gene Ontology Consortium, 2000; Camon et al, 2004). Moreover, we are aware that in zebrafish duplication of some of the genes has occurred (Akimenko et al. 1995; Amores et al.1998; Yan et al. 2004). Zebrafish isoforms of the genes used in *case study 1* are summarized in Table 1.

Obtaining new and existing gene expression data
Zebrafish were maintained under standard conditions (http://zfin.org) in our facilities. Zebrafish embryos were harvested and staged to hours post fertilization, as described by Kimmel et al. (1995) and processed for *in situ* hybridization (ISH) and fluorescent *in situ* hybridization (FISH; Welten et al, 2006) during subsequent stages of pectoral fin development (24 -120 hpf; Kimmel et al, 1995). Imaging was performed as previously described (Welten et al., 2006).
Chicken (*Gallus gallus domesticus)* gene expression data were obtained from ISH experiments for *sox9, bmpr1b* and *wnt-14*. Supplementary to these experimental data a selected panel of genes involved in limb development (cf Table 1) was assembled by literature search.
In addition to the experimental data, gene expression data of the relevant model species (mouse *(Mus musculus), clawed toad (Xenopus laevis / tropicalis)*, and axlolotl *(Ambystoma mexicanum)) were* collected through literature search (Pubmed http://www.ncbi.nlm.nih.gov/entrez/, Google Scholar http://scholar.google.nl/).

Table 1.
Selection of genes used for heterochrony analysis in five model species. Gene function, name, and expression site in fin or limb are given. The corresponding Gene Ontology term refers to the biological process described in Gene Ontology

Gene function	**Gene name and expression site**	**Gene Ontology Term**
Limb initiation and identity	*tbx5;* expressed in forelimb mesenchyme	GO 0030326
Limb patterning and outgrowth	*fgf8;* expressed in Apical Ectodermal Ridge.	GO 0030326 GO 0051216
	sonic hedgehog; expressed in zone of polarizing activity	GO 0030326
	msx2, (*msx–b* for zebrafish), expressed in Apical Ectodermal Ridge	GO 0030326
Cartilage and joint formation	*sox9* (*sox9a* and *sox9b*, zebrafish), expressed before prechondronic condensation	GO 0030326 GO 0001501 GO 0051216
	runx2 (*runx2a* and *runx2b*, zebrafish), expressed in chondrogenic condensation and in osteoblasts	GO 0001501 GO 0051216 GO 0001503
	bmpr1b; expressed in chondrogenic condensation	GO 0001501 GO 0051216
	Wnt-14 (wnt9a): expressed in joints	GO 0030326
	Chondromodulin-1; expressed in chondrogenic cells	GO 0006029
Myogenesis	*myoD,* expressed in myogenic tissue	GO 0007517 GO 0007519
Posterior *hox* genes involved in limb development	*Hoxa9;* tail and pectoral fin mesenchyme	GO 0007275
	hoxb13; tail mesenchyme	GO 0009611 GO 0040008 GO 0008544
	hoxc12; tail mesenchyme fin mesenchyme	GO 0007275
	hoxd9; tail and pectoral fin mesenchyme	GO 0007275
	hoxd11; tail and posterior region of fin / limb bud	GO 0007275 GO 0001501 GO 0001759

Aggregation of spatio-temporal data

We focused on gene expression data that have been obtained from whole mount *in situ* experiments. These give both a spatial and a temporal clue. Both ISH data from literature and data generated by "in house" FISH and ISH (zebrafish and chicken, respectively) are organized in a spreadsheet table. Data are categorized according subsequent developmental stages, from limb bud stages to juvenile.

In the table, gene expression data are attributed a quadruplet consisting of:

1) Normal stage of embryonic development,
2) Corresponding age in developmental units, i.e. embryonic or larval day,
3) A corresponding relative time scale from fertilization to juvenile,
4) Presence at a particular stage.

As an example an excerpt from our spreadsheet table for *sox9a* expression in zebrafish pectoral fin, is given in Table 2.

Table 2. Spreadsheet table of *sox9a* expression in zebrafish pectoral fin.

Gene	Developmental stage (Kimmel et al, 1995)	Age (days)	% of development	Presence
sox9a	Prim 5	1 day	20%	no
sox9a	High pec	2 days	40%	yes
bmpr1b	High pec	2days	40%	yes

Relative time scale of development in comparative study of heterochrony

For the comparative study of the five species, the relative time scale is computed for every single model species. The relative time scale indicates a ratio of complete development, but also relative to limb development. For all species the onset, i.e. 0%, is set up at fertilization. For practical reasons the 100% stage was chosen differently for every model species. As a criterion for 100% of development, independent feeding (zebrafish, mouse, chicken) or juvenile stages (clawed toad, axolotl) was chosen.

For chicken, hatching, and for mouse, birth is considered as 100% of development (Hamburger and Hamilton, 1951; Theiler, 1972 respectively). For zebrafish, the relative time scale is calculated up to 96 hpf, as it reaches the early larval stage, though the pectoral fins are still developing during this stage. The pelvic fins develop during late larval stages (Kimmel et al, 1995, Grandel and Schulte - Merker, 1998). For clawed toad and axolotl, the relative time scale of development is calculated up to juvenile stages, since limb development occurs during larval stages (for *Xenopus:* Nieuwkoop and Faber, 1967; for Axolotl: Bordzilowskaya et al, 1989; Nye et al, 2003).

Gene expression data are organized according to subsequent developmental stages. In Table 3 the relative time scale computation, relative time point of appearance of fore and hind limb buds, as well as references for stages of embryonic development are summarized.

Table 3. Extraction of features used in data collection.

Species	**Stage, 100% of development**	**First appearance of limb/fin bud**		**% of development, first appearance limb/fin bud**		**Reference (cf. References)**
		fore/ pectoral	hind/ pelvic	fore/ pectoral	hind/ pelvic	
Zebrafish	96 hpf (Kimmel, 1995)	prim 18	larva (>21 days)	31%	100%	Kimmel et al, 1995.
Xenopus	Juvenile, 58 days (N & F 66)	NF 48	NF 46	13%	8%	Nieuwkoop and Faber, 1967
Axolotl	Juvenile, > 36 days (Nye 57)	B. 37	Nye 51	19%	82%	Bordzilowskaya et al, 1989; Nye et al, 2003
Mouse	Newborn mouse, 19-20 days (Th 27)	Th 15	Th 16	50%	53%	Theiler, 1972
Chicken	Hatching, 21 days (H&H 46)	H& H 16	H&H 17	Ca.10%	Ca. 11%	Hamburger and Hamilton, 1951

Data analysis

The datasets are collected in spreadsheet tables and subsequently converted to comma separated values (CSV) files; these files are the input for analysis with FEDA (Bathoorn et al 2007). After initialization in the Frequent Episode tree, the Jaccard distance is computed and next a clustering is applied. From the clustering a cladogram can be derived and visualized. In this cladogram, species are expressed in clusters, depending on the rate of difference i.e. Jaccard distance, between the species (Bathoorn et al, in preparation).

Case study 2: Heterochrony in gene expression in the chicken wing and hindlimb

Preprocession of data

For chicken (*Gallus gallus domesticus*), gene expression data of chondrogenesis markers (*sox9, bmpr1b*) and alcian blue staining for cartilage formation from stages 24 – 34 (Hamburger and Hamilton, 1951; Murray and Wilson, 1994) are recorded for the skeletal elements in the fore and hindlimb (Welten et al, 2005). All skeletal elements are recorded in a proximo-distal order: from humerus and femur (upper arm or leg) to the phalanges in the autopodium (hand and foot).

Aggregation of spatio-temporal data

Skeletal elements are organized according to proximal (humerus / femur) to distal position (phalanges) and plotted against onset and duration of gene expression.

Relative time scale of development tin context of wing and hind limb development

For the application of FEDA to gene expression data in the chicken wing and hindlimb, a relative time scale of limb development is implemented. The onset of cartilage formation in the stylopodium i.e., upper arm or leg, is considered as 0 % of development (Hamburger and Hamilton stage 24). Chondrification of the digits is considered as 100% of development (Hamburger and Hamilton stage 34), all total a time span of four days (Hamburger and Hamilton, 1951; Murray and Wilson, 1994). All stages between HH 24 and 34 represent a ratio of development.

In this application FEDA is used to analyze heterochrony in gene expression in morphological structures, to show that morphological differences between fore and hindlimb within one species can be the result of heterochrony in gene expression in these different regions.

In like manner to the previous case study the data are imported to the FEDA as CSV-files.

Data analysis

Application of FEDA in this case study required a different organization of the data with respect to the previous that was concerning more species. Skeletal elements and future skeletal elements are organized according proximo-distal sequence along the limb. Presence of gene expression at a particular developmental stage (Hamburger and Hamilton, 1951) is scored for proximal, carpal and digit I t/m digit V region. In Table 4, an example is presented for *sox9* expression in the chicken wing.

Table 4. Spreadsheet table of s*ox9* gene expression data in the chicken wing. Onset of *sox9* gene expression in future skeletal elements is scored in proximal, carpal and digit regions. Onset of gene expression is scored at stages according to Hamburger and Hamilton (1951) and corresponding percentage of limb development.

Skeletal element	Proximal *sox9* expression	Carpal *sox9* expression	Digit I *sox9* expression	Digit II *sox9* expression
Ulna	HH 24 / 15%			
Ulnare		HH 25 / 30%		
Metacarpal			HH 30 / 50%	HH 30 / 50%

In this application, the occurrence of frequently found patterns, i.e. (future) skeletal elements, is analyzed for the chosen chondrogenesis markers: *sox9* and *bmpr1b* as well as cartilage formation, visualized with alcian blue staining. The computed pattern shift results in a so –called pattern shift diagram. In this diagram, shift in timing of gene expression in different locations in one single organism is shown in relation to percentage of limb development (cf. Figure 3).

RESULTS

Comparative study of heterochrony in gene expression

Application of FEDA to gene expression data in different model species has resulted in a cladogram which is depicted in Fig.1. This tree, based on gene expression data, is

completely consistent with the cladogram described in Metscher and Ahlberg (1999) as well as with cladograms described in the Tree of Life website (http://tolweb.org/tree/phylogeny.html); ergo phylogenetic reconstruction based on gene expression in limb / fin is conform phylogenetic reconstructions based on morphological characters.

From the cladogram it is immediately visible that zebrafish is separated from the tetrapods, while the tetrapod cluster itself contains two groups: the amphibians (*Xenopus* and axolotl) and the amniotes (chicken and mouse).

Analysis of the differences at the nodes of the cladogram is in correspondence with literature. For instance, the genetic pathway responsible for limb initiation, patterning and outgrowth (*tbx5, fgf8, msx2, sonic hedgehog*) is found in all 5 model species, though relative timing and duration of gene expression is different for the 5 model species.

The axis in Fig.1 shows Jaccard distance i.e., the rate of dissimilarity between species. (Bathoorn et al, in preparation). In this cladogram, it does not relate to mutation speed or evolutionary divergence time.

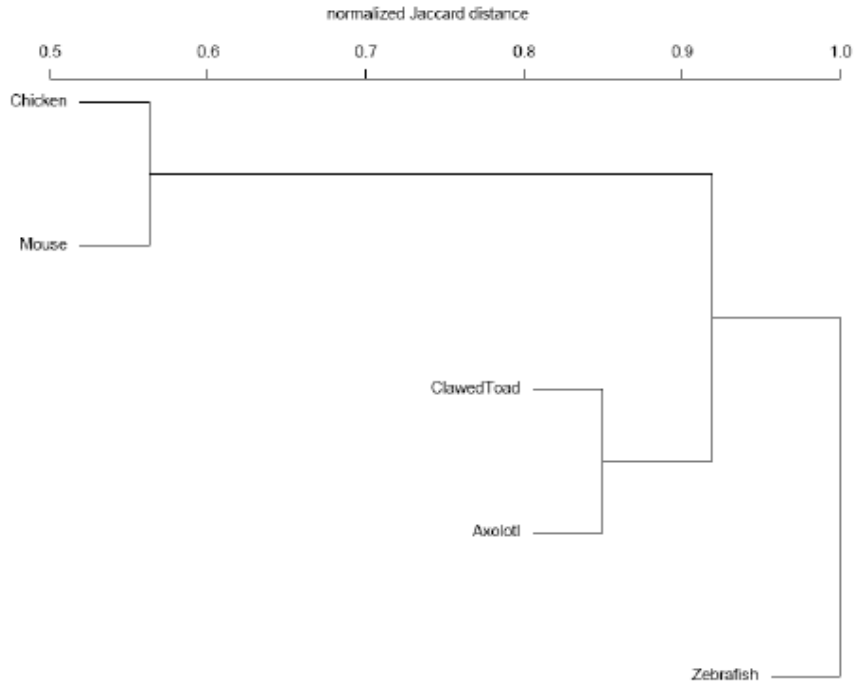

Fig. 1. Phylogenetic tree, based on gene expression data, constructed with Frequent episode mining. The x-axis in the tree depicts Jaccard distance (Bathoorn et al, 2006), which can be explained as the numerical rate of dissimilarity between species. Numbers 0 -1 on the axis indicate increase of dissimilarity. According to the computations (Bathoorn et al, in preparation), the amniote taxa (chicken and mouse) are closest together and are clustered in one group. The amphibians, *Xenopus* and axolotl, showing a high rate of dissimilarity, are clustered in a different group. The zebrafish, which is the lowest vertebrate, show highest dissimilarity to the other species.

In *case study 1*, gene expression data for several markers of chondrogenesis were used (*sox9, runx2, bmpr-1b* and *chondromodulin-1*). Gene expression data for chondrogenesis markers were available from literature for nearly all model systems. For zebrafish however, *bmpr1b* expression has only been described at pre- limb bud stages (Nikaido et al, 1999). For FEDA we concluded that bmpr1b should be part of a certain episode. This could be confirmed by doing a FISH / ISH experiment in zebrafish at 36-72 hpf. Indeed expression of *bmpr1b* was found in the pectoral fins and in skeletal elements at these stages of development (Fig.2). This illustrates that FEDA provides possibility to predict gene activity in a particular species, at absence of gene expression data for this species. From the FEDA output as well as from pilot experiments, functional studies can be carried out to further characterize the role of the gene in this particular species (cf. Discussion).

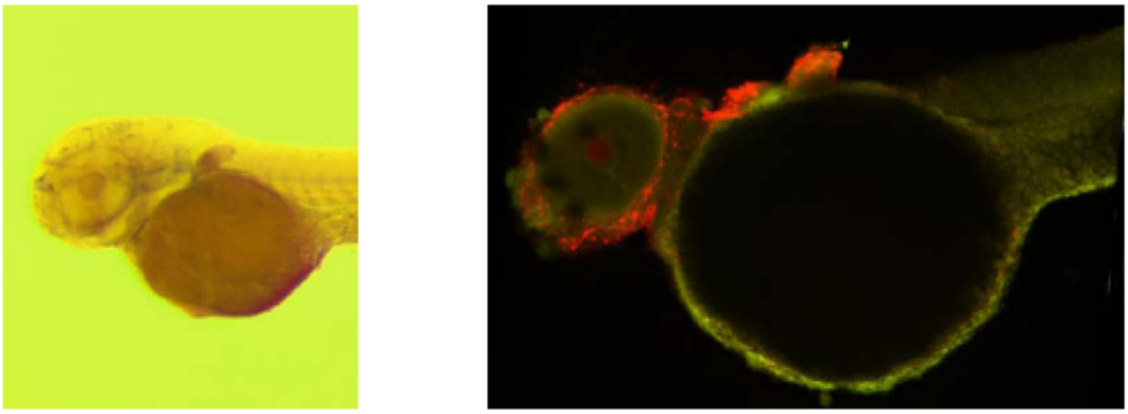

Fig. 2. *bmpr-1b* expression in zebrafish pectoral fin and branchial arches at 48 hpf. Anterior is to the left, dorsal to the top. Left panel : ISH result from AP detection method; Right panel: FISH result. The picture is the result of the projection of a 2 channel 3D confocal image. The expression is in red, i.e. the red channel of the CLSM image, the green depicts a standard staining of the cell nuclei.

Heterochrony in gene expression in the chicken wing and hindlimb

The aim of this application was to show that the apparent differences in fore and hind limb of chicken may be the result of a shift in gene expression timing. Our method clearly visualizes timing shifts at different levels, i.e. on the level of gene expression and on the level of cartilage formation. In the heterochrony study of gene expression in chicken wing and hindlimb, timing differences for *sox9, bmpr1b* expression and cartilage formation are visualized in the pattern shift diagram in Fig.3. Data for wing and hindlimb are displayed in the relative time scale of cartilage formation in wing and hindlimb (cf. Materials and Methods). The onset of cartilage formation in the proximal part of the limb bud is determined as 0 % of development, where completion of cartilage formation in the digits is determined as 100% of development (Murray and Wilson 1994; own experiments). The heterochrony is considered and represented in the form of a so-called pattern shift diagram. In the pattern shift diagram, the relative position of red (wing) and green (hindlimb) along the relative time scale of limb development indicates the onset and duration of gene expression in wing or hindlimb. The onset of *sox9, bmpr1b* and cartilage formation in the metacarpals (mc) and metatarsals (mt), is first observed in mc

and mt IV and V, followed by mc / mt III and II. *sox9* gene expression is present in mc of digit I of both wing and hindlimb. The pattern shift diagram clearly illustrates that *sox9* gene expression in metacarpal I in the wing appears late compared
to hindlimb metatarsal I. From the pattern shift diagram is also visible that no subsequent gene expression for *bmpr1b* and no cartilage formation are observed in metacarpal I in the wing. In the primordia of wing digit II – IV, foot digit I-IV and rudimentary foot digit V, *bmpr1b* expression is found; these primordia develop into fully ossified digits. This is in full agreement with previous studies (e.g. Burke and Feduccia 2002; Larsson and Wagner 2002; Kundrat et al. 2002; Welten et al. (2005)).

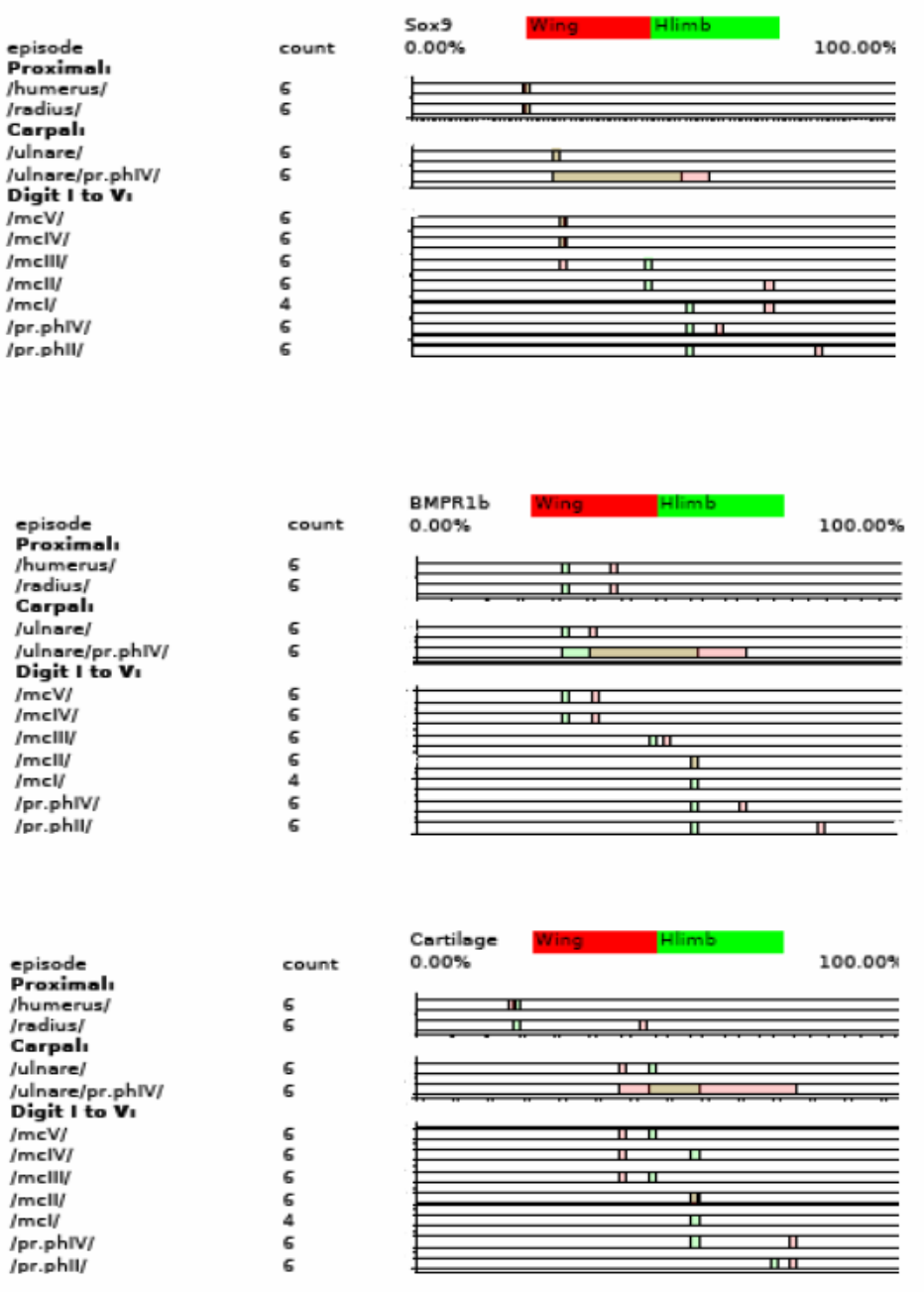

Fig.3

Fig. 3. Pattern shift diagram showing episodes, frequently found sequences (Bathoorn et al, in preparation) of skeletal elements plotted against duration of gene expression, using a relative time scale of chicken limb development. The diagram shows a selection from the total analysis of gene expression timing and cartilage formation in chicken wing and hind limb. Onset and duration of gene expression as well as alcian blue staining for cartilage formation are shown in the red bar (wing) and in the green bar (hind limb). Structures are organized in proximal, carpal and digit region. The pattern shift diagram shows that only *sox9* gene expression is found in the presumptive wing metacarpal (mc) I while no subsequent *bmpr1b* expression and cartilage formation are found in the presumptive wing mc I. The onset of gene expression in presumptive wing mc I is relatively late compared to metacarpals and proximal phalanges of digit II and IV. The pattern shift diagram clearly illustrates that the difference in number of digits between wing and hind limb skeleton is the result of a time shift in gene expression.
mc metacarpal, mt metatarsal, ph phalanx, pr.ph proximal phalanx. Metacarpals / tarsals and digits are indicated with roman numerals (cf. Welten et al., 2005).

DISCUSSION

Several methods have previously been developed for the analysis of heterochrony in a phylogenetic context. Methods include event pairing (Smith, 2002, Jeffery et al, 2002 and 2005), search – based character optimization (Schulmeister and Wheeler, 2004). These methods have been presented based on morphological criteria. In this study, frequent episode mining is used to show that evolutionary relations can be reconstructed on the basis of gene expression data, morphological criteria (Bathoorn et al, 2006), temporal data and combinations of all these data.

First, we present a tree showing the phylogenetic relations of five laboratory model organisms that is produced with our frequent episode-mining algorithm. The reconstruction is based on differences in timing of gene expression in the selected model organisms. The phylogenetic relationships of these model systems are evident from literature; from this evidence we were able to validate our algorithm. In order to be able to compare development, a relative time scale of development from fertilization (0%) to juvenile (100%) is made part of the analysis (Bathoorn et al, 2007). The phylogenetic tree, based on gene expression data and produced from the results of FEDA, is consistent with phylogenetic trees described in literature. The differences at the nodes of the cladogram produced by FEDA are consistent with literature. Although most genes are present in all five model species, onset and duration of expression of these genes show a wide variation between species. For instance, the genetic pathway responsible for limb initiation, patterning and outgrowth is found to be present in all 5 model species. In mouse, chicken, axolotl and zebrafish, *fgf8* expression occurs in pre-limb bud stages. In *Xenopus* however, *fgf8* is expressed at later stages (Christen and Slack, 1997). *Tbx5* expression, which occurs in the forelimb only, is delayed in *Xenopus* since forelimb develops later than hindlimb in *Xenopus* (Kahn et al, 2002).

Analysis of differences at the nodes of the cladogram provides the possibility to predict presence of gene activity (gene expression) in a model species, when no data are available for a particular species. In our study, markers from the molecular cascade of chondrogenesis (*sox9, bmpr1b, runx2*) are found in most of the species. For zebrafish,

bmpr1b data were absent in a certain episode. From literature, no zebrafish *bmpr1b* gene expression data are available in relation to chondrogenesis; only gene expression patterns from younger stages have been described (Nikaido et al, 1999). FISH experiments for our case study exhibit *bmpr1b* expression in the pectoral fin: most likely in the endoskeletal disc and other skeletal structures. Recent images from large – scale screening also display *bmpr1b* expression in the pectoral fin (Thisse et al.; www.zfin.org). Further experiments are needed to investigate the function of *bmpr1b* in zebrafish and its possible role in zebrafish chondrogenesis. In *case study 1* we demonstrate that FEDA is capable of revealing presence of gene expression if no data are available for a particular species. FEDA can be tuned to specifically output such prediction. In our application, the prediction was not focused on. The more gene expression data are available for FEDA, the higher the predictive power of our method will be.

In the phylogenetic tree in Fig. 1, the model species are clustered in different groups. The clustering in the cladogram (Fig. 1) is based on Jaccard distance expressing dissimilarity between species (Bathoorn et al., in preparation). The cladogram shows that chicken and mouse in the amniote cluster display lower numerical dissimilarity than the dissimilarity computed for *Xenopus* and axolotl in the amphibian cluster; according to existing established knowledge. Amphibians show more diverse body plans than amniotes in general. Moreover, amphibians hatch at a relatively early stage, so that juveniles are more subject to evolutionary changes (Bininda- Emonds et al, 2003).

In contrast to methods previously described, application of the FEDA algorithm produces a numerical value to express the rate of difference between species i.e., the Jaccard distance. This distance measure helps to clearly quantify differences between species in the context of gene expression.

The relative time scales we implemented in this study are based either on the developmental stages in which the limbs or fins develop or on the stages in which cartilage develops in the skeletal structures of hind and forelimb. Alternatively, somite number can be used as a time scale indicator on which timing of limb or fin development can be mapped (Richardson, 1995). In our study we chose a relative time scale from fertilization to juvenile, since in some model species, limbs develop long after completion of somitogenesis (Richardson, 1995). FEDA has shown to be able to deal with the different relative timing schemes that we used in the case studies. In future applications this flexibility should be further explored.

In general, lack of data might influence the accuracy for construction of phylogenetic trees. For some species, spatio-temporal gene expression data available from literature are absent or sparse. FEDA is capable to find a solution despite of sparseness or complete lack of data, since it uses episodes, collections of events (Bathoorn et al, in preparation). Missing an event, only means that the episode cannot be found for a particular species, but it can still be found for the other species. This feature again emphasizes the flexibility in data arrangement of FEDA.

In the lizard genus *Hemiergis* digit reduction is found in several closely related species (Shapiro, 2002; Shapiro et al. 2003). The mechanism underlying this phenomenon cannot simply be explained by heterochrony of the process of chondrification and ossification alone but rather by the molecular cascades underlying these processes. When timing of cartilage formation was compared between lizard species, cartilage elements in the digits were formed at approximately the same stages until digits were fully developed (Shapiro,

2002). On the level of gene expression however, a difference in duration of exposure to *shh* expression was observed among the four *Hemiergis* species (Shapiro et al. 2003). The limb buds of the five-fingered *Hemiergis initialis* displayed a later offset of *shh* expression than those of *Hemiergis quadrilineatus*, which has only two digits. This indicates that heterochrony may be found at different levels of developmental processes (Shapiro et al. 2003). In like manner, we analyzed heterochrony in gene expression as well as in cartilage formation in chicken wing and hindlimb digits (cf. *case study 2*). In *case study 2* FEDA is used to analyze heterochrony at different views on developmental processes; i.e. gene expression, organogenesis, morphology. Therefore, FEDA was applied to investigate onset of gene expression in future skeletal structures in the autopodium (hand or foot) of one species. Additionally, timing of cartilage formation was analyzed. With the pattern shift diagram (Fig.3) we demonstrate that FEDA is capable to display heterochrony in various developmental processes.

Different morphological features in fore and hindlimbs of one species may be the result of a shift in gene expression timing in one of these regions in relation to the other. A wide range of genes is involved in digit patterning and specification of digit identity (Dahn and Fallon 2000, Litingtung et al. 2002; Shapiro et al. 2003; Tiecke et al. 2007). It has been shown that *shh* has a direct role in the regulation of *sox9* (Tavella et al. 2004). For our analysis, more gene expression data are needed to further investigate whether heterochrony in *sox9* expression observed in Fig. 3 is caused by changes in timing of gene expression of other genes such as *shh.*

In all cases, an existing dataset can still be used when adding more species to the dataset. Only a new computation for these new species needs to be performed. When more genes are added to the dataset, re-evaluation of the complete dataset is required. In this manner, our method is capable of dealing with large datasets. This is an important characteristic since the amount of gene expression data available from large genomic screens, functional genomics and molecular genetics, is still growing. Analyzing the gene expression patterns in the manner presented will render new insights.

Conclusions and future work

Our two case studies show that heterochrony in gene expression in limb-fin development can be studied very well using the computational approach provided by FEDA. We have shown that heterochrony in gene expression between species (case study 1) and within species (case study 2) was elucidated in both cases. The frequent episode mining on the data that we have aggregated for our studies was sufficient to analyse analyze limb-fin heterochrony in gene expression in both a phylogenetic framework and in relation to different time scales. The development of a relative time scale was crucial to the outcomes presented for this studies; it supported heterochrony analysis of gene expression with FEDA and allowed flexibility in data preparation (Bathoorn et al., in preparation).

We have used standard visualization methods for the phylogenetic analysis; for the pattern shift study a new method was introduced to visualize the results of FEDA. With this visualization method, heterochrony can be revealed at different levels of developmental process. This is a potentially useful tool in evo-devo research problems.

FEDA has shown to be a very powerful and flexible method. Data can be rearranged such that several features can be compared in the analysis; i.e., gene expression, morphological

structures, or species. This flexibility contributes to utility in the analysis of developmental differences such as heterochrony. FEDA computations result in numerical values to express difference between species, i.e., Jaccard distance (cf. figure 1), which represents an objective measure of dissimilarity between entities in data.
FEDA can be engaged in the prediction of gene expression, when data are incomplete.
The computational framework of FEDA will be employed in future work in the analysis of spatiotemporal gene expression data available from structured repositories (Belmamoune and Verbeek, 2006). In the analysis presented in this paper data were based on in situ gene expression data; a next step is to include data from microarray in the analysis. This next step will provide new possibilities in the heterogeneous and comprehensive analysis of genetic networks and evolutionary relationships.

ACKNOWLEDGEMENTS

This project is partially supported by The Netherlands Research Council through the BioMolecular Informatics programme of Chemical Sciences (grant number # 050.50.213). We thank M.A.G. de Bakker and G.E.M. Lamers for their valuable advice, and O. Ayachi, E.M. Dondorp and R.T. Schoon for their help with the *in situ* hybridizations. We also thank M. Akimenko, P.W. Ingham, C. and B. Thisse, J. Postlethwait, N. Ueno, C. Shukunami and J. Bakkers for kindly providing us the cDNA clones for *msxb, tbx5, fgf8, sox9, bmpr1b, chondromodulin-1,* and *myoD,* respectively.

Chapter 7

General discussion and conclusions

General discussion and conclusions

In this thesis we explored *in situ* hybridization techniques and computerized tools to study gene expression patterns during embryonic development. We applied these tools to investigate several developmental processes in both zebrafish and chicken embryos and in two groups of case studies.

In order to study differentiation and patterning of organ systems during embryonic development, both spatial, as true 3D data, and temporal information is required. True 3D data of gene expression patterns and anatomical structures provide most information. In this thesis, the focus was on obtaining 3D spatial and temporal gene expression data during embryonic development. Therefore, we have developed a whole-mount fluorescent *in situ* hybridization protocol: ZebraFISH. The ZebraFISH method is particularly suitable for 3D imaging of whole mount zebrafish embryos with confocal laser scanning microscopy (CLSM).

In **Chapter 2** we describe the ZebraFISH protocol and underlying methodology. Our method is based on Tyramide Signal Amplification (TSA) and proved to be a powerful, sensitive method to visualize gene expression patterns. In this detection method the presence of horseradish peroxidase catalyses the deposit of cyanine labelled tyramide at the site of hybridisation. TSA yields a strong expression signal with a relatively low background in a short defined staining time (Clay and Ramakrishnan, 2005; Zaidi et al. 2000). Even weak probes and small gene expression domains can be visualized. Stronger amplification of weak signal can be obtained by using TSA Plus (Perkin Elmer).

In order to obtain a large amount of 3D gene expression data, we developed a workflow based on the use of ZebraFISH, confocal laser scanning microscopy and 3D modelling with three- dimensional reconstruction software TDR-3Dbase (Verbeek et al. 2000).

In this thesis, all FISH experiments were carried out manually. The one-step antibody detection method used in ZebraFISH is a major advantage for application of ZebraFISH in a high throughput setting and for use in a robot. Subsequent imaging with CLSM is a more time-consuming process than imaging with fluorescent or bright-field microscopy. These images however, provide only 2D information. For the research described in this thesis, each CLSM image slice was sampled to 1024 x 1024 pixels, providing high-resolution 3D images. Although this is a time-consuming process, these high-resolution images allow precise 3D reconstructions. Therefore, in comparison with *in situ* hybridisation (ISH) and subsequent serial sectioning, our workflow provides the possibility to produce a large amount of 3D gene expression data in an accurate and non-destructive manner.

The CLSM work described in this thesis was performed with a Leica TCS/ SP DM IRBE confocal laser scanning microscope equipped with an Ar/Kr laser. Dependent on the laser lines available, a wide range of fluorescent labels can be used to discern gene expression, anatomical structures and the outline of the embryo. Also, tissue-specific fluorescent markers can be used to more accurately annotate gene expression patterns on specific tissues and developing organs.

CLSM proved to be suitable for imaging whole mount zebrafish embryos. In order to overcome the limitations in specimen depth scanning of the CLSM, multiphoton microscopy can be applied to obtain images of complete embryos. In like manner, excellent results with Optical Projection Tomography (OPT) have been presented for mouse (Sharpe et al. 2002; http://genex.hgu.mrc.ac.uk/OPT_Microscopy), for human

(Kerwin et al. 2004; http://www.ncl.ac.uk/ihg/EADHB/) and for zebrafish (Bryson-Richardson et al. 2007; http://www.fishnet.org.au). Imaging with CLSM is limited to fluorescently labelled specimens only, whereas OPT allows 3D imaging of chromogenic ISH as well as many other experiments (Sharpe et al. 2002).
The voxel size in OPT is about 10x10x10 μm (http://genex.hgu.mrc.ac.uk/Emage/database). With CLSM, depending on the NA of the lens, a much smaller voxel size can be achieved; this resolution is more suitable for small samples like zebrafish embryos and the visualization of gene expression at the cellular level. For most of the work done in this thesis a 10 x plan apo lens (NA = 0.24, long working distance) was applied. The resolution in the xy-plane was used as a guide for z-axis sampling to achieve isotropic voxels in the image. With given NA, each image slice was sampled in 1024x1024 pixels; next choosing the right z-displacement a voxel size of around 1 μm^3 can be achieved. For subcellular localization of gene expression in zebrafish embryos however, a magnification of 63 x is required.
ZebraFISH can also be used in experiments with multiple FISH labelling, in combination with fluorescent immunostaining and Green Fluorescent Protein (GFP) transgenic zebrafish. In multiple FISH experiments only a limited number of fluorescently tagged genes can be visualized in the same embryo. More complex patterns of coexpression and colocalization can be analyzed using dedicated resources such as the zebrafish gene expression database (Belmamoune & Verbeek, 2007).
Other fluorescent techniques comprise transgenic zebrafish lines expressing GFP, and fluorescent immunolabelling. GFP is used as a reporter for gene expression; immunohistochemistry shows expression at the protein level. While FISH and immunolabelling are only possible in fixed samples, GFP can be applied to live samples as well as in combination with FISH, i.e. in fixed embryos (Langford et al., 2006).
In order to further improve the quality of the CLSM images, deconvolution can be applied to images acquired with a higher magnification. This process eliminates the distortions and blurring caused during capture of the image. Deconvolution will result in a sharper and clearer image than could be obtained with the available optics alone (Boutet de Monvel et al. 2003).
Spatio-temporal analysis and 3D modelling of gene expression patterns were applied to study relationships between genes in both spatial and temporal context. It also allowed an accurate characterization of more complex gene expression patterns. This is illustrated through application of methods to two groups of case studies:
1) Early zebrafish development:

- Characterization of 14-3-3 gene expression during zebrafish development (**Chapter 3**)
- 3D reconstructions of gene expression patterns in the developing innate immune system (**Chapter 4**)

In this group of case studies, we analysed complex gene expression patterns as well as gene expression patterns in small domains, i.e. in single cells scattered over the embryo.

2) Late zebrafish and cross species development:
- Gene expression and digit homology in the chicken wing (**Chapter 5**)
- Limb/fin heterochrony, analysis of gene expression data with Frequent Episode Mining in Developmental Analysis (FEDA, **Chapter 6**).

In this group of case studies, the focus was on marker genes, involved in zebrafish pectoral fin and chicken limb development. Gene expression data of these marker genes were compared with data from other tetrapods.

Case study Early zebrafish development
In **Chapter 3**, ZebraFISH and 3D modelling were applied to characterize complex gene expression patterns.

Recently, expression patterns of genes encoding 14-3-3 proteins were studied in zebrafish embryos. The 14-3-3 isoforms exhibited complex gene expression patterns (Besser et al. 2006). These gene expression patterns were not yet studied in 3D. In order to employ zebrafish as a model to study cancer and neurological disorders, the role of 14-3-3 proteins in zebrafish brain development needs to be characterized.

In this chapter, gene expression patterns for genes encoding two 14-3-3 isoforms were analyzed using our workflow (cf. **Chapter 1**). Application of the ZebraFISH protocol yielded more 14-3-3 gene expression domains and at earlier developmental stages than by ISH detection in previous studies. To confirm our ZebraFISH results, samples from ISH detection were overstained for 3-4 days. Serial sections were made from these overstained samples. The serial sections were then processed for 3D reconstruction (Verbeek et al. 2002). Using 3D modelling, we were able to establish an accurate characterization of zebrafish genes encoding 14-3-3 γ and τ in developing anatomical structures.
From earlier work two subtypes for the genes encoding the zebrafish γ and τ isoforms have been described. Data from microarray analysis (Besser et al. (2006) revealed that the two γ subtypes displayed very diverse expression profiles, suggesting different roles for 14-3-3 γ1 and γ2 during development. Microarray expression profiles for the 14-3-3 τ1 and τ2 subtypes were less distinct (Besser et al. 2006) and ZebraFISH as well as ISH yielded almost similar gene expression patterns (Besser et al. 2006, this thesis). Our initial analysis was based on the 14-3-3 γ1 probe used by Besser et al.(2006). In order to specifically analyze gene expression of γ1 and γ2, recently two new probes were synthesized for the 14-3-3 γ1 and γ2 subtypes. Results from ZebraFISH and CLSM imaging with these probes suggest that the expression patterns for the two subtypes of the gene encoding 14-3-3 γ can be distinguished. FISH results for the "new" 14-3-3 γ1 and γ2 subtype display expression in the domains previously described (Besser et al. 2006; this thesis Chapter 3). The expression patterns of the two 14-3-3 γ subtypes are partially overlapping and partially complementary to each other (Welten et al., in preparation). 3D modelling of the CLSM images confirmed these data. Thus, the methods presented stablish the specificity of probes.

Although the 14-3-3 proteins are highly conserved among amniotes, a large variation in isoform number can be observed in higher organisms (Wiker and Yaffe, 2004). Alterations in expression or function of the 14-3-3 isoforms in relation to human disorders indicate specific functions for the different isoforms (Wiker and Yaffe, 2004).

For zebrafish, the function of the distinct 14-3-3 isoforms and the cell type in which the isoforms are expressed, are still under study. FEDA (cf. Chapter 6) can be applied to analyze timing data of gene expression of the 14-3-3 isoforms in anatomical structures, within one species and across species. Moreover, application of the FEDA algorithm to location and function of the distinct 14-3-3 isoforms in various model organisms (e.g. fruitfly, zebrafish, mouse, rat) and human may help predicting location and function of the isoforms in zebrafish. However, some basic features of the teleost fish brain are different from those in higher vertebrates. For example, in teleost fish neurogenesis occurs in a wide range of brain structures and continues during adulthood (Miramura and Nakayasu, 2001; Zupanc et al. 2005) whereas in higher vertebrates, adult neurogenesis occurs only in restricted areas (Zupanc et al. 2005). This aspect might involve different roles for 14-3-3 isoforms in zebrafish and higher vertebrates such as mammals.

In **Chapter 4**, we applied ZebraFISH and 3D modelling to study gene expression patterns in single white blood cells (and precursors thereof).
Zebrafish macrophages and granulocytes are essential cell types in the innate immune system. These cells behave strikingly similar to their counterparts in mammals. Marker genes expressed by zebrafish macrophages and granulocytes are found to be homologous to those of mammals. This is one of the reasons that the zebrafish can be employed as a model to study the response of both the innate and the adaptive immnune system to inflammation. Experimental findings from zebrafish can be used for understanding these systems in human.
In this case study we focused on *l-plastin*, a general marker of leukocytes, and *mpx*, a specific marker of neutrophil granulocytes. An exploratory study was carried out to analyze cell distribution and migration behaviour of *mpx* and *l-plastin* expressing cells in relation to vascularization and haematopoietic events.

The distribution patterns of *mpx* and *l-plastin* expressing cells during zebrafish development matched the vascularization and haematopoietic events described in literature (Herbomel et al.1999 and 2001, Isogai et al. 2001, Lieschke et al. 2001, Murayama et al.2006). With the schematic 3D modelling gene expression can be inspected in single cells and give a clue about the distribution patterns of these cells in relation to anatomical structures.
Application of ZebraFISH and schematic 3D modelling allow a quantitative approach in future studies. For example, cell numbers and distribution patterns can be analyzed in infection experiments, or in mutants in which the vascular system is affected. Consequently, further understanding of the innate immune system in zebrafish can be achieved.

3D gene expression data and models from several other marker genes were made, but not used in the analysis presented in Chapter 4. These markers comprise *draculin*, an early marker of macrophages and erytrhroblasts (Herbomel et al.1999); *fms*, a marker of macrophages, early microglia and neural crest derivatives (Herbomel et al. 2001) and *lysozyme C*, previously suggested as macrophage marker (Berman et al. 2005; Liu and Wen 2001) though recent multiple FISH experiments revealed expression of *lysozyme C* in neutrophil granulocytes (Meijer et al. 2007). In order to characterize these overlapping cell populations, multiple FISH experiments as well as FISH combined with fluorescent

immunolabeling or with known GFP lines can be useful in analysis. Subsequent 3D modelling allows a better inspection of these overlapping cell populations and their expression domains in other tissues.

Gene expression data from the developing innate immune system can also be compared over different animal models, using the FEDA algorithm (cf. Chapter 6). This computational approach can be helpful to elucidate characters such as locations of embryonic and adult haematopoietis or differences in function of early macrophages (Shepard and Zon 2000), across zebrafish, amphibians and amniote model systems.

Case study Late zebrafish and cross species development

In this case study we focused on marker genes involved in zebrafish pectoral fin and tetrapod limb development. Though data from the fossil record indicate that the fin / limb transition occurred about 410 million years ago (Shubin et al, 2006), many similarities can be found during both teleost fin and tetrapod limb development (Hinchliffe, 2002; Tickle, 2002). First, we made a side step to another model organism: the chicken **(Chapter 5)**. The chicken is extensively studied in a developmental as well as in an evolutionary context and a large number of molecular data has become available. Gene expression data from zebrafish pectoral fin and chicken limb development obtained by our own experiments were then compared with data from known orthologues in other tetrapod model systems **(Chapter 6)**. In **Chapter 5,** *in situ* hybridization and 3D reconstruction were used to investigate a rudimentary structure in the chicken wing in relation to bird evolution. In the wing, the transcription factor *sox9* exhibits a transient gene expression pattern anterior to the digit II primordium, which we identified as a rudimentary digit I domain. The receptor molecule *bmpr1b* displayed no hybridisation signal in the same region at the same stage, suggesting that the presumptive digit I domain is arrested during development and shows no further differentiation into cartilage

In our study, ISH and 3D reconstruction were applied to whole mount chicken wings and hindlimbs. Recent studies reveal excellent FISH results for whole mount chicken embryos (Denkers et al. 2004). Repeating our experiments with FISH and subsequent imaging with CLSM will result in an accurately aligned stack of optical sections, in a relatively short time. Since the TSA detection proved to be more sensitive, we may be able to detect the onset and offset of *sox9* and *bmpr-1b* gene expression patterns in the digit primordia and cartilage elements more precisely. During later stages of chicken development, CLSM may not be capable to scan through tissues like cartilage. To overcome this problem, thick sections of the samples can be scanned with CLSM (Sharpe, 2003).

To compare differences in timing of gene expression in wing and hindlimb, a computational method was applied: FEDA (**Chapter 6**). Though a wide variety of genes are involved in digit formation, analysis with FEDA revealed a delay in *sox9* expression in the presumptive digit I domain in the chicken wing, compared with that of the hindlimb. The pattern shift diagram in **Chapter 6** also reveals that FEDA can visualize heterochrony at different levels within one analysis. Investigation of more gene expression data from in chicken wing and hindlimb development with FEDA might provide a clue about genetic networks involved in digit formation and identity.

In the skink *Chalcides chalcides*, a similar conflict between embryonic and adult digit identity exists as in birds (Wagner, 2005). Anatomical evidence suggests that the digits of *Chalcides chalcides* fore and hindlimb are digit I, II and III. Embryological evidence however, suggests that these digits develop from the digit II, III and IV primordia. The reduction of digits in *Chalcides chalcides* as well as in theropod dinosaurs might be the result of an adaptive modification during evolution. Digit reduction is also observed in *Hemiergis*, another skink genus. In this lizard, loss of digits is correlated with shifts in timing, i.e. heterochrony - in sonic hedgehog expression (Shapiro et al. 2003, Smith et al. 2003). Since FEDA showed to be a very flexible method in data organisation, it can be applied to data from at different levels, such as anatomical structures, gene expression data and developmental events. Analysis of data from skinks, birds and other tetrapods might reveal a link between digit reduction and heterochrony in gene expression, chondrogenesis or other processes.
To solve the problem of homology of avian wing digits with those of other tetrapods, several models are proposed (reviewed by Wagner, 2005). The Frame Shift Hypothesis (Wagner and Gauthier, 1999) proposes that embryonic digit domains II-IV have undergone a homeotic transformation and adopted the identity of digit I-III. The Pyramid Reduction Hypothesis (Kundrat et al. 2002) solves the problem by proposing a bilateral reduction of digits, and that the remaining digits (II-IV) have been remodelled during evolution, into the I-III phenotype. In **Chapter 5** we discuss an alternative model, the polydactyly model. This model provides continuity between digit position and identity across the theropod and bird phylogeny. However, recent findings point towards a possible frame shift in bird digit identity in the theropod –bird lineage. This might be caused by a change of *hox* gene expression in the wing (Vargas and Fallon 2004; Wagner, 2005), though a wide range of genes are involved in the specification of digit identity (Dahn and Fallon 2000, Litingtung et al. 2002; Shapiro et al. 2003; Tiecke et al. 2007). Further studies of the molecular mechanisms underlying digit development and identity, as well as new fossils from bird ancestors will give more insight in the evolution of birds.

Besides the analysis of gene expression patterns in single species, in situ gene expression data were compared across species, with zebrafish as key model.
In **Chapter 6**, gene expression patterns were analyzed using Frequent Episode Mining in Developmental Analysis (FEDA). The FEDA algorithm was applied in two case studies:

1) Gene expression data from zebrafish fin and chicken limb development were compared with data from other tetrapod model systems to analyse heterochrony in gene expression during fin and limb development.
2) Heterochrony in gene expression was analyzed within one species.

We demonstrated that heterochrony in gene expression in limb and fin development could be elucidated very well using the FEDA algorithm, in a phylogenetic context as well as within one species. The use of relative time scales is essential for analysis with FEDA.

We demonstrated that FEDA is flexible in the arrangement of data and capable of handling large datasets such as 14 species, 25 developmental events and 17 gene expression data. Sparseness of gene expression data from a certain species might influence the accuracy of phylogenetic trees. FEDA is capable of finding a solution, even

if data are sparse. The computations with FEDA produce a numerical value to express distance between species, the Jaccard distance. This provides a true objective measure to express differences between species or other entities.
Comparison of ZebraFISH and ISH data from zebrafish as well as extraction of ISH data from literature might influence the accuracy for construction of phylogenetic trees. For zebrafish pectoral fin development, data were generated using ZebraFISH and ISH in parallel. The probes used for detection of the fin markers were strong and specific; no discrepancies between FISH and ISH data were found for the fin markers and the projections of the FISH were consistent with ISH data from literature. The data that were extracted from literature were generated in different research groups where different ISH protocols are used. Though ISH protocols are optimised for every model species, these gene expression data may show slight differences in sensitivity in relation to each other. However, we did not observe differences in timing of gene expression when we compared images from one species that were generated in different research groups. Timing of gene expression and development of morphological characters is compared using a relative time axis; no absolute data were used.
FEDA showed to be a very flexible method in the both arrangement and type of the data. It is not only useful to study heterochrony, but also to compare location and functions of different subtypes of genes within species or across species.
In the near future, in situ gene expression data will be combined with microarray as well as morphological data. Also, the computational framework of FEDA will be employed in spatiotemporal analysis of gene expression data from structured repositories (Belmamoune and Verbeek, 2006).

Conclusions and future work
The work described in this thesis is concerned with the analysis of gene expression and tools to establish spatiotemporal analysis of gene expression.

- We demonstrated that the fluorescent mRNA *in situ* hybridisation (ISH) technique is an efficient and powerful tool to study developmental processes at the level of gene expression. Fluorescent *in situ* hybridisation (FISH) by means of Tyramide Signal Amplification improves the sensitivity of the method and goes hand in hand with 3D CLSM imaging.
- 3D modelling using TDR-3Dbase enabled us to establish an accurate characterization of gene expression in relation to anatomical structures. The methods presented, produced relevant biological data. For the zebrafish 14-3-3 γ proteins, we were able to distinguish and accurately characterize gene expression domains for two isoforms.
  In functional studies, 3D modelling allows analytical approaches.
- The FEDA algorithm has shown to be a very flexible and powerful method to analyse gene expression, timing, species, morphological characters and combinations of all these data. Moreover, FEDA is very flexible in the arrangement of data.

Optimisation of imaging techniques will contribute to further improvement of the analysis of whole mount specimens such as zebrafish embryos. Given the size of the embryo and the limitations of our CLSM it was not possible to produce 3D images of

complete embryos. In future studies, multiphoton microscopy can be used to accomplish a higher depth penetration so that complete embryos can be scanned (Centonze and White, 1998) and a more complete analysis of cell numbers over time can be obtained. For multiphoton microscopy other fluorescent labels with longer wavelength are required, usually in the infrared spectrum (Centonze and White, 1998). This needs to be tuned with our ZebraFISH method.

Application of FEDA to spatial gene expression data in combination with microarray data and morphological characters will provide a clue about the genetic networks present developmental processes in zebrafish as well as in other model systems. In the near future, FEDA can be applied to a wide variety of characters such as subtypes, location and function of genes, and comparison of these with other model systems.

REFERENCES

Ahn, S. and Joyner, A. L. 2004. Dynamic changes in the response of cells to positive hedgehog signaling during mouse limb patterning. Cell 118: 505–516.

Aitken, A., Howell, S., Jones, D., Madrazo, J. and Patel, Y. 1995. 14-3-3 α and δ are the phosphorylated forms of Raf-activating 14-3-3 β and ζ. The Journal of biological chemistry 270 (11) 5706-5709

Aitken, A. 1996. 14-3-3 and its possible role in co-ordinating multiple signalling pathways. Trends in cell biology 6: 341-347

Akimenko, M.A., Johnson, S.L., Westerfield, M. and Ekker, M., 1995. Differention induction of four *Msx* homeobox genes during fin development and regeneration in zebrafish. *Development* 121: 347-357

Akiyama, H., Chaboissier, M.C., Martin, J.F., Schedl, A. and de Crombrugghe, B.2002. The transcription factor Sox9 has essential roles in successive steps of the chondrocyte differentiation pathway and is required for expression of Sox5 and Sox6. Genes Dev 16(21):2813-28.

Alberch, P. and Gale, E. A. 1983. Size dependence during the development of the amphibian foot. Colchicine-induced digital loss and reduction. J. Embryol. Exp. Morphol. 76: 177–197.

Amores, A., Force, A., Yan, Y.L., Joly, L., Amemiya, C., Fritz, A., Ho, R.K., Langeland, J., Prince, V., Wang, Y.L., Westerfield, M., Ekker, M. and Postlethwait, J. H.1998. Zebrafish hox clusters and vertebrate genome evolution. Science 282: 1711-1714

Bardeleben, K. 1889. On the præpollex and præhallux, with observations on the carpus of Theriodesmus phylarchus. Proc. Zool. Soc. Lon. 259–262.

Bartosik-Psujek, H. and Archelos, J.J. 2004.Tau protein and 14-3-3 are elevated in the cerebrospinal fluid of patientswith multiple sclerosis and correlate with intrathecal synthesis of IgG. J Neurol 251: 414–420

Bathoorn, R.and Siebes, A.J.P.M. 2004. Constructing (Almost) Phylogenetic Trees from Developmental Sequences Data. 8th European Conf on Principles and Practice of Knowledge Discovery in Databases: 500-502.

Baxter, H.C., Liu, W.G., Forster, J.L., Aitken, A. and Fraser, J.R. 2002. Immunolocalisation of 14-3-3 isoforms in normal and scrapie-infected murine brain. Neuroscience Vol. 109, No. 1, pp. 5-14

Bei,Y., Belmamoune, M. and Verbeek, F.J. 2006. Ontology and image semantics in multimodal imaging: submission and retrieval. Proc SPIE Internet Imaging VII 6061:C1–C12

Bellairs, R. and Osmond, M. 2005. Atlas of Chick Development. Second Edition. Elsevier Academic press.

Belmamoune, M. and Verbeek, F.J. 2006. Heterogeneous Information Systems: bridging the gap of time and space. Management and retrieval of spatio-temporal Gene Expression data. Proc. Int. Conf. Multidisciplinary Information Sciences and Technologies, InSCit2006 (in press).

Bennett, C.M., Kanki, J. P., Rhodes, J., Liu, T. X., Paw, B. H., Kieran, M. W.,. Langenau, D. M, Delahaye-Brown, A., Zon, L. I., Fleming, M. D. and Look, A. T. (2001). Myelopoiesis in the zebrafish, *Danio rerio* Blood 98: 643-651.

Besser, Y., Bagowski, C.P., Salas – Vidal, E., Hemert, M.J., Bussman, J. and Spaink, H.P. 2006. Expression analysis of the family of 14-3-3 proteins in zebrafish development. Gene expression patterns 7 (4):511-20.

Biesecker, L. G. 2002. Polydactyly: how many disorders and how many genes? Am. J. Med. Genet. 112: 279–283.

Bininda-Emonds, O.R.P, Jefferey, J.E. and Richardson, M.K. 2003. Is sequence heterochrony an important evolutionary mechanism in mammals? Jounal of mammalian evolution 10 (4):335-361.

Blanco, M. J. and Alberch, P. 1992. Caenogenesis, developmental variability, and evolution in the carpus and tarsus of the marbled newt *Triturus marmoratus*. Evolution 46: 677–687.

Blanco, M. J., Misof, B. Y. and Wagner, G. P. 1998. Heterochronic differences of Hoxa-11 expression in Xenopus fore- and hind limb development: evidence for lower limb identity of the anuran ankle bones. Dev. Genes Evol. 208: 175–187.

Bordzilowskaya, N.P., Detlaff, T.A., Duhon, S.H. and Malacinski, G.M. 1989. Developmental-stage series of Axolotl embryos. In: Armstrong, J.B., and Malacinski, G.M. (eds). Developmental biology of the Axolotl. Oxford University Press, Oxford, pp. 201-219.

Boutet de Monvel, J., Le Calvez, S. and Ulfendahl, M. 2001. Image Restoration for Confocal Microscopy: Improving the Limits of Deconvolution, with Application to the Visualization of the Mammalian Hearing Organ. Biophys J 80 (5): 2455-2470.

Bryson-Richardson, R.J., Berger, S., Schilling, T.F., Hall, T.E., Cole, N.J., Gibson, A.J., Sharpe, J., Currie, P.D. 2007. FishNet: an online database of zebrafish anatomy. BMC Biol. 2007 Aug 17;5(1):34

Burke, A. C. and Alberch, P. 1985. The development and homology of the chelonian carpus. J. Morphol. 186: 119–131.

Burke, A. C. and Feduccia, A. 1997. Developmental patterns and the identification of homologies in the avian hand. Science 278: 666–668.

Burns, C. and Zon, L. 2006. Homing Sweet Homing: Odyssey of Hematopoietic Stem Cells. Immunity 25 (6):859-862

Camon, E., Magrane, M., Barrell, D., Lee, V., Dimmer, E., Maslen, J., Binns, D., Harte, N., Lopez, R. and Apweiler, R. 2004. The Gene Ontology Annotation (GOA) Database: sharing knowledge in Uniprot with Gene Ontology. Nucleic Acids Research, Vol.32 Database issue DOI: 10.1093/nar.gkh021

Carroll, R. L. 1987. Vertebrate Paleontology and Evolution. W.H. Freeman and Company, New York.

Centonze, V.E. and White, J.G. 1998. Multiphoton Excitation Provides Optical Sections from Deeper within Scattering Specimens than Confocal Imaging. Biophysical Journal 75: 2015–2024

Chamberlain, F. W. 1943. Atlas of Avian Anatomy. Michigan State College Agricultural Experiment Station, East Lansing, Michigan.

Chatterjee, S. 2004. Counting the fingers of birds and dinosaurs. Science 280: 355a.

Chaudhri, M., Scarabel, M. and Aitken, A. 2003.Mammalian and yeast 14-3-3 isoforms form distinct patterns of dimers in vivo. Biochemical and Biophysical Research Communications 300 679–685.

Chen, X-D. and Turpen, J.B . (1995). lntraembryonic Origin of Hepatic Hematopoiesis in Xenopus laevis. The journal of Immunology 154: 2557-2567

Chiang, C., Litingtung, Y., Harris, M.P., Simandl, B. K., Li ,Y., Beachy, P.A. and Fallon, J.F. 2001. Manifestation of the limb prepattern: limb development in the absence of Sonic hedgehog function. Dev. Biol. 236: 421–435.

Chimal-Monroy, J., Rodriguez-Leon, J., Montero, J.A., Ganan, Y., Macias, D., Merino, R. and Hurle, J.M. 2003 Analysis of the molecular cascade responsible for mesodermal limb chondrogenesis : sox genes and BMP signalling. *Developmental Biology* 257 Issue 2, pp 292-301

Christen, B. and Slack, J.M.W. 1997. FGF-8 is associated with anteroposterior patterning and limb regeneration in *Xenopus*. Developmental Biology 192: 455-466.

Christiansen, P. and Bonde, N. 2004. Body plumage in *Archaeopteryx*: a review, and new evidence from the Berlin specimen. Comptes Rendus Palevol 3: 99–118.

Clack, J. A. 2002. An early tetrapod from 'Romer's Gap.' Nature 418: 72–76.

Clay, H. and Ramakrishnan, L. 2005. Multiplex Fluorescent In Situ hybridization in zebrafish embryos using tyramide signal amplification. Zebrafish 2(2):105-111

Coates, M. I. and Clack, J. A. 1990. Polydactyly in the earliest tetrapod limbs. Nature 347: 66–69.

Coates, M.I. and J. Cohn, M.J. 1998. Fins, limbs, and tails: outgrowths and axial patterning in vertebrate evolution. BioEssays 20:371-381

Cohn, M. J., Lovejoy, C. O., Wolpert, L. and Coates, M. I. 2002. Branching, segmentation and the metapterygial axis: pattern versus process in the vertebrate limb. Bioessays 24: 460–465.

Cole, N.J., Tanaka, M., Prescott, A. and Tickle, C. 2004. Expression of limb initiation genes and clues to the morphological diversification of threespine stickleback. Current Biology 13:24 R951-952

Corredor-Adámez, M., Welten, M.C.M., Spaink, H.P., Schoon, R.T., De Bakker, M.A.G., Bagowski, C.P., Meijer, A.H., Jeffery, J.E., Verbeek, F.J., and Richardson, M.K. 2005. Genomic annotation and transcriptome analysis of the *Danio rerio* hox complex with description of a novel member, hoxb13a. Evol Dev.7(5):362-75.

Crossman, A.R. and Neary, D. Neuroanatomy: An Illustrated Colour Text. Churchill Livingstone; 3rd edition (2005)

Crowhurst, M.O., Layton, J.E. and Lieschke, G.J. (2002) Developmental biology of zebrafish myeloid cells. Int. J. Dev. Biol. 46, 483-492.

Dahn, R. D. and Fallon, J. F. 2000. Interdigital regulation of digit identity and homeotic transformation by modulated BMP signalling. Science 289: 438–441.

Davidson, D., Bard, J., Brune, .R, Burger, A., Dubreuil, C., Hill, W., Kaufman, M., Quinn, J., Stark, M. and Baldock, R. 1997. The mouse atlas and graphical gene-expression database. Semin Cell Dev Biol. 8(5):509-17.

De Jong, J.L.O. and Zon, L.I. 2005. Use of the zebrafish system to study primitive and definitive hematopoiesis. Annual Review of Genetics 39: 481-501.

Denkers, N., Garcýa-Villalba, P., Rodesch, C.K., Nielson, K.R. and Mauch, T.J. 2004. FISHing for Chick Genes: Triple-Label Whole-Mount Fluorescence In Situ Hybridization Detects Simultaneous and Overlapping Gene Expression in Avian Embryos. Developmental Dynamics 229:651–657.

Dougherty, M.K. and Morrison D.K. 2004. Unlocking the code of 14-3-3. Journal of cell science 117 (10):1875-1884

Driever, W., Solnica-Krezel, L., Schier, A.F., Neuhauss, S.C., Malicki, J., Stemple, D.L., Stainier, D.Y., Zwartkruis, F., Abdelilah, S., Rangini, Z., Belak, J. and Boggs, C. 1996. A genetic screen for mutations affecting embryogenesis in zebrafish. Development. 123: 37-46

Dudley, A. T., Ros, M. A. and Tabin, C. J. 2002. A re-examination of proximodistal patterning during vertebrate limb development. Nature 418: 539–544.

Duprez, D. 2002. Signals regulating muscle formation in the limb during embryonic development. Int.J.Dev. Biol. 46: 915-925

Efthimios M., Skoulakis, C. and Davis, R.L. 1996. Olfactory Learning Deficits in Mutants for leonardo, a Drosophila Gene Encoding a 14-3-3 Protein. Neuron Vol. 17, 931–944.

Feduccia, A. 1999. 1,2,352,3,4: accommodating the cladogram. Proc. Natl. Acad. Sci. USA 96: 4740–4742.

Feduccia, A. and Nowicki, J. 2002. The hand of birds revealed by early ostrich embryos. Naturwissenschaften 89: 391–393.

Forster, C. A., Sampson, S. D., Chiappe, L. M. and Krause, D. W. 1998. The theropod ancestry of birds: new evidence from the late cretaceous of Madagascar. Science 279: 1915–1919.

Forster, S.A. and Baker, J.A. 2004. Evolution in parallel: new insights from a classic system. Trends in Ecology and Evolution 19 (9):456-459.

Fountoulakis, M., Cairns, N. and Lubec, G. 1999. Increased levels of 14-3-3 gamma and epsilon proteins in brain of patients with Alzheimer's disease and Down syndrome. J Neural. Transm. Suppl. 57: 323-35

Galis, F., Kundrát, M. and Sinervo, B. 2003. An old controversy solved: bird embryos have five fingers. Trends Ecol. Evol. 18: 7–9.

Garner, J. P. and Thomas, A. L. R. 2004. Counting the fingers of birds and dinosaurs. Science 280: 355a.

Gauthier, J. A. 1986. Saurischian monophyly and the origin of birds. Mem. Calif. Acad. Sci. 8: 1–55.

Gegenbaur, C. 1864. Untersuchungen zur vergleichenden Anatomie der Wirbelthiere: Erstes heft. Carpus und Tarsus. Engelmann, Leipzig.

Gerth, V.E. and Vize, P.D. 2004. A Java tool for dynamic web-based visualization of anatomy and overlapping gene or protein expression patterns.
Bioinformatics 21(7):1278-9.

Gerth, V.E., Katsuyama, K., Snyder, K.A., Bowes, J.B., Kitamyama, A., Ueno, N. and Vize, P.D. 2007. Projecting 2D gene expression data into 3D and 4D space. Developmental Dynamics 236:1036-1043.

Goff, D.J. and Tabin, C.J.1997. Analysis of Hoxd-13and Hoxd-11misexpression in chick limb buds reveals that Hox genes affect both bone condensation and growth. Development 124, 627-636

Godin, I. and Cumano, A. 2005. Of birds and mice; hematopoietic stem cell development. Int. J. Dev. Biol. 49: 251-257

Goodwin, B. C. and Trainor, L. E. H. 1983. The ontogeny and phylogeny of the pentadactyl limb. In B. C. Goodwin, N. Holder, and C. C. Wylie (eds.). Development and Evolution. Cambridge University Press, Cambridge, UK, pp. 75–98.

Graham A, Begbie J. 2000. Neurogenic placodes: a common front. Trends Neurosci. 2000 Jul;23(7):313-6. Review.

Grandel, H. and Schulte- Merker, S.1998. The development of the paired fins in the Zebrafish (*Danio rerio*). Mechanisms of Development 79 99-120

Grunwald, D.J. and Eisen, J.S. Headwaters of the zebrafish -- emergence of a new model vertebrate. Nat Rev Genet. 2002 Sep;3(9):717-24.

Haffter, P. and Nusslein – Volhard C. 1996. Large scale genetics in a small vertebrate, the zebrafish. Int J Dev Biol.40(1):221-7.

Hamburger, V. and Hamilton, H. L. 1951. A series of normal stages in the development of the chick embryo. J. Morphol. 88: 49–92.

Hanken, J. 1993. Model Systems versus Outgroups Alternative Approaches to the Study of Head Development and Evolution. Am. Zool. **33**(4), 448-456.

Harfe, B. D., Scherz, P. J., Nissim, S., Tian, H., McMahon, A. P. and Tabin, C. J. 2004. Evidence for an expansion-based temporal Shh gradient in specifying vertebrate digit identities. Cell 118: 517–528.

Hartmann, C. and Tabin, C. J. 2001. Wnt-14 plays a pivotal role in inducing synovial joint formation in the developing appendicular skeleton. Cell 104: 341–351.

Hasumi, M. and Iwasawa, H. 1993. Geographic variation in the pes of the salamander *Hynobius lichenatus*: a comparison with tetradactyl *Hynobius hidamontanus* and pentadactyl *Hynobius nigrescens*. Zool. Sci. 10: 1027.

He, M., Zhang, J., Shao, L., Huang, Q., Chen, J., Chen, H., Chen, X., Liu, D. and Luo, Z. Upregulation of 14-3-3 isoforms in acute rat myocardial injuries induced by burn and lipopolysaccharide. Clinical and Experimental Pharmacology and Physiology (2006) 33, 374–380

Healy, C., Uwanogho, D. and Sharpe, P. T. 1999. Regulation and role of Sox9 in cartilage formation. Dev. Dyn. 215: 69–78.

Hecht, M. K. 1985. The biological significance of Archaeopteryx. In M. K. Hecht, J. H. Ostrom, G. Viohl, and P. Wellnhofer (eds.). The Beginnings of Birds: Proceedings of the International Archaeopteryx Conference, Eichstätt. Freunde des Jura-Museums Eichstätt, Willibaldsburg, Eichstätt, pp. 149–160.

Hecht, M. K. and Tarsitano, S. 1982. The paleobiology and phylogenetic position of *Archaeopteryx*. Gebios Mem. Spec. 6: 141–149.

Herbomel, P., Thisse, B. and Thisse, C. 1999. Ontogeny and behaviour of early macrophages in the zebrafish embryo. Development 126: 3735- 3745.

Herbomel, P., Thisse, B. and Thisse, C. 1999. Zebrafish early macrophages colonize cephalic mesenchyme and developing brain, retina, and epidermis through an M-CSF receptor- dependent invasive process. Development 238: 274-288.

Hinchliffe, J. R. 1977. The chondrogenic pattern in chick limb morphogenesis: a problem of development and evolution. In D. A. Ede, J. R. Hinchliffe, and M. Balls (eds.). Vertebrate Limb and Somite Morphogenesis. Cambridge University Press, Cambridge, UK, pp. 293–309.

Hinchliffe, J. R. 1985. ‘One, two, three’ or ‘two, three, four’: an embryologist’s view of the homologies of the digits and carpus of modern birds. In M. K. Hecht, J. H. Ostrom, G. Viohl, and P. Wellnhofer (eds.). The Beginnings of Birds: Proceedings of the International Archaeopteryx Conference, Eichstätt. Freunde des Jura-Museums Eichstätt, Willibaldsburg, Eichstätt, pp. 141–147.

Hinchliffe, J. R. and Hecht, M. K. 1984. Homology of the bird wing skeleton: embryological versus paleontological evidence. Evol. Biol. 18: 21–39.

Hinchliffe, J.R. 2002. Developmental basis of limb evolution. *Int. J. Dev. Biol*. 46: 835-845.

Holmgren, N. 1933. On the origin of the origin of the tetrapod limb. Acta Zool. 14: 185–295.

Holmgren, N. 1952. An embryological analysis of the mammalian carpus and its bearing upon the question of the origin of the tetrapod limb. Acta Zoologica 33: 1–115.

Holzschuh J, Wada N, Wada C, Schaffer A, Javidan Y, Tallafuβ A, Bally-Cuif L, Schilling TF. 2005. Requirements for endoderm and BMP signalling in sensory neurogenesis in zebrafish. Development 132:3731-3742

Horie, M., Suzuki, M., Takahashi, E. and Tanigami, A. 1999. Cloning, expression, and chromosomal mapping of the human 14-3-3γ gene (YWHAG) to 7q11.23. Genomics 60: 241-243.

Isogai, S., Horiguchi, M. and Weinstein, B. M. The vascular anatomy of the developing zebrafish: an atlas of embryonic and early larval development. Developmental Biology, Volume 230, pp. 278-301.

Ivanov, D., Dvoriantchikova, G., Nathanson, L., McKinnon, S.J., and Shestopalov, V.I. 2006. Microarray analysis of gene expression in adult retinal ganglion cells. FEBS Letters 580: 331–335

Jeffery, J.E., Bininda-Emonds, O.R.P., Coates, M.I. and Richardson, M.K. 2002. Analyzing evolutionary patterns in amniote embryonic development. *Evolution & Development* 4:4. 292-302 .

Jeffery, J.E. Richardson, M.K., Coates, M.I. and Bininda-Emonds, O.R.P.. 2002. Analyzing Developmental Sequences Within a Phylogenetic Framework. Systematic Biology 51 (3): 478-491.

Jeffery, J.E., Bininda-Emonds, O.R.P., Coates, M.I. and Richardson, M.K.2005. A new technique for identifying sequence heterochrony. *Syst. Biol.* (2):230-240.

Ji, Q., Currie, P. J., Norell, M. A. and Ji, S. A. 1998. Two feathered dinosaurs from north eastern China. Nature 393: 753–761.

Ji, Q., Norell, M. A., Gao, K. Q., Ji, S. A. and Ren, D. 2001. The distribution of integumentary structures in a feathered dinosaur. Nature 410: 1084–1088.

Jones, S.L., Wang, J., Turck, W. et al. (1998) A role for the actin-bundling protein L-plastin in the regulation of leukocyte integrin function. Proc. Natl. Acad. Sci. USA 95, 9331-9336.

Jowett, T. 2001. Double *in situ* hybridization techniques in zebrafish. Methods 23:345-358

Karsenty, G. and Wagner, E.F. 2002. Reaching a genetic and molecular understanding of skeletal development. *Developmental Cell,* Vol 2, 389-406

Kawamoto, Y.,MD; Akiguchi, I., MD; Tomimoto, H., MD; Shirakashi, Y., MD; Honjo, Y., MD; and Budka, H.,MD. 2006. Upregulated Expression of 14-3-3 Proteins in Astrocytes From Human Cerebrovascular Ischemic Lesions. Stroke 37:830-835

Kearny, J.B., Wheeler, S.R., Estes, P., Parente, B. and Crews, S.T. 2004. Gene expression profiling of the developing *Drosophila* CNS midline cells. Dev Biol 275:473-492.

Kerwin, J., Scott ,M., Sharpe, J., Puelles, L., Robson, S.C., Martinez-de-la-Torre, M., Ferran, J.L., Feng, G., Baldock, R., Strachan, T., Davidson, D., Lindsay, S. 2004. 3 dimensional modelling of early human brain development using optical projection tomography. BMC Neurosci. 2004 Aug 6;5:27.

Khan, P., Linkhart, B. and Simon, H.G. 2002. Different regulation of T-box genes Tbx4 and Tbx5 during limb development and limb regeneration. Developmental Biology 250

Kimbrell, D.A. and Beutler, B. 2001. The evolution and genetics of innate immunity. Nature Genetics 2, 256-267

Kimmel, C.B., Ballard, W.W., Kimmel, S.R., Ullman, B. and Schilling, T.F. 1995. Stages of embryonic development of the zebrafish. Dev Dyn 203:253-310.

Koskinen, H., Krasnov, A., Rexroad, C., Gorodilov, Y., Afanasyev, S. and Molsa, H. 2004. The 14-3-3 proteins in the teleost fish rainbow trout (Oncorhynchus mykiss). J Exp Biol. 207(Pt 19):3361-8.

Kousteni, S., Tura, F., Sweeney, G.E. and Ramji, D.P.1997. Sequence and expression analysis of a Xenopus laevis cDNA which encodes an homologue of mammalian 14-3-3 zeta protein. Gene 190 279-285

Kundrát, M., Seichert, V., Russell, A.P. and Smetana, K jr.2002 Pentadactyl pattern of the avian wing autopodium and pyramid reduction hypothesis. *Journal of Experimental zoology* (mol. Dev. Evol.) 294: 152-159

Langford, K.J., Askham, J.M., Lee, T., Adams, M. and Morrison, E.E. 2006. Examination of actin and microtubule dependent APC localisations in living mammalian cells. BMC Cell Biol. 7:3.

Larsson, H.C.E. and Wagner, G.P., 2002 Pentadactyl Ground State of the Avian Wing. Journal of Experimental zoology (mol. Dev. Evol.) 294: 146-151

Lau, J.M.C., Wu, Ch. and Muslin, A. 2006. Differential role of 14-3-3 family members in *Xenopus* development. Developmental Dynamics 235:1761-1776.

Lau, N.C. Lim, L.P. Weinstein, E.G. and Bartel, D.P. 2001. An abundant class of tiny RNAs with probable regulatory roles in *Caenorhabditis elegans*. Science 294:858-862

Lieschke, G.J., Oates, A.C., Crowhurst, M.O., Ward, A.C. and Layton, J.E. 2001. Morphologic and functional characterization of granulocytes and macrophages in embryonic and adult zebrafish. Blood;98(10):3087-3096.

Linney, E., Dobbs-McAuliffe, B., Sajadi, H. and Malek, R.L. 2004. Microarray gene expression profiling during the segmentation phase of zebrafish development. Comp Biochem Physiol C Toxicol Pharmacol. 138(3):351-62

Lipshutz, R.J., Morris, D., Chee, M., Hubbell, E., Kozal, M.J., Shah, N., Shen, N., Yang, R. and Fodor, S.P. 1995. Using oligonucleotide probe arrays to access genetic diversity. Biotechniques. 19(3):442-7. Review.

Liu, F. and Wen, Z. 2002. Cloning and expression pattern of the lysozyme C gene in zebrafish. Mechanisms of Development 113: 69-72.

Lu, G., de Vetten, N.C., Sehnke, P.C., Isobe, T., Ichimura,T., Fu, H., van Heusden, G.P. and Ferl, R.J. 1994. A single *Arabidopsis* GF14 isoform possesses biochemical characteristics of diverse 14-3-3 homologues. Plant Mol Biol. 25(4):659-67.

Lun, K. and Brand, M. 1998. A series of no isthmus (noi) alleles of the zebrafish pax2.1 gene reveals multiple signalling events in development of the midbrain-hindbrain boundary. Development 125:3049-3062

Mabee, P. 2000.Developmental Data and Phylogenetic Systematics: Evolution of the Vertebrate Limb. AMER. ZOOL., 40:789–800

Manders, E.M.M., Verbeek, F.J. and Aten, J.A. 1993. Measurement of co-localisation of objects in dual colour confocal images. J.Microscopy ;1 69:375-382.

McKenzie, J.C. and Klein, R.M. 2000. Basic concepts in Cell Biology and Histology. McGraw-Hill companies inc. New York.

Meijer, A.H., Van der Sar, A.M., Cunha, C., Lamers, G.E.M., Laplante, M.A.,

Kikuta, H., Bitter, W., Becker, T.S. and Spaink, H.P. 2007. Identification and real-time imaging of a myc-expressing neutrophil population involved in inflammation and mycobacterial . granuloma formation in zebrafish. Dev Comp Immunol. 2007 May 22

Mercier, P., Simeone, A., Cotelli, F. and Boncinelli, E. Expression pattern of two otx genes suggest a role in specifying anterior body structures in zebrafish. Int J Dev Biol 1 995;39:559-573.

Merino, R., Ganan, Y., Macias, D., Economides, A. N., Sampath, K. T. and Hurle, J. M. 1998. Morphogenesis of digits in the avian limb is controlled by FGFs, TGF betas, and noggin through BMP signaling. Dev. Biol. 200: 35–45.

Metscher, B.D. and Ahlberg, P.E. 1999. Zebrafish in context: uses of a laboratory model in comparative studies. *Developmental Biology* 210, 1-14

Meuleman,W., Welten, M.C.M. and Verbeek, F.J. 2006. Construction of correlation networks with explicit time-slices using time-lagged, variable interval standard and partial correlation coefficients. Lecture Notes in Computer Science, Volume 4216, Computational Life Sciences II, pp 236-246.

Miyamura, Y. and Nakayasu, H. 2001. Zonal distribution of Purkinje cells in the zebrafish cerebellum: analysis by means of specific monoclonal antibody. Cell Tissue Res 305:299-305.

Moinar, R. E. 1985. Alternatives to Archaeopteryx: a survey of proposed early or ancestral birds. In M. K. Hecht, J. H. Ostrom, G. Viohl, and P. Wellnhofer (eds.). The Beginnings of Birds: Proceedings of the International Archaeopteryx Conference, Eichstätt. Freunde des Jura-Museums Eichstätt, Willibaldsburg, Eichstätt, pp. 209–217.

Montagna, W. 1945. A re-investigation of the development of the wing of the fowl. J. Morphol. 76: 87–113.

Morgan, B. A., Izpisua-Belmonte, J. C., Duboule, D. and Tabin, C. J.1992. Targeted misexpression of Hox-4.6 in the avian limb bud causes apparent homeotic transformations. Nature 358: 236–239.

Mueller, T. and Wulliman, M.F. 2005. Atlas of early zebrafish brain development. First edition 2005. Amsterdam, The Netherlands: Elsevier B.V. 183 p.

Murayama, E., Kissa, K., Zapata, A., Mordelet, E., Briolat, V., Lin, H-F., Handin, R.I. and Herbomel Ph. 2006. Tracing Hematopoietic Precursor Migration to Successive Hematopoietic Organs during Zebrafish Development.
Immunity 25, 963–975.

Murray, B. M. and Wilson, D. J. 1994. A scanning electron microscopic study of the normal development of the chick wing from stages 19 to 36. Anat. Embryol. 189: 147–155.

Nelson, C.E., Morgan, B.A., Burke, A.C., Laufer, E., DiMambro, E., Murtaugh, L.C., Gonzales, E., Tessarollo, L., Parada, L.F. and Tabin, C. 1996. Analysis of Hox gene expression in the chick limb bud. Development 122(5):1449-66

Nieuwkoop, P.D. and Faber, J. 1967. Normal table of Xenopus laevis. Daudin, North Holland, Amsterdam.

Nikaido, M., Tada, M. and Ueno, N. 1999. Restricted expression of the receptor serine /threonine kinase BMPR1b in Zebrafish. Mechanisms of Development 82 (1-2): 219-222

Nye, H.L.D., Cameron, J. A., Chernoff, E.A.G. and Stocum, D.L 2003. Extending the table of stages of normal development of the axolotl: limb development. Developmental Dynamics 226:555-560.

Norman J.R. and Greenwood P.H., *A history of Fishes.* Third Edition, 1975. Ernest Benn Ltd, London.

Old, J.M. and Deane, E.M. 2003. The lymphoid and immunohaematopoietic tissues of the embryonic brushtail possum (*Trichosurus vulpecula*). Anat Embryol 206:193-97

Osborn, H. F. 1916. Skeletal adaptations of Ornitholestes, Struthiomimus, Tyrannosaurus. Bull. Am. Mus. Nat. Hist. 35: 733–771.

Ostrom, J. H. 1969. Osteology of Deinonychus antirrhopus, an unusual theropod from the Lower Creataceous of Montana. Bull. Peabody Mus. 30: 1–165.

Ostrom, J. H. 1976. Archaeopteryx and the origin of birds. Biol. J. Linn. Soc. 8: 91–182.

Paddock, S.W. An introduction to confocal imaging. In Confocal Microscopy:Methods and Protocols. Paddock SW (ed), pp 1-34, Humana Press, Totowa, NJ, 1999.

Padian, K., Hutchinson, J. R. and Holtz, T. R. 1999. Phylogenetic definitions and nomenclature of the major taxonomic categories of the carnivorous Dinosauria (Theropoda). J. Vertebr. Paleontol. 19: 69–80.

Paton, R. L., Smithson, T. R. and Clack, J. A. 1999. An amniote-like skeleton from the Early Carboniferous of Scotland. Nature 398: 508–513.

Phelps, H.A. and Neely, M. N. 2005. Review paper: Evolution of the Zebrafish Model: From development to Immunity and Infectious Disease. Zebrafish 2: 87- 103.

Pizette, S. and Niswander, L. 2000. BMPs are required at two steps of limb chondrogenesis: formation of prechondrogenic condensations and their differentiation into chondrocytes. *Developmental Biology* volume 219, Issue 2, 15 March 2000, pp 237-249

Pozdeyev, N., Taylor,C., Haque, R., Chaurasia,S.C., Visser, A., Thazyeen, A., Du, Y., Fu, H., Weller, J., Klein, D.C. and Iuvone, P.M. 2006. Photic Regulation of Arylalkylamine N-Acetyltransferase Binding to 14-3-3 Proteins in Retinal Photoreceptor Cells. The Journal of Neuroscience 26(36): 9153–9161

Renshaw, S.A., Loynes, C.A., Trushell, D.M.I., Elworthy, S., Ingham, P.W. and Whyte, M.K.B. 2006. A transgenic zebrafish model of neutrophilic inflammation. Blood 108:3976-3979.

Richardson, M.K. 1995. Heterochrony and the phylotypic period. *Developmental Biology* 172**:** 412-421

Richardson, M.K. and Oelschlager, H.A. 2002. Time, pattern, and heterochrony: a study of hyperphalangy in the dolphin embryo flipper. *Evolution & Development* 4:6 435–444

Richardson, M. K., Jeffery, J. E. and Tabin, C. J. 2004. Proximodistal patterning of the limb: insights from evolutionary morphology. Evol. Dev. 6: 1–5.

Robb, L. 1997. Hematopoiesis: origin pinned down at last? Curr. Biol. 7 (1): R10-2.

Rombout, J.H.W.M., Huttenhuis, H.B.T., Picchietti, S. and Scapigliati, G. 2005. Phylogeny and ontogeny of Fish leucocytes. Fish & Shell.sh Immunology 19 441e455

Romer, A. S. 1956. Osteology of the Reptiles. University of Chicago Press, Chicago.

Rosner, M. and Hengstschlager, M. 2006. 14-3-3 proteins are involved in the regulation of mammalian cell proliferation. Amino Acids 30(1):105-9.

Ruvkun, G. 2001. Glimpses of a tiny RNA world. Science 294: 797-799

Santa Luca, A. P. 1980. The postcranial skeleton of *Heterodontosaurus tucki* (Reptilia, Ornithischia) from the Stormberg of South Africa. Ann. S. Afr. Mus. 7: 159–211.

Sanz-Ezquerro, J. J. and Tickle, C. 2003. Digital development and morphogenesis. J. Anat. 202: 51–58.

Schena M. 1996. Genome analysis with gene expression microarrays. Bioessays. 1996 May;18(5):427-31.

Schestakowa, G. S. 1927. Die Entwicklung des Vlogelflügels. Bull. Soc. Nat. Moscou. (Biol.) 36: 163–210.

Schindler, C.K., Heveri, M. and Henshall, D.C. 2006. Isoform- and subcellular fraction-specific differences in hippocampal 14-3-3 levels following experimentally evoked seizures and in human temporal lobe epilepsy . Journal of Neurochemistry 99, 561–569

Schlosser, G. 2001. Using heterochrony plots to detect the dissociated coevolution of characters. *Journal of experimental zoology* (mol dev evol) 291:282-304.

Schulmeister, S. and Wheeler, W.C. 2004. Comparative and phylogenetic analysis of developmental sequences. *Evolution and development* 6:1, 50-57

Sereno, P. C. 1993. The pectoral girdle and forelimb of the basal theropod *Herrerasaurus ischigualastensis*. J. Vertebr. Paleontol. 13: 425–450.

Sereno, P. C. 1999. The evolution of dinosaurs. Science 284: 2137–2147.

Shapiro, M.D. 2002. Developmental Morphology of Limb Reduction in *Hemiergis* (Squamata: Scincidae): Chondrogenesis, Osteogenesis, and Heterochrony. Journal of Morphology 254:211–231

Shapiro, M.D., Hanken, J. and Rosentahl, N. 2003. Developmental Basis of evolutionary digit loss in the Australian lizard *Hemiergis*. Journal of Experimental Zoology. 297B,1:48-56

Shapiro, M.D., Marks, E.M., Peichel, C.L., Blackman, B.K., Nereng, K.S., Jonsson, B., Schluter, D. and Kingsley, D.M. 2004. Genetic and developmental basis of evolutionary pelvic reduction in threespine sticklebacks. Nature 428(6984):717-23. Erratum in: Nature. 2006 Feb 23;439(7079):1014.

Sharpe, J., Ahlgren, U., Perry, P., Hill, W., Ross, A., Hecksher-Sorensen, J., Baldock, R. and Davidson, D. 2002. Science 296(5567):541-5.

Sharpe, J. 2003. Optical projection tomography as a new tool for studying embryo anatomy. J Anat. Feb;202(2):175-81.

Shiga, Y., Wakabayashi, H., Miyazawa, K., Kido, H. and Itoyama, Y. 2006. 14-3-3 protein levels and isoform patterns in the cerebrospinal fluid of Creutzfeldt-Jakob disease patients in the progressive and terminal stages. J Clin Neurosci. 13(6):661-5.

Shubin, N. H. and Alberch, P. 1986. A morphogenetic approach to the origin and basic organisation of the tetrapod limb. In M. K. Hecht, B. Wallace, and G. I. Prance (eds.). Evolutionary Biology. Plenum Press, New York, pp. 319–387.

Shubin, N.H., Daeschler, E.B. and Jenkins, F.A. Jr. 2006. The pectoral fin of *Tiktaalik roseae* and the origin of the tetrapod limb. Nature Apr 6;440(7085):764-71.

Smith, K.K. 2002. Sequence heterochrony and the evolution of development. *Journal of morphology* 252:82-97.

Smith, K.K 2003. Time's arrow: heterochrony and the evolution of development. *Int. J. Dev. Biol.* 47:613-621

Smith, S.J., Kotecha, S., Towers, N., Latinkic, B.V. and Mohun T.J. 2002. XPOX2-peroxidase expression and the XLURP-1 promoter reveal the site of embryonic myeloid cell development in Xenopus. Mechanisms of Development 117 173–186

Stern, H.M. and Zon L.I. 2003. Cancer genetics and drug discovery in the zebrafish. Nat Rev Cancer 3(7):533-539.

Streisinger, G., Walker, C., Dower, N., Knauber, D. and Singer, F. 1981. Production of clones of homozygous diploid zebra fish (*Brachydanio rerio*).
Nature 28;291 (5813): 293-6.

Swanson, K.D. and Ganguly, R. 1992. Characterization of a Drosophila melanogaster gene similar to the mammalian genes encoding the tyrosine/tryptophan hydroxylase activator and protein kinase C inhibitor proteins. Gene. Apr 15;113(2):183-90.

Tarsitano, S. and Hecht, M. K. 1980. A reconsideration of the reptilian relationships of *Archaeopteryx.* Zool. J. Linn. Soc. 69: 149–182.

Tavella, S., Biticchi, R., Schito, A., Minina, E., Di Martino, D., Pagano, A., Vortkamp, A., Horton, W.A., Cancedda, R. and Garofalo, S.2004. Targeted Expression of SHH Affects Chondrocyte Differentiation, Growth Plate Organization, and Sox9 Expression. Journal of bone and mineral research 19 (10):1678-1688

The Gene Ontology Consortium. 2000. Gene Ontology: tool for the unification of biology. Nat. Genet. 25, 25-29

Theiler, K. 1972. In *The House Mouse: Development and normal stages from fertilization to 4 weeks of age.* Springer-Verlag, New York.

Thisse, C., Thisse, B., Schilling, T.F. and Postlethwait, J.H. 1993. Structure of the zebrafish *snail1* gene and its expression in wild-type, *spadetail* and *no tail* mutant embryos. Development 119:1203–1215.

Thisse, B., Heyer, V., Lux, A., Alunni, V., Degrave, A., Seiliez, I. et al. 2004. Spatial and temporal expression of the zebrafish genome by large scale *in situ* hybridization screening. Methods Cell Biol;77:505–519.

Thulborn, R. A. and Hamley, T. L. 1982. The reptilian relationships of *Archaeopteryx*. Aust. J. Zool. 30: 611–634.

Tickle, C. 2002. Molecular basis of vertebrate limb patterning.Am J Med Genet. 112(3):250-5.

Tiecke, E., Turner, R., Sanz-Ezquerro, J.J., Warner, A. and Tickle, C. 2007. Manipulations of PKA in chick limb development reveal roles in digit patterning including a positive role in Sonic Hedgehog signaling. Developmental Biology 305: 312–324

Umahara, T., Uchihara, T., Tsuchiya, K., Nakamura, A., Iwamoto, T., Ikeda, K. and Takasaki, M. 2004. 14-3-3 proteins and zeta isoform containing neurofibrilary tangles in patients with Alzheimer's disease. Acta Neuropathol. 108: 279-286

Van Everbroeck, B.R.J., Boons, J. and Cras, P. 2005. 14-3-3 γ-isoform detection distinguishes sporadic Creutzfeldt–Jakob disease from other dementias. J Neurol Neurosurg Psychiatry 76:100–102

Vargas, A.O. and Fallon, J.F. 2004. Birds Have Dinosaur Wings: The Molecular Evidence. Journal of Experimental Zoology (Mol Dev Evol) 000:1–5 (2004)

Verbeek F.J., Lawson, K.A. and Bard, J.B. Developmental bioinformatics: linking genetic data to virtual embryos. Int J Dev Biol 1999;43:761–771.

Verbeek, F.J., Den Broeder, M.J., Boon, P.J., Buitendijk, B., Doerry, E., Van Raaij, E.J. and Zivkovic, D. 2000. A standard atlas of zebrafish embryonic development for projection of experimental data. Proc SPIE, Internet Imaging I 3964:242-252

Verbeek, F.J. 2000. Theory & Practice of 3D-reconstructions from serial sections. In Image Processing, A Practical Approach. R.A. Baldock and J. Graham, eds. (Oxford: Oxford University Press), pp. 153-195

Verbeek, F.J., Boon, P.J., Sloetjes, H., Van der Velde, R. and Vos, N. 2002. Visualization of complex data sets over Internet: 2D and 3D visualisation of the 3D digital atlas of zebrafish development. Proc SPIE Internet Imaging III 4672:20–29.

Verbeek,F.J., Rodrigues, D.D., Spaink, H.P. and Siebes, A.J.P.M. 2004. Data submission of 3D image sets to a bio-molecular database using active shape models and a 3D reference model for projection. Proc SPIE Internet Imaging V 5304:13–23.

Wagner, G.P. 2005. The developmental evolution of avian digit homology: An update Theory in Biosciences 124 (2005) 165–183

Wagner, G. P., and Gauthier, J. A. 1999. 1,2,352,3,4: a solution to the problem of the homology of the digits in the avian hand. Proc. Natl. Acad. Sci. USA 96: 5111–5116.

Walker, A. 1985. The braincase of Archaeopteryx. In M. K. Hecht, J. H. Ostrom, G. Viohl, and P. Wellnhofer (eds.). The Beginnings of Birds: Proceedings of the International Archaeopteryx Conference, Eichstätt. Freunde des Jura-Museums Eichstätt, Willibaldsburg, Eichstätt, pp. 123–134.

Wang, W. and Shakes, D.C. 1996. Molecular evolution of the 14-3-3 protein family.J Mol Evol. 43(4) 384-98.

Watanabe, M., Isobe, T., Ichimura, T., Kuwano, R., Takahashi, Y., Kondo, H. and Inoue, Y.1994. Molecular cloning of rat cDNAs for the and 0 subtypes of 14-3-3 protein and differential distributions of their mRNAs in the brain. Molecular Brain Research 25 113-121

Watanabe, M., Isobe, T., Ichimura, T., Kuwano, R., Takahashi,Y. and Kondo, H. 1993. Developmental regulation of neuronal expression for the subtype of the 14-3-3 protein, a putative regulatory protein for protein kinase **C.** *Developmental Brain Research,* 73 225-235 225

Watanabe, M., Isobe, T., Ichimura, T., Kuwano, R., Takahashi,Y. and Kondo, H. 1993. Molecular cloning of rat cDNAs for/3 and 3/subtypes of 14-3-3 protein and developmental changes in expression of their mRNAs in the nervous system. *Molecular Brain Research,* 17 135-146 135

Weinberg, E.S., Allende, M.L., Kelly, C.S., Abdelhamid, A., Murakami, T., Andermann, P. et al. 1996. Developmental regulation of zebrafish *MyoD* in wild type, *no tail* and *spadetail* embryos. Development 122:271-280

Wellnhofer, P. 1985. Remarks of the digit and pubis problems of *Archaeopteryx*. In M. K. Hecht, J. H. Ostrom, G. Viohl, and P.Wellnhofer (eds.). The Beginnings of Birds: Proceedings of the International Archaeopteryx Conference, Eichstätt. Freunde des Jura-Museums Eichstätt, Willibaldsburg, Eichstätt, pp. 113–122.

Wilker, E. and Yaffe, M.B. 2004. 14-3-3 Proteins – a focus on cancer and human disease. J. Mol Cell Cardiol. 37 (3):633-42

Wilkinson, D.G. 1998. *In situ* hybridization, a practical approach. Oxford university press, Oxford, England

Willett, C.E., Cortes, A., Zuasti, A. and Zapata, A.G. 1999. Early hematopoiesis and developing lymphoid organs in the zebrafish. Developmental dynamics 214: 323- 336.

Wolpert, L. and Hornbruch, A. 1990. Double anterior chick limb buds and models for cartilage rudiment specification. Development 109: 961–966.

Wilson AL, Shen Y-C, Babb-Clendenon SG, Rostedt J, Liu B, Barald KF, Marrs JA, Liu Q. 2007. Cadherin-4 plays a role in the development of zebrafish cranial ganglia and lateral line system. Developmental Dynamics 236:893-902

Wolpert, L., Beddington, R., Jessell, T.M., Lawrence, P., Meyerowitz, E.M. and Smith, J. Principles of Development, 2nd Ed., 2002

Woo, K. and Fraser, S.E. 1998. Specification of the Hindbrain fate in the zebrafish. Dev biol 197:283-296

Wu, C. and Muslin, A.J. 2002. Role of 14-3-3 proteins in early *Xenopus* development. Mech Dev. 119(1):45-54.

Yan, Y.L., Willoughby, J., Liu, D., Gage Crump, J., Wilson, C., Miller, C.T., Singer, A., Kimmel, C., Westerfield, M. and Postlethwait, J.H. 2004. A pair of Sox: distinct and overlapping functions of zebrafish *sox9* co-orthologs in craniofacial and pectoral fin development. Development 132: 1069-1083

Yang, Y., Drossopoulou, G., Chuang, P.T., Duprez, D., Marti, E., Bumcrot, D., Vargesson, N., Clarke, J., Niswander, L., McMahon, A. and Tickle C. 1997. Relationship between dose, distance and time in Sonic-Hedgehog-mediated regulation of anteroposterior polarity in the chick limb. Development 124: 4393–4404.

Yasuda, M. 2002. The Anatomical Atlas of Gallus (English Edition). University of Tokyo Press, Tokyo.

Zaidi, A.U., Enomoto, H., Milbrandt, J. and Roth, K.A. 2000. Dual fluorescent *in situ* hybridization and immunohistochemical detection with tyramide signal amplification. J Histochem Cytochem. 48(10):1369-75

Zakany, J., Gerard, M., Favier, B. and Duboule, D. 1997. Deletion of a HoxD enhancer induces transcriptional heterochrony leading to transposition of the sacrum. EMBO J. Jul 16; 16(14):4393-402.

Zakany, J., Fromental-Ramain, C., Warot, X. and Duboule, D. 1997. Regulation of digit number and size of digits by posterior Hox genes: a dose-dependent mechanism with potential evolutionary implications. Proc. Natl. Acad. Sci. USA 94: 13695–13700.

Zakany, J., Kmita,M. and Duboule, D. 2004. A dual role for Hox genes in limb anterior-posterior asymmetry. Science 304: 1669–1672.

Zhou, Z., Barrett, P. M. and Hilton, J. 2003. An exceptionally preserved Lower Cretaceous ecosystem. Nature 421: 807–814.

Zupanc, G.K.H., Hinsch, K. and Gage, F.H. 2005. Proliferation, Migration, Neuronal Differentiation, and Long-Term Survival of New Cell in the Adult Zebrafish Brain Journal of Comparative Neurology 488:290–319 (2005)

Summary

In developmental biology, the expression of genes is studied to understand normal development, phenotypes and to construct models to understand disease. In this thesis, we explore and validate biological as well as computerized tools, to address research questions in developmental biology. Based on these techniques, we developed a workflow to generate a large number of 3D spatio-temporal patterns of gene expression.
The analysis of developmental processes has specific problems. For example, many genes are active and many events occur in a short time span, gene expression patterns in differentiating structures do not always correspond with the boundaries of anatomical structures, and expression patterns of different genes need to be compared for colocalization and coexpression. Though several techniques for gene expression analysis are available, most spatial gene expression data are only in 2D. In order to study gene expression and differentiation of structures during development at the same time, both spatial 3D information, and temporal data are essential. Nowadays there is a tendency towards combining molecular biological as well as computational tools and techniques.

In the research group Imaging and Bioninformatics, we have developed a 3D Atlas of zebrafish development. This atlas is intended to serve as an on line reference for researchers. In addition to the anatomical information of the 3D Atlas, a zebrafish gene expression database is under construction (Belmamoune and Verbeek, 2006). This gene expression database can be considered as the molecular counterpart of the 3D atlas. Spatial and temporal expression patterns of genes involved in developmental processes can be mapped on developing anatomical structures in the 3D atlas and compared for co-localization and co-expression of genes; providing a clue about development of complex organs and tissues.
These spatio-temporal patterns of gene expression have to be generated. To that end, we have developed a workflow based on fluorescent *in situ* hybridization (FISH) (ZebraFISH; cf **Chapter 2**), confocal laser scanning microscopy (CLSM) and subsequent three-dimensional modeling with, in our case, TDR-3Dbase software - but comparable results could be obtained with other 3D reconstruction softwar e- resulting in a large amount of 3D spatio-temporal patterns of gene expression obtained in a straightforward and non-destructive manner.

In **Chapter 2,** we describe the methodology of ZebraFISH. This fluorescent *in situ* hybridization method is based on the high-resolution whole mount *in situ* hybridization protocol described by Thisse et al (1993, 2004). The strength of our approach is that it enables 3D imaging with confocal laser scanning microscopy. In our ZebraFISH protocol, Tyramide Signal Amplification (TSA) is used to visualize gene expression patterns. The work in this thesis (Chapter 2 and 3) demonstrates that the ZebraFISH method yields a high signal and relatively low background in a short, defined staining period.
For the work described in this thesis, we applied our workflow to a wide variety of genes in two groups of case studies:

1) *Case study Early zebrafish development*
2) Case study Late zebrafish and cross species development

Case study Early zebrafish development

In **Chapter 3,** the expression of 14-3-3 isoforms was analyzed in zebrafish embryos in a developmental series ranging from 18 hpf up to 48 hpf. In this study, we applied ZebraFISH to investigate complex gene expression patterns with a diffuse appearance. With our workflow, based on ZebraFISH, CLSM and 3D modelling, we were able to detect more gene expression domains and at earlier stages of development than in previous studies. Our methods provided an accurate characterization of genes encoding 14-3-3 γ and τ proteins in subsequent stages of zebrafish development.

In **Chapter 4**, ZebraFISH was applied to analyze gene expression in single white blood cells and precursors thereof. Gene expression patterns of *l-plastin*, a general marker for leukocytes, and *mpx*, a marker for neutrophil granulocytes, were characterized in developmental series of zebrafish. In addition, a pilot study was carried out to analyze the distribution of *l-plastin* and *mpx* expressing cells from 24 hpf up to 72 hpf in relation to haematopoietic events. The schematic 3D modeling presented in this study, allows better inspection of the distribution of the single *l-plastin* and *mpx* expressing cells and their relation to anatomical structures.

Case study Late zebrafish and cross species development

In this case study the focus is on genes involved zebrafish fin and tetrapod limb development.

In **Chapter 5**, ISH and 3D modelling are used to investigate a rudimentary digit in the wing of developing chicken embryos. Gene expression patterns from two markers genes of early cartilage formation, *sox9* and *bmpr1b*, were analyzed in chicken wings and hindlimbs. In the wing, anterior to digit II primordium and close to the ectoderm, we found an expression domain for *sox9* that we identified as a rudimentary digit I domain.
No subsequent *bmpr1b* expression and no cartilage formation were found in this domain, suggesting that the presumptive digit I domain is arrested in development and shows no further differentiation.

In Chapter 6, timing of expression of genes involved in zebrafish pectoral fin and chicken limb development is compared among other vertebrate model systems. Zebrafish and chicken gene expression data were obtained by our own experiments. Data for mouse, axolotl and clawed toad, as well as supplemental data for chicken, were extracted from the literature. A relative time scale was calculated for every model species, from zygote up to hatching, birth or juvenile stages. Gene expression data were processed with the Frequent Episode Mining algorithm (FEDA) to analyze evolutionary relationships between model species, based on heterochrony, i.e. difference in timing, of gene expression. The relative time scale was made part of the computation.
The FEDA algorithm showed to be a powerful and flexible method. Data can be rearranged such that several features can be compared in the analysis; i.e., gene expression, morphological structures, species and timing data.

In **Chapter 7**, a general discussion and conclusions are presented. A perspective of the work described in this thesis is given in relation to recent literature and the most important conclusions from **Chapter 2-6** are summarized

Samenvatting

In de ontwikkelingsbiologie wordt activiteit van genen, genexpressie, bestudeerd om inzicht te krijgen in ontwikkelingsprocessen, en om modellen te ontwikkelen voor ziekten en afwijkingen. In dit proefschrift zijn biologische en digitale methoden ontwikkeld, toegepast en gevalideerd om genetische en morfologische vraagstukken tijdens embryonale ontwikkeling te kunnen analyseren in 3D, in plaats en in tijd.
Op basis van deze technieken hebben we een protocol ontwikkeld, een zogenaamde workflow, om grote aantallen driedimensionale genexpressie-patronen in plaats en op vershillende tijdstippen tijdens de ontwikkeling.
Het bestuderen van ontwikkelingsprocessen heeft specifieke uitdagingen. Er komen vele genen tegelijkertijd tot expressie en veel processen vinden in relatief korte tijd plaats. Genexpressie-patronen komen niet altijd overeen met de anatomische structuren, en expressie – patronen van verschillende genen moeten met elkaar vergeleken worden in plaats en tijd om het verloop van de ontwikkelingsprocessen en de vorming van organen te kunnen volgen. Er zijn verscheidene technieken voor de analyse van genexpressie voorhanden; de meeste gegevens over genexpressie zijn echter alleen in 2D beelden.. Om genexpressie en de differentiatie van structuren te kunnen volgen gedurende de ontwikkeling, zijn zowel spatiële gegevens, in 3D, als gegevens over tijd noodzakelijk. Met huidige moleculair-biologische en beeldanalyse technieken kunnen dergelijke analyses gedaan worden.
In de onderzoeksgroep Imaging and Bioinformatics van de Imagery and Media Group is een “3D Atlas of Zebrafish development “ ontworpen. Deze atlas is bedoeld als on line referentie voor onderzoekers en kan uiteindelijk gebruikt worden om genexpressie-patronen op te projecteren. Als aanvulling op deze 3D Atlas is momenteel een “ zebrafish gene expression database” in ontwikkeling. Deze genexpressie-database kan beschouwd worden als de moleculair – biologische tegenhanger van de 3D Atlas. Genexpressie-gegevens in plaats en tijd, kunnen geprojecteerd worden op de anatomische structuren van een virtueel embryo in de 3D Atlas, en vergeleken worden op co-expressie (tegelijkertijd tot expressie komen) en co-lokalisatie (op dezelfde plaats tot expressie komen). Zo krijgt men een goed inzicht in de staat van ontwikkeling zelf, en in activiteit van genen die betrokken zijn bij de ontwikkeling van specifieke weefsels of organen.
Deze spatio-temporele gegevens moeten op een of andere wijze gegenereerd worden. Hiertoe hebben wij een werkschema ontwikkeld, gebaseerd op fluorescente in situ – hybridisatie (FISH), confocale laser scanning microscopie (CLSM), 3D reconstructie met – in dit geval – TDR-3Dbase software en software voor data-analyse Frequent Episode Mining in Developmental Analysis (FEDA). Met deze tools kunnen grote 3D gegevens van genexpressie verkregen worden, op betrekkelijk eenvoudige en non-destructieve wijze.
Om 3D opnamen van genexpressie-patronen mogelijk te maken, hebben we een protocol ontwikkeld voor fluorescente *in situ* hybridisatie (FISH): ZebraFISH.

In **Hoofdstuk 2** wordt de methode en techniek van ZebraFISH besproken. Voor deze fluorescente *in situ* hybridizasatie wordt gebruik gemaakt van Tyramide Signal Amplification (TSA), gebaseerd op het veelgebruikte *in situ* hybridisatie – protocol voor zebravis (Thisse et al. 1993). Deze kleurmethode levert in een korte reactietijd een sterk signaal op, terwijl er weinig achtergrondkleuring optreedt.

Het voordeel van deze benadering is dat van genexpressie-patronen, aangetoond met behulp van ZebraFISH, 3D opnamen gemaakt kunnen worden m.b.v. confocale laser scanning microscopie (CLSM).
We hebben de technieken en het werkschema toegepast op twee case studies tijdens de embryonale ontwikkeling:

1) De vroege ontwikkeling van de zebravis.
2) De latere ontwikkeling van zebravis en vergelijking met andere modelorganismen.

Case study Early zebrafish development
In **Hoofdstuk 3** zijn de expressiepatronen van de genen die coderen voor de 14-3-3 eiwitten geanalyseerd in zebravis-embryo's van 18 tot 48 uur oud. In deze studie hebben we ZebraFISH, CLSM en 3D reconstructie toegepast om complexe genexpressie-patronen te lokaliseren. Door de toepassing van onze methoden vonden we meer genexpressie-patronen en in eerdere stadia van ontwikkeling dan in voorgaande studies. Onze methoden maakten het mogelijk om expressie-patronen van genen die coderen voor 14-3-3 gamma en tau eiwitten in de zebravis, nauwkeurig in kaart te brengen tijdens opeenvolgende stadia van ontwikkeling.

In **Hoofdstuk 4** zijn de ZebraFISH methode, CLSM en 3D reconstructie toegepast op losse cellen: leukocyten of voorlopers daarvan. De genexpressie-patronen voor *l-plastin,* een algemene marker voor leukocyten, en *mpx,* een marker voor neutrofiele granulocyten zijn bestudeerd in verschillende stadia van ontwikkeling (24 tot 72 uur). Aanvullend hierop, als basis voor verdere studie, is de verdeling van de *l-plastin* en *mpx* expresserende cellen genanalyseerd met betrekking tot de formatie van bloed en de aanleg van bloedvaten. De schematische 3D modellen die in deze studie gepresenteerd worden, laten nauwkeurige inspectie toe van deze cellen en hun relatie tot anatomische structuren.

Case study Late zebrafish and cross species development
In deze case studie ligt de nadruk op genen die een rol spelen in de aanleg van de gepaarde vinnen van vissen en de ledematen van tetrapoden (viervoeters).

In **Hoofdstuk 5** zijn *in situ* hybridisatie en 3D reconstructie gebruikt om een rudimentaire structuur te bestuderen met betrekking tot de evolutie van vogels. De genexpressie-patronen van moleculaire markers die een rol spelen bij kraakbeenvorming, de transcriptiefactor *so*x9 en de receptor *bmpr1b,* zijn bestudeerd in van vleugel en poot in kippenembryo's van 4.5 tot 8 dagen oud. *In situ* hybridisatie met *sox9* leverde een specifiek genexpressiepatroon op in de vleugel, dat wij hebben geïdentificeerd als een digit I-domein. Deze structuur ontwikkelt zich niet verder tot kraakbeen.

In **Hoofdstuk 6** is de timing van expressie van genen die een rol spelen bij ontwikkeling van vinnen bij de zebravis en ledematen van de kip, vergeleken met die van andere modelorganismen, om inzicht krijgen in genetische netwerken die een rol spelen bij de ontwikkeling van de verschillende modelorganismen. Genexpressie-patronen voor zebravis en kip zijn geproduceerd met behulp van eigen experimenten. Gegevens voor

muis (*Mus musculus*), axolotl (*Ambystoma mexicanum*), klauwpad (*Xenopus laevis* en *X. tropicalis)* zijn verkregen door literatuurstudie.
Een belangrijke stap waarmee het mogelijk wordt ontwikkelingsgegevens te vergelijken is de relatieve tijdschaal voor ontwikkeling Voor elk organisme is zo'n relatieve tijdschaal berekend. De gegevens van genexpressie zijn uitgezet in deze relatieve tijdschaal van ontwikkeling. De methode "Frequent Episode Mining" (FEDA) is gebruikt voor analyse van evolutionaire relaties, gebaseerd op heterochronie - verschil in timing – van genexpressie tijdens de ontwikkeling van vin en ledemaat. De relatieve tijdschaal van ontwikkeling is hierbij opgenomen in de analyse. Het FEDA algoritme is flexibel: het kan op verschillende data worden toegepast, zoals op functies van genen, locaties van expressie, anatomische structuren, verschillende diersoorten en timing.

In **Hoofdstuk 7** wordt het werk, beschreven in dit proefschrift, beschouwd in perspectief met de meest recente literatuur. De belangrijkste conclusies uit de hoofdstukken worden in dit hoofdstuk samengevat.

Publications

• Welten, M.C.M.,. Sels, A., Lamers, G.E.M., Spaink, H.P. and Verbeek, F.J.
Expression analysis of the genes encoding 14-3-3 gamma and tau proteins using the 3D digital atlas of zebrafish development. In submission, 2007
.

• Bathoorn, R[a]., Welten, M.C.M.[b], Siebes, A.P.J.M., Richardson, M.K., Verbeek, F.J
Limb - fin heterochrony: a case study analysis of molecular and morphological characters using frequent episode mining. (a and b equally contributed)
In submission, 2007. (Evolution and Development).

• Witte, F., Welten, M., Heemskerk, M., Van der Stap, I., Ham, L., Rutjes, C. and Wanink, J. Major morphological changes in a Lake Victoria cichlid species within two decades.
Accepted for publication, 2007 (Biological Journal of the Linnaean Society).

• Meuleman, W., Welten, M.C.M. and Verbeek, F.J.
Construction of correlation networks with explicit time-slices using time-lagged, variable interval standard and partial correlation coefficients.
Lecture notes in computer science (2006).

• Welten, M.C.M., De Haan, S.B., Van den Boogert, N., Noordermeer, J.N., Lamers, G.E.M., Spaink, H.P, Meijer, A.H. and Verbeek, F.J.
ZebraFISH: Fluorescent *in situ* hybridization protocol and 3 D imaging of gene expression patterns.
ZEBRAFISH 3:4, 465-476 (2006)

• M. Corredor-Adamez, M.C.M. Welten, H.P. Spaink, J.E. Jeffery, R.T. Schoon, M.A.G. De Bakker, C.P. Bagowski, A.H. Meijer, F.J. Verbeek and M.K. Richardson
Genomic annotation and transcriptome analysis of the *Danio rerio* hox complex with description of a novel member, *hoxb13a*.
.Evolution & Development 7:5, 362-375 (2005)

• M.C.M. Welten, F.J. Verbeek, A.H. Meijer and M.K. Richardson.
Gene expression and digit homology in the chicken wing.
Evolution & Development 7:1, 18-28 (2005)

• M.C.M.Welten, P. A. J.Audiffred and W. F. Prud'homme van Reine.
Notes on Marine Algae Collected in Guinea-Bissau,Tropical West Africa.
Botanica Marina Vol. 45, 380–384 (2002)

Presentations

• **Seminar: TSA (Tyramide Signal Amplification) for FISH, IHC and Flow Cytometry. Perkin Elmer Benelux, University of Antwerp, Belgium. 20 September, 2007.**
Presentation: Spatio-temporal gene expression analysis from 3D *in situ* hybridization images (invited talk).

• **Benelux Congress of Zoology, Leuven, Belgium. 27-28 October, 2006.**
Presentation, 27 October:
Limb - fin heterochrony: a case study analysis of molecular and morphological characters using frequent episode mining. M.C.M. Welten, R. Bathoorn, A.P.J.M. Siebes, M.K. Richardson and F.J. Verbeek

• **8th International Conference Limb Development & Regeneration, Dundee, Scotland UK. July 15-/19 2004**.
Presentation, 18 July:
Spatio –temporal analysis of limb development as a case study for the 3D atlas of Zebrafish development and the Spatio-temporal zebrafish gene expression database. M.C.M. Welten, M.K. Richardson and F.J. Verbeek.

• **Benelux Congress of Zoology, Antwerp, Belgium, 7-8 November, 2002**
Presentation, 8 November:
Differences in gill area in natural populations of *Haplochromis pyrrhocephalus.*
M.C.M. Welten, M. Heemskerk, I. Van der Stap and F. Witte

Poster presentations
• **Designing the body plan. Lorentz Center, Leiden University. 4-8 June , 2007.**
Poster presentation, 7 June 2007:
From cell to organ: gene expression analysis of 14-3-3 gamma and tau proteins using the 3D digital atlas of zebrafish development. M.C.M. Welten, A. Sels, M.I. Van den Berg – Braak, G.E.M. Lamers, H.P. Spaink and F.J. Verbeek.

• **SIREN 2005, TU Eindhoven, the Netherlands; 6 October, 2005**
Poster presentation:
A digital zebrafish helps fishing for knowledge.
M. Belmamoune, R. Bathoorn, M.C.M. Welten, E. Lindoorn, M.K. Richardson, H.P. Spaink, A.P.J.M. Siebes and F.J. Verbeek.

• **4th European Zebrafish Genetics and Development meeting 2005, Dresden, Germany, 13-19 July, 2005.**
Poster presentation:
Construction of Phylogenetic trees by comparative analysis using gene expression derived heterochrony with zebrafish as principal experimental model system.
M.C.M. Welten, R. Bathoorn, A.J.P.M. Siebes, M.K. Richardson and F.J. Verbeek.

Curriculum vitae

Monica Cornelia Maria Welten werd geboren op 2 juni 1960 te Heemstede. In 1979 behaalde zij het HAVO diploma aan het Sint-Antoniuscollege te Gouda. Zij vervolgde haar opleiding aan het Van 't Hoff Instituut te Rotterdam (de huidige Hogeschool Rotterdam). In 1981 behaalde zij het diploma Hogere Laboratoriumopleiding, richting Medische Microbiologie. Na het afronden van deze opleiding werkte zij als analist: van 1981 tot 1990 bij het Streeklaboratorium voor de Volksgezondheid te Gouda en van 1990 tot 2000 bij het Universitair Medisch Centrum Utrecht.

Omdat zij al sinds haar jeugd de wens had om Biologie te studeren en zelf onderzoek te doen, besloot zij in september 2000 haar vaste baan op te zeggen en Biologie te gaan studeren aan de Universiteit Leiden. De werkervaring als microbiologisch analist kwam hierbij uitstekend van pas.

Tijdens haar eerste onderzoeksstage werkte zij aan "Identification of marine algae collected in Guinea Bissau", onder supervisie van Dr. W.F. Prud'homme van Reine. Deze studie werd in 2002 gepubliceerd in Botanica Marina. Het onderwerp van haar tweede onderzoeksstage was "Rapid increase in gill surface in natural populations of the Lake Victoria Cichlid *Haplochromis pyrrhocephalus" ,* onder supervisie van Dr. F. Witte. In 2002 behaalde zij het doctoraal diploma Biologie.

In 2003 werkte zij bij Prof. Dr. M. K. Richardson aan het project "Gene expression and digit homology in the chicken wing". Vanaf januari 2004 begon zij aan het in dit proefschrift beschreven promotieonderzoek onder begeleiding van Dr. Ir. F. J. Verbeek en in samenwerking met Prof. Dr. H. P. Spaink, Prof. Dr. M. K. Richardson en Dr. A. H. Meijer. Dit promotieonderzoek werd gesubsidieerd door NWO.
Sinds 1 juli 2007 werkt zij aan de Universiteit Leiden als post doc bij Dr. G.E.E.J.M. Van den Thillart aan het project "Cloning and gene expression analysis of the gonadotropin receptors in the European eel, *Anguilla anguilla*". Vanaf 1 december 2007 zal zij haar werk als post doc voortzetten bij Prof. Dr. S. Lindsay aan het Institute of Human Genetics van de universiteit van Newcastle (UK).

Color supplement

Chapter 2

FIG. 1. A panel of marker genes expressed in 24 hpf zebrafish embryos. Row **A** depicts the results of the standard AP detection. Row **B** depicts a characteristic optical section from the 3D image obtained with zebraFISH, using TSA/Cy3-SYTOX Green. Row **C** is a projection of that same image stack into one image. Row **D** depicts 3D reconstructions of the expression pattern, the embryo outline, and some surrounding tissues as obtained from the 3D image.
Column **1** shows *myoD* expression in the somites: (**B1, C1**) *myoD* expression detected in an image stack of 64 slices; (**D1**) 3D reconstruction of *myoD* expression in white, yolk extension in green, and embryo outline in blue. Column 1 is visualized in oblique dorsal orientation. Column **2** shows *krox20* expressed in rhombomeres 3 and 5: (**B2, C2**) *krox20* gene expression in an image stack of 13 slices; (**D2**) 3D reconstruction of *krox20* expression in white, third ventricle in cyan, partial eye outline in salmon, and embryo outline in blue. Column 2 is visualized in oblique lateral orientation. Column **3** shows the *pax2.1* expression pattern at the midbrain-hindbrain boundary and the optic stalk: (**B3, C3**) show gene expression detected in an image stack of 97 slices; (**D3**) 3D reconstruction of *pax2.1* gene expression patterns in white, embryo outline in blue, optic cup in salmon. Column 3 is visualized in oblique lateral orientation. Column **4** shows *otx2* expressed in the diencephalon and mesencephalon: the image stack in (**B4, C4**) is 74 slices; (**D4**) 3D reconstruction of *otx2* gene expression in white, embryo outline in blue, optic cup in salmon. Column 4 is visualized in oblique lateral orientation. For all four genes, the pattern generated with zebraFISH corresponds to the pattern generated with AP detection. The 3D reconstructions give insight into the extension of the pattern within the embryo as well as clear spatial relations with a number of anatomical domains. These domains coincide exactly with the domains annotated in the three-dimensional digital atlas of zebrafish development (bio-imaging.liacs.nl).
FIG. 2. Gene expression patterns of *mpx* in 36 hpf and 48 hpf zebrafish embryos with TSA/Cy3 detection. (**A**) At 36 hpf, an image stack of 70 slices. For this image only TSA detection was applied. The *mpx* expressing cells are clearly visible as dispersed over the yolk and also visible in the head; *mpx* expressing cells also accumulate in the ventral venous plexus (not shown). (**B–D**) At 48 hpf, image stacks of 78 slices using TSA/Cy3-SYTOX Green detection. Expression is visible in single cells scattered over the yolk and in the head. Characteristic slices show single cell imaging (arrow pointing to *mpx* expressing cell) in the brain (**B**) and yolk sac (**C**). (**D**) A projection of the whole stack showing the pattern of the *mpx* gene at 48 hpf.

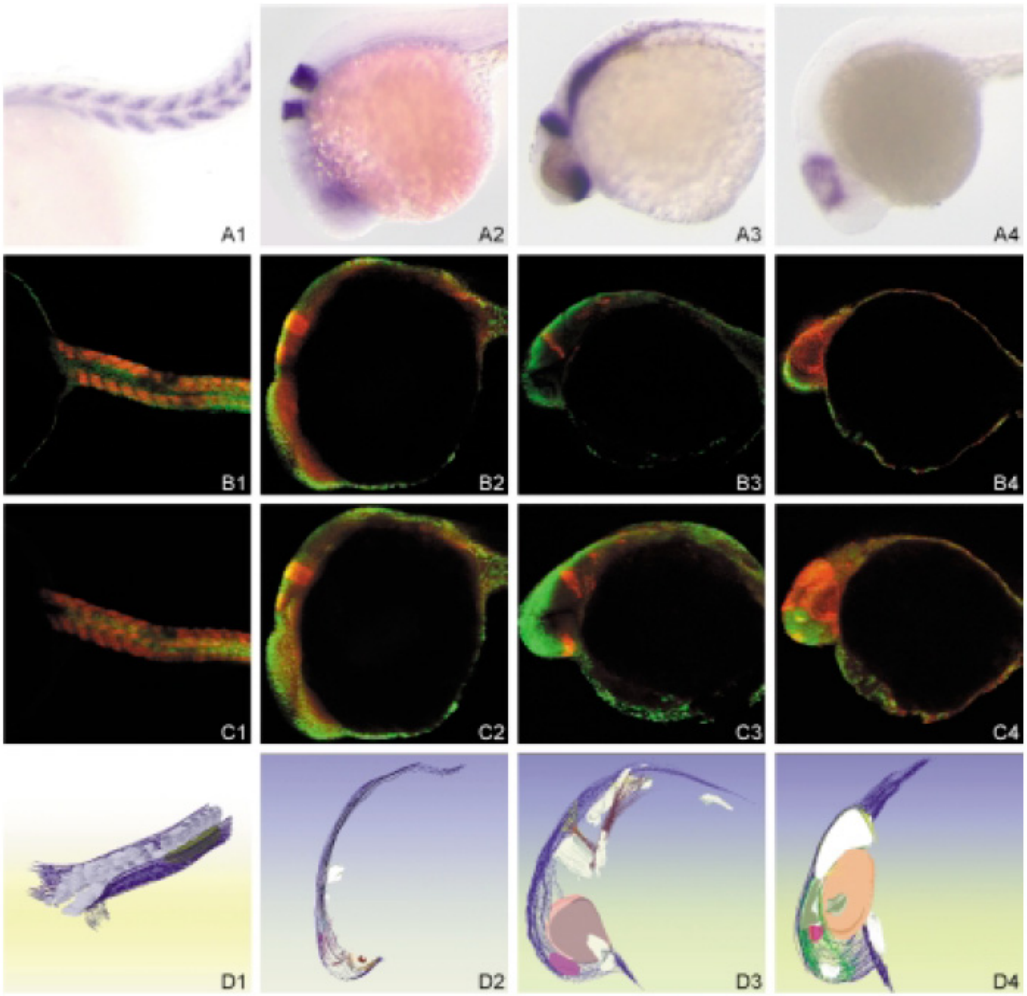

FIG. 1.

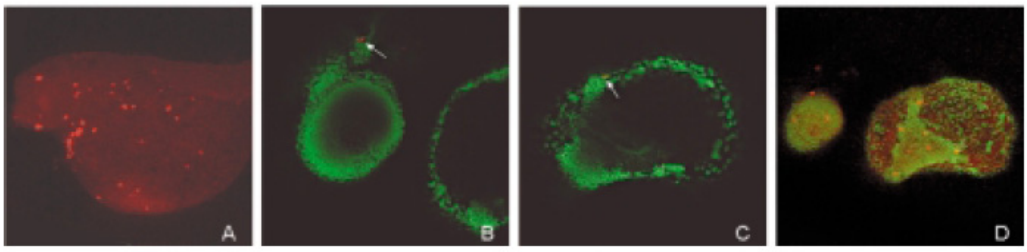

FIG. 2.

Chapter 2 Fig 1 and 2

Chapter 3

Fig.2 A: FISH result for the gene encoding 14-3-3γ in a 24 hpf embryo. The picture is a confocal image**.**

C: 14-3-3 **γ** FISH result in a 48 hpf embryo; a so-called z-projection of the confocal image. Gene expression is in red, i.e. the red channel of the CLSM image. The green depicts a background staining of the cell nuclei with SYTOX Green.
2 B,D: 3D reconstruction of the embryos shown in 2A and 2B respectively. Gene expression for 14-3-3 **γ** is depicted in white. Both FISH images and 3D reconstruction clearly reveal gene expression patterns in otic vesicle (salmon) , optic stalk (orange), cranial ganglia (light yellow), ganglion V (light organge), spinal cord neurons and heart primordium (red) at 24 and 48 hpf.
2 E, F: ISH results for 14-3-3 **γ** at 24 and 48 hpf. Dorsal view; anterior is to the left.
G: 14-3-3 γ ISH result at 24 hpf. Tissue section after overstaining, revealing gene expression in eye, tectum of the mesencephalon, cranial ganglia and otic vesicle.
H: 3D reconstruction of the embryo shown in 5A. In 5B, gene expression is displayed in relation to anatomical structures. 14-3-3 γ gene expression domains are depicted in white.
In all images, anterior is to the left, dorsal is to the top.
The findings after overstaining, tissue sectioning and 3D reconstruction of ISH results confirm our findings with FISH.
Abbreviations: ccv, common cardinal vein; cer, cerebellum; c g, cranial ganglia; c g V, fifth cranial ganglion; di, diencephalon; h: heart primordium; o v, otic vesicle; sp n, spinal cord neurons; tec, tectum of the mesencephalon; rh: rhombencephalon.
Color legend: gene expression: white; gill primordia: light green; cerebellum: blue; common cardinal vein: clear blue; diencephalon: orange; eye: salmon; lens: brown; heart primordium: red; otic vesicle: dark green; rhombencephalon: lilac; tectum (mesencephalon): purple; telencehpalon: dark blue; 4^{th} ventricle: clear blue.

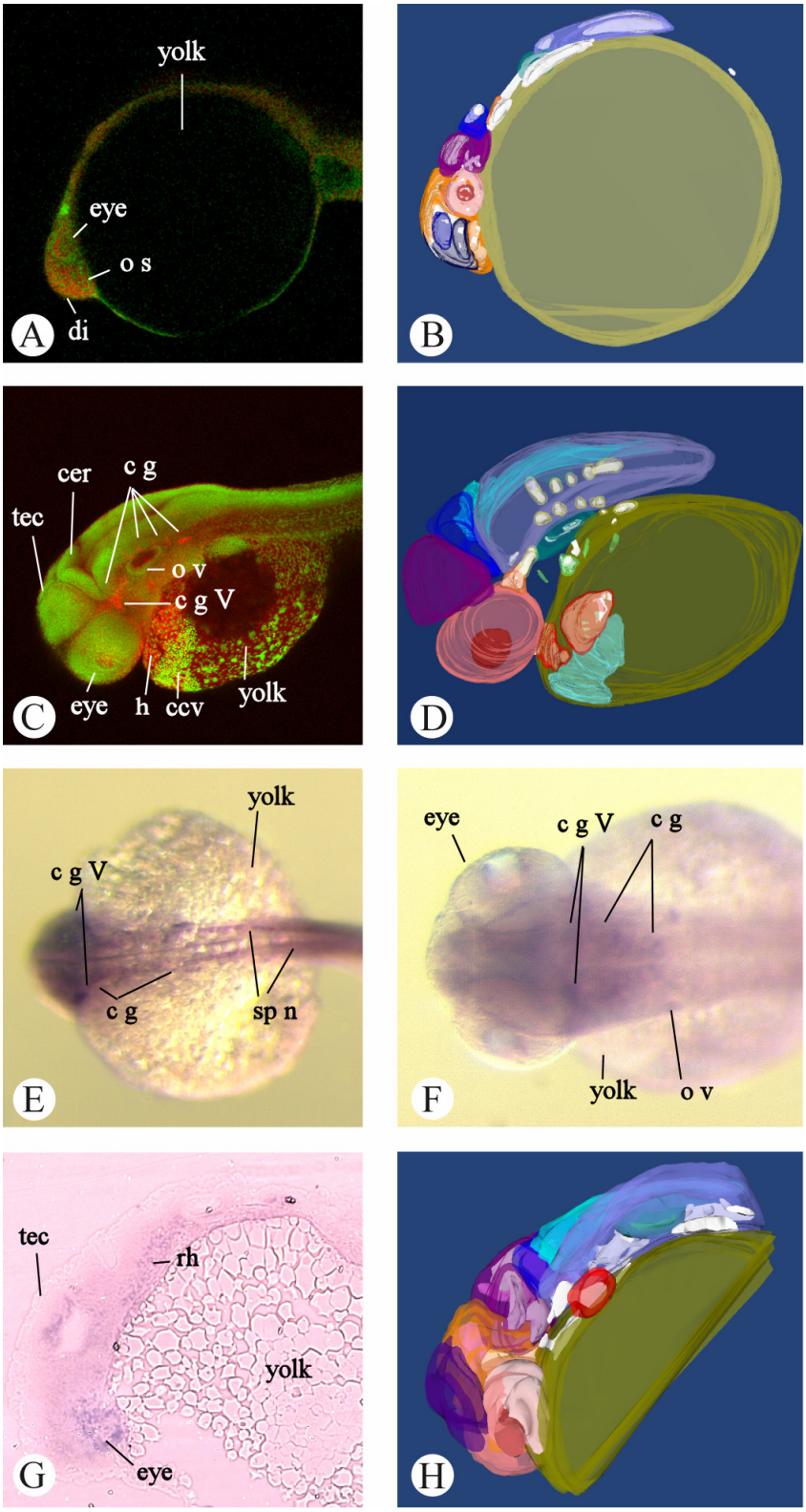

Chapter 3 Fig.2

Chapter 3

Fig. 3 A: 14-3-3 τ FISH result in a 24 hpf embryo; z-projection of a confocal image.
B: 3D reconstruction of the embryo shown in 3A. 14-3-3 τ gene expression (white) is visible in most brain structures.
C: Gene expression for 14-3-3 τ at 36 hpf, ISH detection.
D: Reference image from the 3D atlas, in the same orientation as the embryo in 3A and B.
Abbreviations: cer, cerebellum; f b: fin bud; o v, otic vesicle; tec, tectum of the mesencephalon; tel: telencephalon. In all images, anterior is to the left, dorsal is to the top.
Color legend: gene expression: white; cerebellum: blue; diencephalon: orange; eye: salmon; lens: brown; otic vesicle: dark green; rhombencephalon: lilac; tectum (mesencephalon): purple; 4th ventricle: clear blue.

Fig.4 A, B: 3D reconstructions of *pax2* (4A) and *otx2* (4B) expression domains at 24 hpf, used as a reference for the brain structures.
In all images, anterior is to the left, dorsal is to the top. Color legend: gene expression: white; optic cup: salmon; embryo outline: dark blue

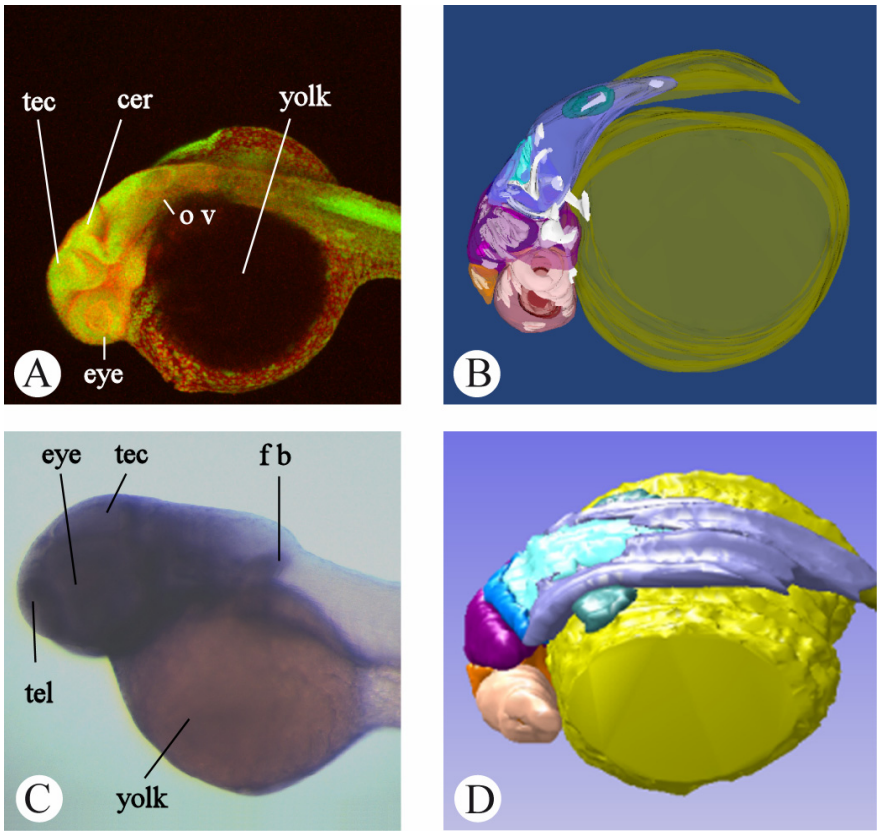

Chapter 3 fig. 3

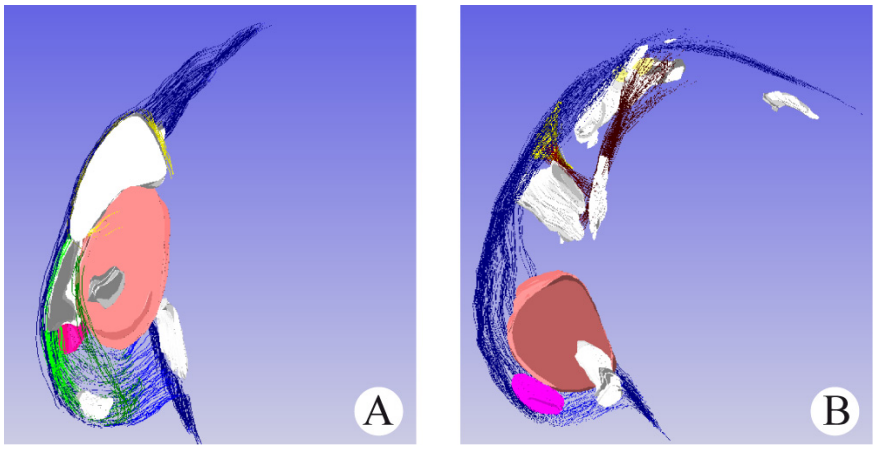

Chapter 3 fig. 4

Fig. 3. Panels A-D: developmental series of *l-plastin* expression in zebrafish embryos at 24, 36, 48 and 60 hpf.
Panels E-H: developmental series of *mpx* expression at 24, 36, 48 and 72 hpf. TSA detection.
A is a dorsal view, anterior is to the left; B-H: Anterior is to the left, dorsal to the top. Images are so-called z-projections of confocal images. Gene expression is in red (TSA signal), counterstaining is in green (SYTOX Green).
Abbreviations: cer: cerebellum; fb: fin bud; h: head; mb: midbrain; pros: prosencephalon; t: tail; ye: yolk extension.

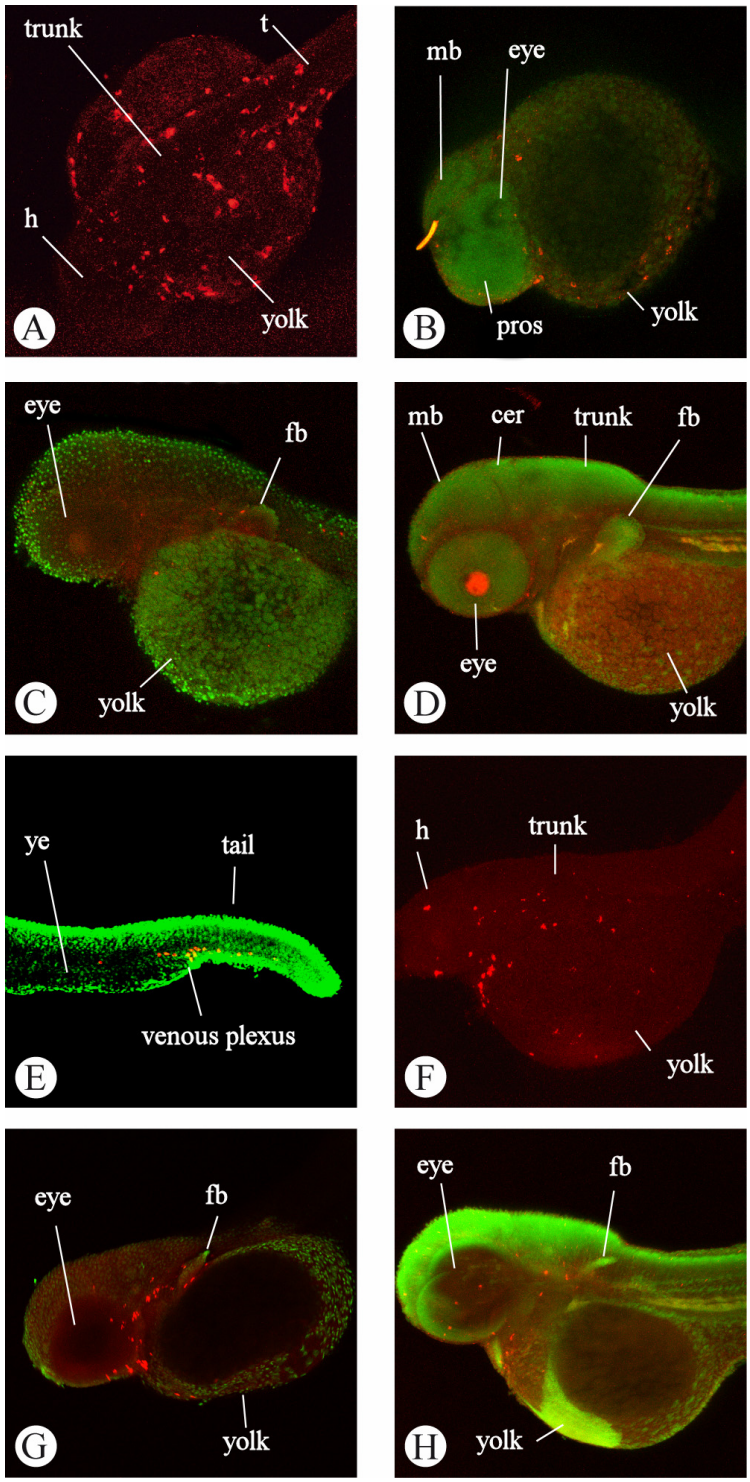

Chapter 4 fig 3

Fig.6. A-D: *l-plastin* gene expression at 36 hpf (panel A and B) and at 60 hpf (panel C and D), In panel B and D, the 3D reconstructions of the embryos in panel A and C are depicted.

E: *mpx* expression in a 48 hpf embryo. F: 3D reconstruction of the same embryo, depicting *mpx* expressing cells in the common cardinal vein i.e. the light blue structure on the yolk (ochre), visible from the confocal image as well as in the 3D reconstruction.
G: *mpx* expression in the tail of a 72 hpf embryo. H: 3D reconstruction of the same embryo, portraying *mpx* expressing cells in the CHT.
The images of the embryos in panel A, C, E and G are the result of TSA detection; The images are so-called z-projections of a confocal image stack. Gene expression is in red (TSA signal), counter staining is in green (SYTOX Green signal). Anterior is to the left, dorsal to the top.

Color legend for the 3D reconstructions in panel B, D, F and H:

l-plastin or *mpx* positive cells (white). embryo outline (dark blue, diencephalon (orange), yolk and yolk extension (ochre), mesencephalon (purple) optic cup (salmon), pectoral fin (red).

Abbreviations: ccv: common cardinal vein; cer: cerebellum; CHT: caudal haematopoietic tissue; fb: fin bud; h: head; mb: midbrain; pros: prosencephalon; t: tail; ye: yolk extension. **Fig. 5**. A: *l-plastin* expression in the tail of a 96 hpf embryo in the dorsal longitudinal anastomotic vessels. B: *mpx* expression in the tail of a 96 hpf embryo. Notice the clusters of cells in the spaces between the somites, as a part of the CHT (Murayama et al. 2006). ISH detection with AP staining. Anterior is to the left, dorsal to the top.
DLAV: dorsal longitudinal anastomotic vessels; CHT: caudal haematopoietic tissue.

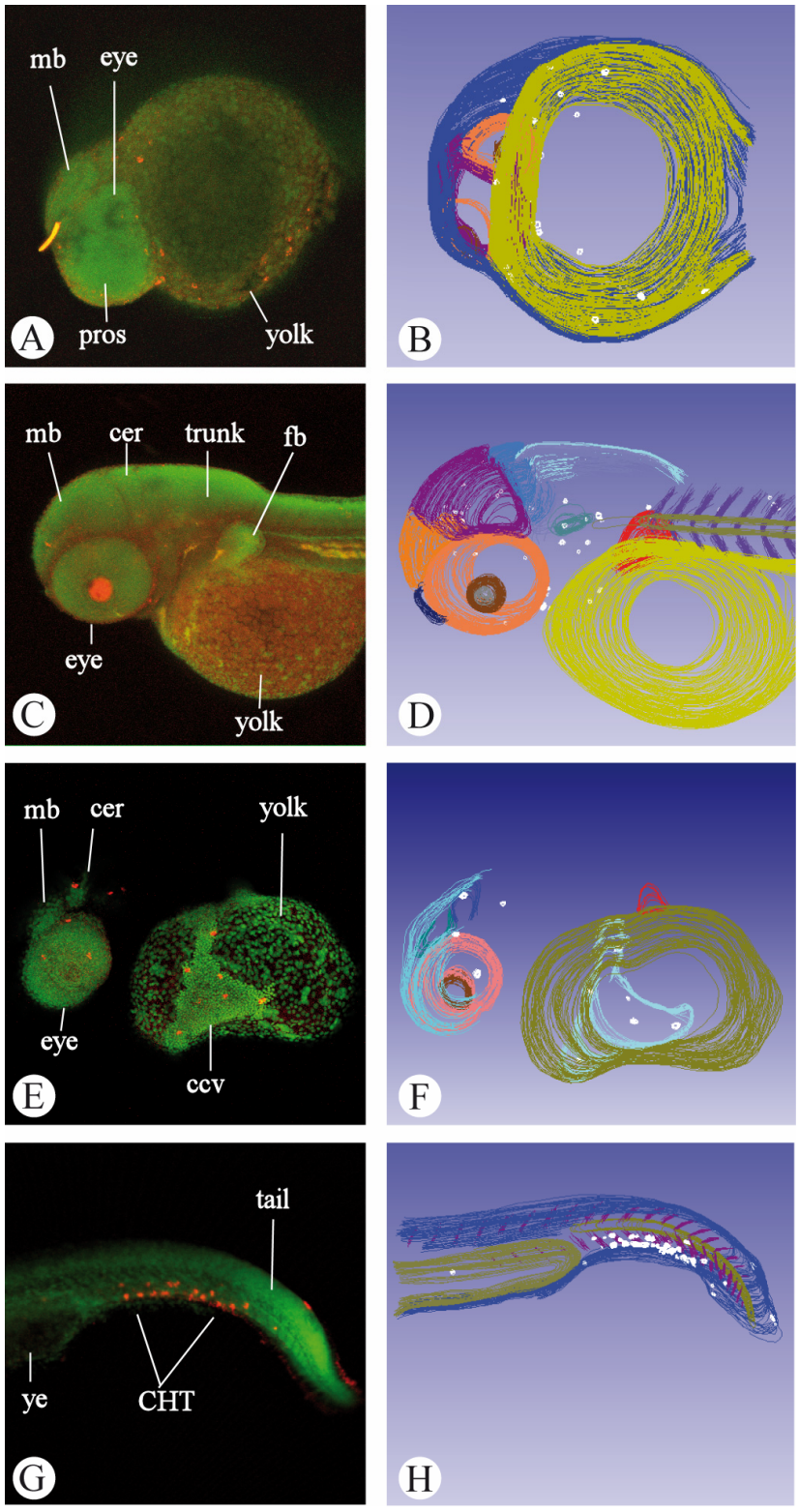

Chapter 4 fig 6

Fig. 3. (A–E) Left chicken wings stage 26–30, after in situ hybridization with *Sox9* probe (anterior is to the top, ventral aspect). (F–H) Left chicken hindlimbs stage 26, 27, and 30, respectively, *Sox9* probe. Anterior is to the top, ventral aspect. Roman numerals, digit or metacarpal number; mc, metacarpal; R, radius; U, ulna; Ue, ulnare; ph, phalanx; p?, pisiform?; [mc IV1V], common expression domain for metacarpals IV and V. Some images were inverted to make the orientation consistent.

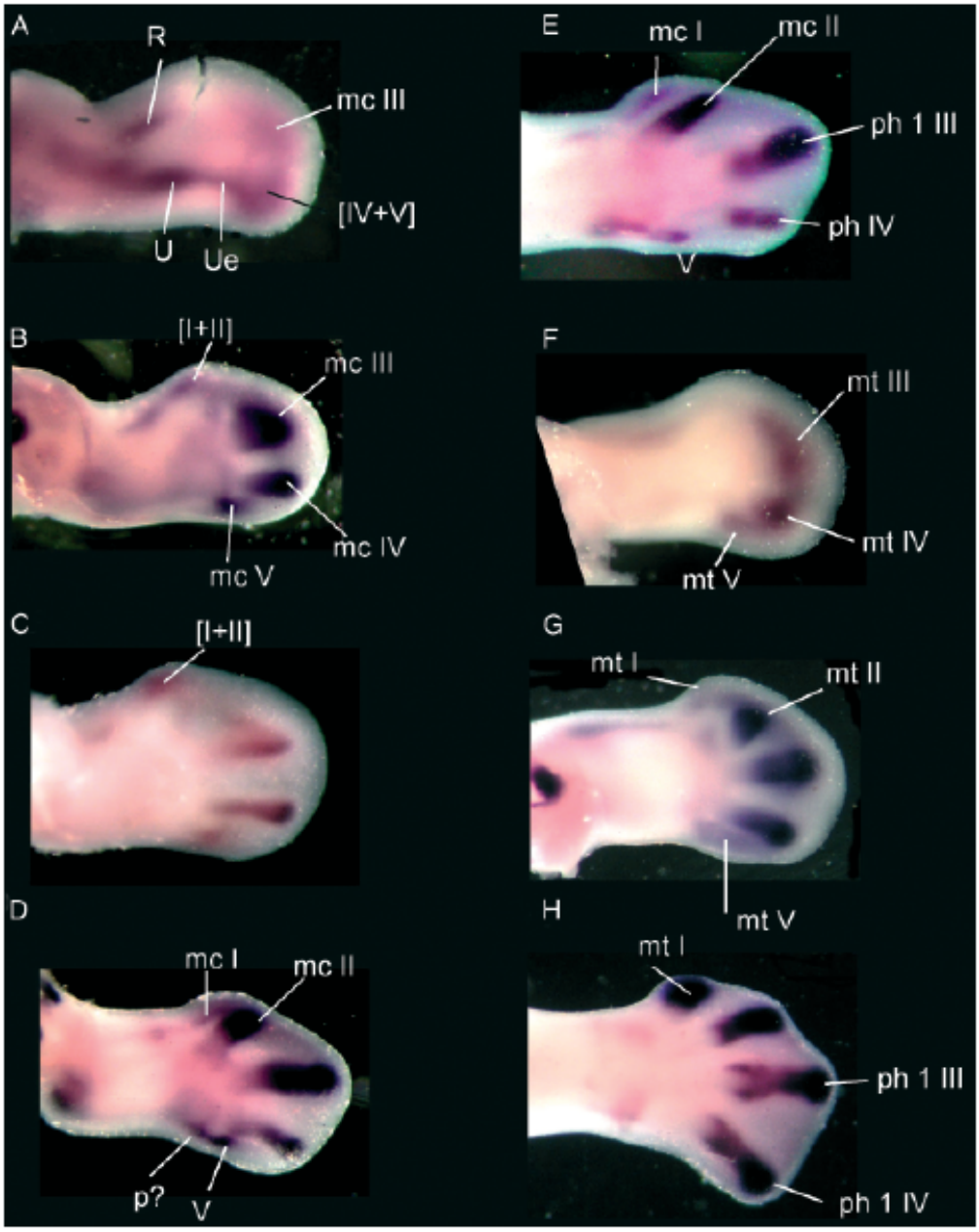

Chapter 5 fig. 3

Fig. 4. (A) Schematic interpretation of the *Sox9* gene expression patterns superimposed on cartilage pattern (alcian blue/ in situ double stains). Roman numerals, digits; vertical green line, plane of section in B; vertical blue line, plane of section in C; dark red box, area reconstructed in D, E. (B and C) Transverse sections of wings (stage 30, hybridized with *Sox9* probe), neutral red counterstain. Sections from the same specimen, C more proximal than B. (C) Detail from boxed area in B, showing expression of *Sox9* in the noncondensed mesenchyme anterior to digit II. (D) Three-dimensional (3D) reconstruction of the same specimen. Yellow, cartilage; dark blue, gene expression digits II–V; light blue, *Sox9* expression, presumptive digit I. Anterior is to the top. Ventral view. (E) Proximal view of the 3D reconstruction. Anterior to the top. The element at the level ‘‘V’’ may consist of mc V1element X. (F) Left chicken wing, stage 30, *Bmpr-1B* probe. Anterior to the top, ventral view. Distinct prechondrogenic domains are seen in digits II–IV, but not anterior to digit II (labeled II). p?, pisiform. (G) Wing, stage 30, oblique posterior–ventral view, *Sox9* probe. X, element ‘‘X’’; p?, pisiform. (H) Wing, stage 30, overstained in NBT/BCIsubstrate after *Sox9* hybridization, then counterstained with alcian blue and cleared in methyl salicylate. p?, pisiform; ue, ulnare.

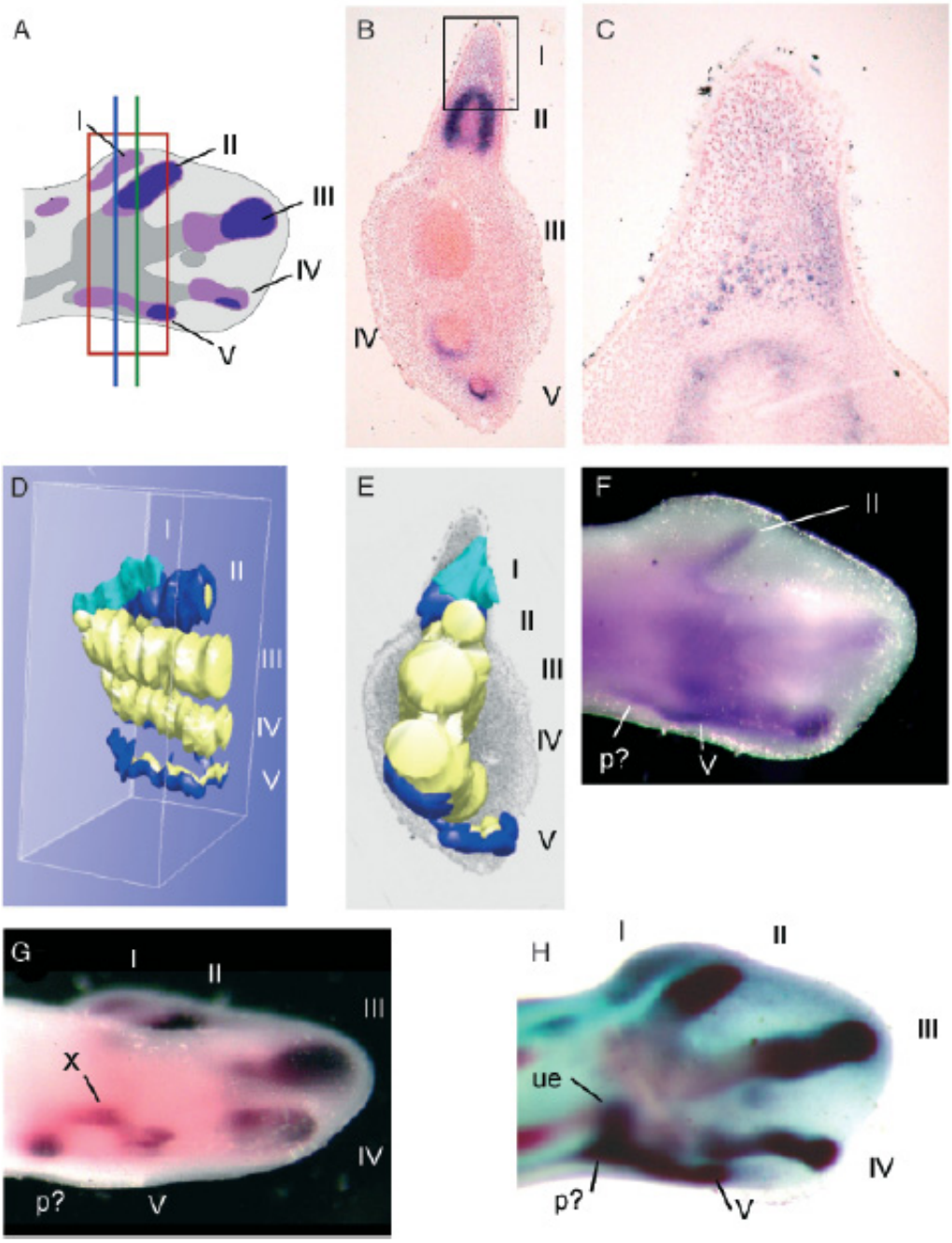

Chapter 5 Fig. 4

Fig. 2. *bmpr-1b* expression in zebrafish pectoral fin and branchial arches at 48 hpf. Anterior is to the left, dorsal to the top. Left panel : ISH result from AP detection method; Right panel: FISH result. The picture is the result of the projection of a 2 channel 3D confocal image. The expression is in red, i.e. the red channel of the CLSM image, the green depicts a standard staining of the cell nuclei.

Fig. 3. Pattern shift diagram showing episodes, frequently found sequences (Bathoorn et al, in preparation) of skeletal elements plotted against duration of gene expression, using a relative time scale of chicken limb development. The diagram shows a selection from the total analysis of gene expression timing and cartilage formation in chicken wing and hind limb. Onset and duration of gene expression as well as alcian blue staining for cartilage formation are shown in the red bar (wing) and in the green bar (hind limb). Structures are organized in proximal, carpal and digit region. The pattern shift diagram shows that only *sox9* gene expression is found in the presumptive wing metacarpal (mc) I while no subsequent *bmpr1b* expression and cartilage formation are found in the presumptive wing mc I. The onset of gene expression in presumptive wing mc I is relatively late compared to metacarpals and proximal phalanges of digit II and IV. The pattern shift diagram clearly illustrates that the difference in number of digits between wing and hind limb skeleton is the result of a time shift in gene expression

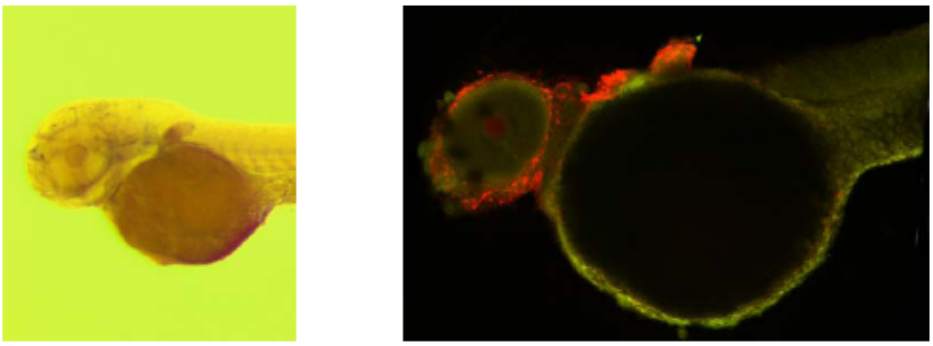

Chapter 6 fig 2

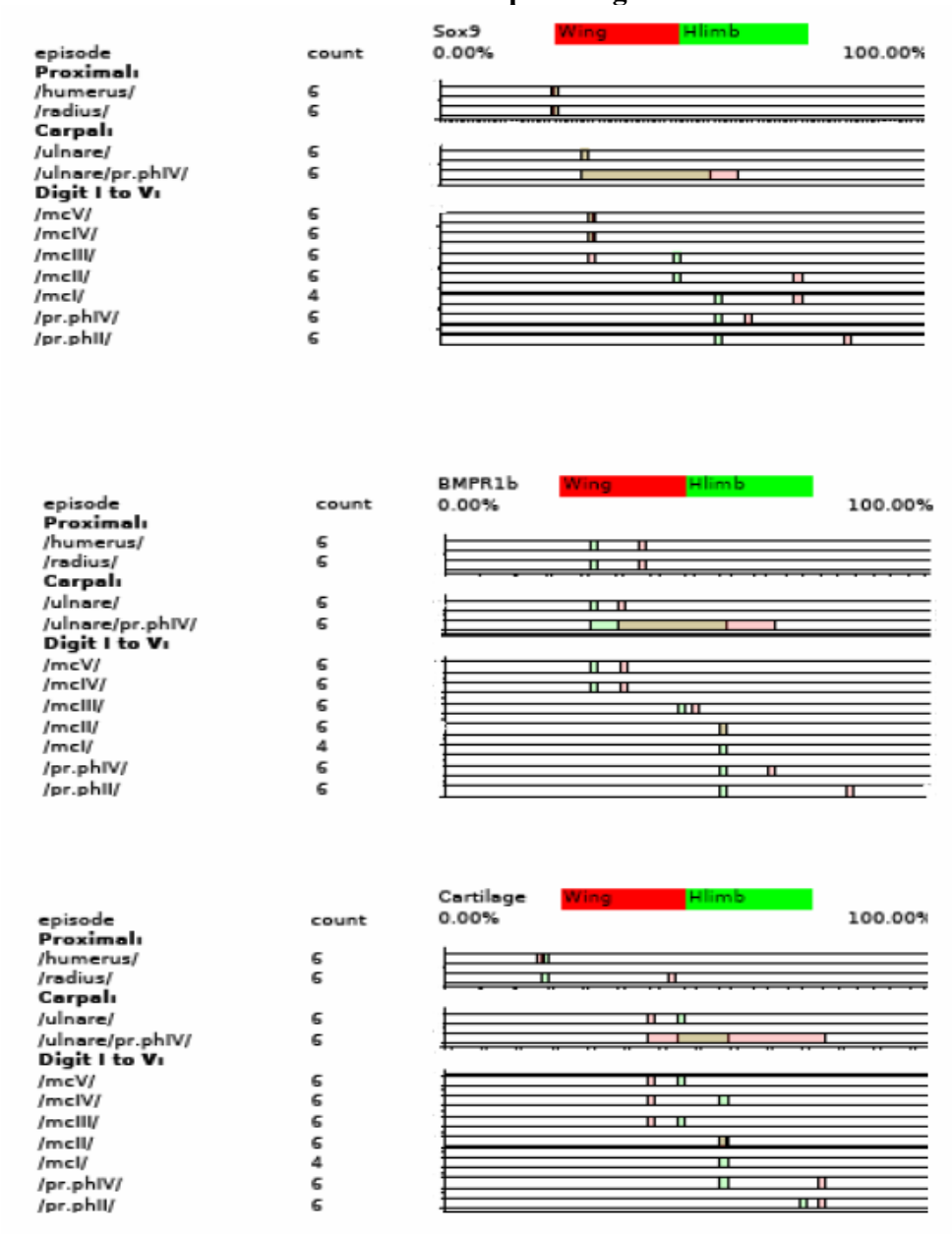

Fig 3